Decreased Stability of Erythroblastic Islands in Integrin β3 Deficient Mice

---

Dissertation

zur

Erlangung der naturwissenschaftlichen Doktorwürde

(Dr. sc. nat.)

vorgelegt der

Mathematisch-naturwissenschaftlichen Fakultät

der

Universität Zürich

von

Zhenghui Wang

aus

Kanada

Promotionskomitee

Prof. Dr. med. vet. Max Gassmann (Vorsitz)
Prof. Dr. med. Johannes Vogel (Leitung der Dissertation)
Prof. Dr. Christian Grimm
Prof. Dr. Carsten Wagner

Zürich, 2013

TABLE OF CONTENTS

ABSTRACT

In both, normal and stress erythropoiesis in hematopoietic organs, erythroblasts proliferate and differentiate while associated with a central macrophage. This distinct structure has been termed erythroblastic island. Growing evidence revealed the crucial role of macrophage/erythroblast and erythroblast/erythroblast interactions within erythroblastic islands during erythropoiesis. The formation and stability of this special niche depend on various adhesion molecules that are believed to mediate both erythroblast/erythroblast and erythroblast/macrophage interactions. Among these molecules, integrin family proteins, expressed by both central macrophage and erythroblasts have been identified to be involved in the attachment of macrophage with erythroblasts.

The Landsteiner-Weiner blood group glycoprotein protein intercellular adhesion molecule-4 (ICAM-4) has been shown to bind to integrin heterodimers such as αLβ2, αMβ2, αIIbβ3, αvβ1, αvβ5 and αvβ3. Among these, the interaction of ICAM with αv appeared to be involved in the formation and maintenance of the integrity of erythroblastic island. However, which β integrin is the heterodimerization partner of αv remained unknown.

By comparing stress erythropoiesis in the anemic integrin β3 lacking mice and transgenic mice with constant overexpression of human erythropoietin (tg 6) we delineated the role of integrin β3 for stabilization of erythroblastic islands. Integrin β3 lacking mice showed reduced numbers of erythroblast per erythropoietic island and a lower percentage of the late stage erythroblasts and premature reticulocytes in erythropoiesis tissues. In addition, in peripheral blood of these mice we found abnormally premature erythroid cells containing calnexin that is normally completely lost before reticulocytes are released into the circulation. In conclusion, our data suggest that the absence of integrin β3 impairs adhesion of the erythroid at the latest developmental stage to the central macrophage of erythropoietic islands resulting in preterm release of abnormally immature erythrocytes into the circulation.

ZUSAMMENFASSUNG

Sowohl während der normalen als auch der stimulierten Blutbildung (Erythropoiese) differenzieren die Erythroblasten in direktem Kontakt mit einem zentralen Makrophagen. Diese mikroanatomische Struktur wird erythroblastische Insel genannt. Bishereige Forschungdaten zeigen, dass die Zellkontakte nicht nur zwischen Erythroblasten und dem zentralen Makrophagen sondern auch die Kontakte zwischen den Erythroblasten innerhalb der erythroblastischen Inseln entscheidend für die korrekte Reifung der Erythrozyten ist.

Die Stabilität der erythroblastischen Inseln wird durch eine Vielzahl von Adhäsionsmolekülen vermittelt, welche im Wesentlichen der Integrin-Proteinfamilie zuzuordnen sind. Zentral scheint hier das Landsteiner-Weiner Blutgruppen Glykoprotein intercellular adhesion molecule-4 (ICAM-4) zu sein, das die Integrinheterodimere αLβ2, αMβ2, αIIbβ3, αvβ1, αvβ5 and αvβ3 binden kann. Von diesen ist wohl αv essentiell für die Bildung und Stabilisierung der erythroblastischen Inseln durch direkte Interaktion mit ICAM-4. Allerdings ist bisher unbekannt, welches β-Integrin der Heterodimerisationspartner von αv in dieser Struktur ist.

Durch Vergleich der Stresserythropoiese in Mäusen, denen das β3-Integrin fehlt mit Mäusen, die Erythropoietin konstant überexprimieren konnte eine Rolle β3-Integrin für die Stabilisierung von erythroblastischen Inseln gefunden werden. Mäuse ohne β3-Integrin hatten eine reduzierte Anzahl von Erythroblasten pro Insel und einen reduzierten Anteil der Zellen der spätesten Erythrozytenentwicklungsstadien im Knochenmark. Zudem enthielten diese Mäuse im peripheren Blut abnorm unreife Erythrozyten, da diese Calnexin enthielten, ein Protein, das normalerweise vollständig aus den Erythozyten verschwindet, bevor sie in den Kreislauf gelangen. Somit legen unsere Daten nahe, dass das Fehlen von β3-Integrin die Haftung der späten Erythrozytenentwicklungstadien an den zentralen Makrophagen stört, was zu einer Freisetzung von abnorm unreifen Zellen in die periphere Zirkulation führt.

LIST OF ABBREVIATIONS

BFU-E	burst forming unit erythroid
CFU-E	colony forming unit erythroid
CSF	colony stimulating factor
DMT1	divalent metal transporter 1
EI	erythroblastic island
EMP	erythroblast macrophage protein
EPO	erythropoietin
GAPDH	glyceraldehyde 3-phosphate dehydrogenase
GAS6	growth arrest specific gene 6
HIF	hypoxia inducible factor
HOX-1	heme oxygenase-1
HRE	hypoxia-response element
HSCs	hematopoietic stem cells
ICAM-4	erythroid intercellular adhesion molecule-4
IgG	immunoglobulin G
IRE	iron responsive element
IRP	IRE/iron regulatory protein
JAK2	Janus kinase 2
MAPK	mitogen-activated protein kinase
PHD	prolyl hydroxylase domain
PIGF	placenta growth factor
RB	retinoblastoma protein
RBCs	red blood cells
RCAS	receptor binding cancer antigen expressed in SiSo cell
SCF	stem cell factor
SIRPα	signal regulatory protein α
TNF	tumor necrosis factor
VCAM-1	vascular cell adhesion molecule-1
VEGF	vascula endothelial growth factor
VHL	Von Hippel-Lindau tumor suppressor protein

CHAPTER 1. INTRODUCTION

1.1. ERYTHROPOIESIS

Erythropoiesis is necessary for large multicellular organisms such as mammals to ensure oxygen transport to all cells. Primitive hematopoiesis occurs in the yolk sac/blood islands, later at the aorta-gonad mesonephros region, the chorio-allantoic placenta, and releases nucleated red blood cells (RBCs) into the circulation. Nuclei gradually condense before being extruded. Definitive erythropoiesis begins in fetal liver and finally shifts from the fetal liver to the bone marrow to produce enucleated RBCs (figure 1) (1). In addition, stress erythropoiesis can be induced in adult mice in the spleen to generate more red cells (2,3,4,5).

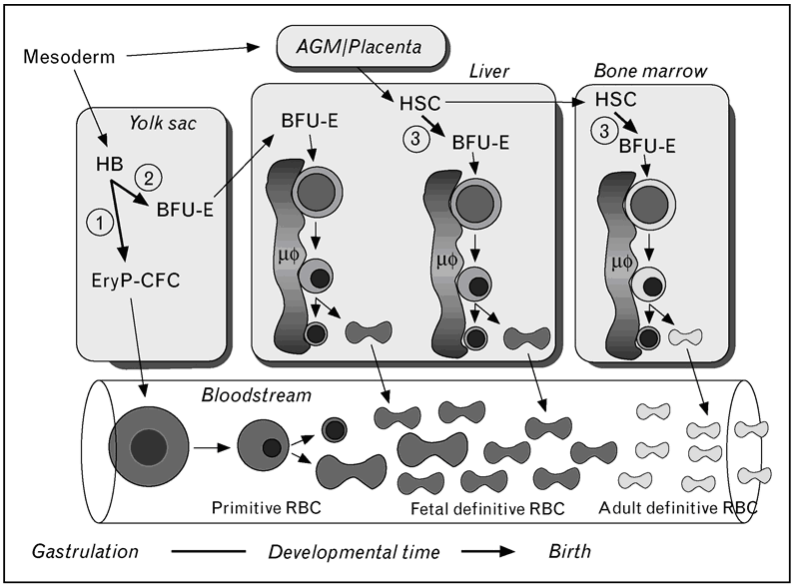

Figure 1. In mammalian embryonic development, primitive erythropoietic progenitors differentiated from hemangioblasts originated from yolk sac. These cells mature in the bloodstream and develop into enucleated reticulocytes. At later stage of fetal development, a population of transient embryonic burst forming unit erythroid (BFU-E) emerges from the yolk sac and later seeds in the fetal liver. There they enucleate to become the first definitive RBCs of fetus. Eventually, in the late gestation liver and postnatal bone marrow definitive erythroid progenitors originated from hematopoietic stem cells. There these erythroid precursors mature within erythroblast islands. μΦ: macrophage cells (1).

1.1.1. Primitive erythropoiesis

The formation of mesoderm cells initiates the generation of erythroid cells in the embryo of mammal. These mesoderm cells possess a pluripotent nature and can differentiate into both erythropoietic cells, epithelial cells and other mesenchyme-derived tissues (12,13,14). In the yolk sac, mesoderm cells committed to primitive erythropoietic cells pool into so-called blood islands (6,7). Each blood island contains a central core consists of erythropoietic progenitors surrounded by a rim of outer endothelial cells, which later form the initial vascular plexus of the yolk sac (8,9). The close spatial and temporal appearance of primitive erythropoietic cells and endothelial cells had suggested that these lineages share a common origin, which were later identified and termed hemangioblasts (10,11). In adult erythropoiesis, nuclear transcription factor GATA-2 is crucial for the survival and proliferation of hematopoietic stem cells (HSCs) (15,16). However, GATA-1 promotes specifically the survival of erythroid precursors through inducing Bcl-xL expression (17,18). GATA-1, GATA-2 have been shown to regulate hemangioblast precursors as well (19,20). Nucleated primitive erythroblasts in the blood islands begin to circulate in the cardiovascular system starting at E8.25 in mice (21,22,23). Over the next 8 days, primitive erythroid cells undergo cell divisions, hemoglobin accumulation, decrease in cell size, nuclear condensation and ultimately loss of euchromatin (24,25).

The primitive erythroblast enucleation results in a transient appearance of a population of very small, globin containing, nucleated cells in the circulation of mouse embryos. These cells are reminiscent of extruded nuclei, termed pyrenocytes (26,27). The discovery of primitive pyrenocytes in the fetal bloodstream suggests that late-stage primitive erythroblasts enucleate in the circulation. However, primitive erythroblasts do not enucleate spontaneously when cultured (26). Interestingly, they are capable of physically interacting with F4/80-positive macrophage cells in vitro. These interactions are mediated in part through α4β1 integrins present on primitive erythroid cells and vascular cell adhesion molecule-1 (VCAM-1) expressed by fetal liver macrophage. Taking together, these observations raise the possibility that primitive erythroid cells enucleate while associated with macrophage cells in vivo (26,27).

1.1.2. Definitive erythropoiesis

At later stages of mammalian fetal development, more red blood cells are needed to meet the demand for growth. Prior to the formation of bone marrow, fetal liver serves as the site of definitive erythropoiesis. External erythropoietic elements such as BFU-Es from the yolk sac invade the fetal liver soon after it begins to form as an organ. BFU-Es proliferate and differentiate into colony forming unit erythroids (CFU-Es), which subsequently expand exponentially in numbers and generate definitive erythroid cells (28,29).

In mammalian embryo, definitive erythropoiesis moves from the fetal liver to the newly formed bone marrow towards the end of gestation. Postnatal definitive erythropoiesis is a continuous process of proliferation and differentiation starting with bone marrow HSCs and resulting in anucleate erythrocytes (Figure 2) (33,34). In the adult bone marrow, HSCs present less than 0.01% of the nucleated cells in the bone marrow and possess the capacities to self-renew and differentiate into all cells of the blood and immune system. The earliest stage of progenitor cell differentiation that is committed to the erythroid lineage is BFU-E which could develop into more mature CFU-E, both have been identified by in vitro colony-forming assays. Although fundamentally similar, adult and fetal erythroid progenitors differ with some distinctive features. First, fetal hepatic BFU-Es proliferate more rapidly than their adult counterpart. Second, fetal liver BFU-Es, in contrast to adult bone marrow BFU-Es, are capable of proliferating in response to erythropoietin (EPO) in the absence of added colony-stimulating factor (CSF) or interleukin-3 (30,31). Lastly, CFU-Es in the murine fetus are more sensitive to EPO (32).

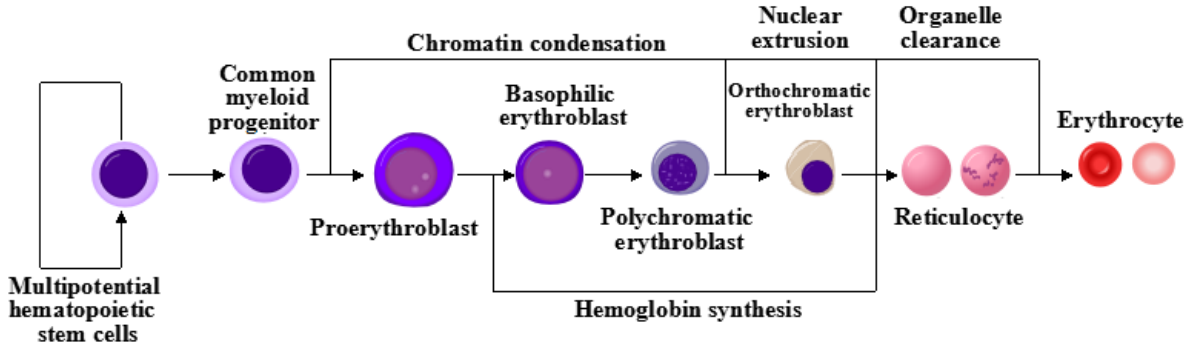

Figure 2. Erythroblasts differentiation stages from dividing self-renewing HSCs through the mature erythrocytes (adapted from https://commons.wikimedia.org/wiki/File: Hematopoiesis _(human)_diagram.png).

In definitive erythropoiesis, CFU-E gives rise to proerythroblast, basophilic, polychromatic and orthochromatic erythroblast. They are morphologically distinct and could be identified by means of cell-surface markers (35,36). During the process of maturation, erythroblasts gradually lose all the organelles before fully matured. In contrast to primitive erythroid cells that enucleate in the blood stream, the definitive erythroid precursors in the fetal liver and postnatal bone marrow enucleate in the erythroblastic islands (EI). The extruded nuclei are surrounded by a rim of plasma membrane of definitive erythroid cells and undergo rapid loss of the phosphatidylserine asymmetry of the cell membrane, which leads to recognition and engulfment by the associated macrophage cells (37,38,39,40). Therefore, erythrocytes in the circulation are devoid of nucleus and internal organelles (37).

1.1.2.1. Erythropoiesis niche: EI

Proliferation and differentiation of erythroblasts occur within the microenvironment EI (Figure 3). The first description of this erythropoietic unit dates back to the 1950's when French hematologist Marcel Bessis identified it. Based on transmission electron microscopic analysis of bone marrow sections, Bessis characterized EI as developing erythroblasts surrounding a central macrophage (41). Originally assumed by Bessis, the central macrophage serves as a "nursing" cell, supplying nutrients and growth factors to the developing erythroblasts and phagocytose extruded nuclear (42).

EI exists in hematopoietic organs such as fetal liver as well as bone marrow. In normal erythropoiesis, the EI is composed of a central macrophage surrounded by erythroblast at different stages of erythropoiesis from nucleated proerythroblasts through multilobulated reticulocytes (43). In mice, the central macrophage can be distinguished from the heterogeneous population of monocytes and macrophages as well as other stromal cells by expression of F4/80 antigen and Forssman glycosphingolipid. In the bone marrow, EIs are found with equal distribution adjacent and non-adjacent to the sinusoid. Of note, the islands more distant to the sinusoids contain more proerythroblasts while islands neighboring sinusoids have more differentiated erythroblasts (44,45).

A diverse array of adhesion molecules mediates both erythroblast/erythroblast and erythroblast/macrophage interactions (Figure 3). Erythroblast macrophage protein (EMP) was the first molecule identified to be involved in the attachment of macrophage/erythroblast and erythroblast/erythroblast through homophilic binding. EMP is a transmembrane protein with a molecular weight of 36-kDa and expressed by both macrophage and erythroblasts (46). In vitro, when EMP-mediated interaction of erythroblasts with central macrophage was blocked by antibodies, erythroid cells matured to the late erythroblast stage but failed to enucleate and underwent apoptosis (47). In vivo, fetuses with deficient of EMP became severely anemic and then die in uterus, which provides further evidence on the important role of EMP in erythropoiesis (48). Subsequently another set of receptor/countereceptor, α4β1 integrin in erythroblasts and VCAM-1 in central macrophages was found to contribute to the erythroblast/macrophage interactions within the islands. Most recently, the interaction of erythroid intercellular adhesion molecule-4 (ICAM-4) and macrophage αv integrin has been identified to participate in island formation (49,50,51). The yet unanswered question is the role of this adhesive molecular attachment. It is speculated that these receptor-counterreceptor interactions may trigger signaling pathways coordinating adhesion and timely release of the reticulocytes and gene expression (37).

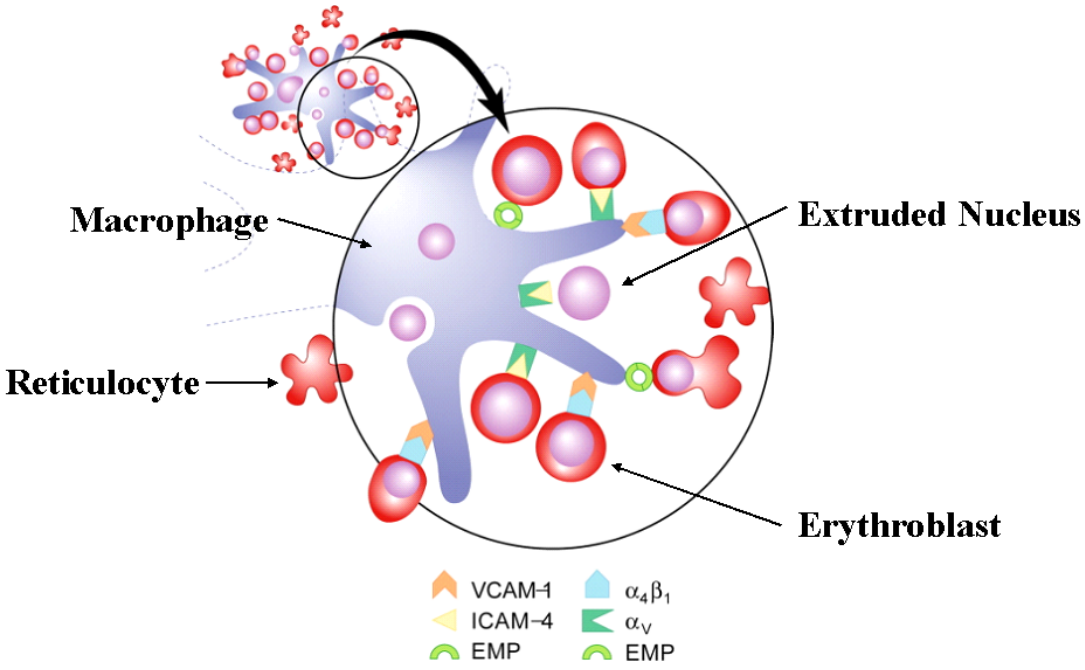

Figure 3. Erythroblasts extrude their nucleus within the niche. Expelled nuclei are phagocytosed by the central macrophage. An array of adhesion molecules is involved in the attachment of the macrophage with erythroblasts, including homophilic interaction of EMP, VCAM-1 with integrin α4β1 and ICAM-4 with integrin αv (54).

As described by Bessis and other researchers, one of the key functions of the central macrophage is to engulf nuclei extruded during the terminal RBC differentiation (52,53). The extruded nucleus is surrounded by plasma membrane separated from erythroblast cytoplasm. It has been reported that during enucleation, the erythroblast plasma membrane components were sorted to the plasma membranes of the nascent reticulocyte and/or the expelled nucleus. In this process, the erythroblast membrane protein EMP and β1 integrin predominantly remain on the extruded nuclei and enable their attachment to the macrophage surface (54,55). Evidence from in vitro co-culture of erythroblasts and macrophages indicated that nuclei expelled from fetal liver erythroblasts expose phosphatidylserine on their surface that is recognized subsequently by macrophages, resulting in phagocytosis and degradation by DNase II within the central macrophage (38,56).

Furthermore, Bessis proposed an important role of macrophage in the transfer of iron to adherent erythroblasts (42). Indeed using co-culture it was shown that macrophages synthesize and secrete ferritin under transferrin free conditions. Iron released from this ferritin

was used by erythroblasts for heme synthesis (57). However, this idea remains controversial and other research groups found evidence indicating that central macrophages are irrelevant for delivering of iron to erythroblasts (37).

Perturbations in macrophage function affect red cell production and result in anemia. There is evidence indicating that the retinoblastoma protein (RB) mediates this process through regulating the maturation of macrophages. RB is a nuclear protein with ubiquitous expression and is essential to the cell's decision to transverse the cell cycle. Mice lacking RB have deficiencies in the nervous system, placenta, eye lens as well as in erythropoiesis. The most recent evidence revealed that RB-deficient fetuses fail to form functional erythroid islands due to the severe defects in the macrophage lineage (58,59). However, the role of RB might be much more complex as a number of recent findings from in vivo investigations suggested that anemia in RB-null mice may involve also to erythroblast defects (60,61).

Despite the fact that progress is made in elucidating the role of the central macrophage in regulating erythropoiesis, little is known concerning the molecular mechanisms through which macrophages enhance erythroid proliferation and how regulatory factors operating in the EI to regulate erythropoiesis (54).

1.1.2.1.1. Regulatory factors within EI

During terminal differentiation, the adhesive proteins of the erythroblast membrane appear to be lost gradually. This implies that the cell-cell adhesive interactions are involved in the erythroblast differentiation. Growing evidence are demonstrating the crucial role of both macrophage/erythroblast and erythroblast/erythroblast interaction within EI during erythropoiesis (60). It has been speculated that erythroblast development is regulated through a balance between positive and negative feedback mechanisms. Cell-cell interactions and soluble factors are regulators in this process (54).

1.1.2.1.1.1. Cell-cell interactions

Macrophage interaction with erythroblasts

In vitro co-culture of macrophages and erythroblasts in the presence of physiological concentrations of EPO indicates that direct contact with macrophage enhances the proliferation of erythroblasts. Cell cycle analysis showed that the improved erythroblast proliferation resulted from a decreased transit time in the G0/G1 phase. More cell divisions were completed during a limited period and consequently more reticulocytes were generated (46,63,64,65). The candidate proteins identified to govern these changes in cell-cycle dynamics are the macrophage membrane protein Ephrin-2 (HTK ligand) and its receptor EphB4 (HTK) expressed by CFU-E (66,67,68).

The negative mechanism existing between cellular components of the EI involves receptor binding cancer antigen expressed in SiSo cells (RCAS) and its receptor. RCAS1 is secreted by bone marrow macrophages and immature erythroblasts express RCAS1 receptor. The binding of RCAS1 to the RCAS1 receptor activates proapoptotic caspases 8 and 3, leading to apoptotic death in immature erythroblasts (69).

Interaction between erythroblasts

In a study of erythroblast terminal differentiation, Fas/Fas ligand interaction was found to regulate survival of erythroblasts. Erythroblasts express Fas throughout terminal differentiation. Crosslinking of Fas/FasL transduces apoptotic death signal to the immature early stage erythroblasts, but mature erythroblasts remained unaffected. At the end of maturation, FasL was induced in orthochromatic erythroblasts, which demonstrates a Fas based cytotoxicity against less mature early erythroblasts within EI (70). EPO counteracts erythroblast apoptosis initiated by Fas ligation, thus provides protection to early erythroblasts (71).

It has long been recognized that the level of transcription factor GATA-1 is crucial for completion of normal erythroblast differentiation. Absence of GATA-1 expression is embryonically lethal and results in proerythroblast apoptosis (72,73,74,75), whereas, GATA-1

overexpressing erythroblasts are unable to complete terminal differentiation (76,77). However, co-culture of wild-type with GATA-1 overexpressing erythroblasts rescued the GATA-1 overexpressing erythroblasts to complete terminal differentiation. It was proposed that a signal generated by wild-type cells overcomes the intrinsic defect in GATA1-overexpressing erythroid cells. This pinpoints the importance of homotypic signaling between erythroblasts within EI niches as a mechanism for regulating GATA-1 activity (78).

1.1.2.1.1.2. Soluble factors

Macrophages within EI secrete macrophage cytokines, including burst promoting activity and insulin-like growth factor, inducing growth of both BFU-Es and CFU-Es (79,80,81). Erythroblasts also secrete soluble factors. A very recent discovery is that erythroblasts release growth arrest specific gene 6 (GAS6) in response to EPO. GAS6 could bind to its receptor also located on erythroblasts, this way activates phosphoinositide 3 kinase and its effector AKT to enforce EPO receptor signaling, thus enhancing proliferation and survival of erythroid cells. Moreover, binding of GAS6 to macrophages decreases macrophage secretion of erythroid inhibitory factors (82). Differentiating erythroblasts also secrete angiogenic factors, vascular endothelial growth factor A (VEGF-A) and placenta growth factor (PIGF). The absence of VEGF-A and PIGF receptors on erythrocytes suggests that these secreted angiogenic factors may serve as paracrine effectors, mediating crosstalk between receptor-expressing macrophages and developing erythroblasts and may regulate island structure and/or localization (83).

In inflammation and malignancy, elevated cytokines secreted by central macrophage such as tumor necrosis factor (TNF), Interleukin-6 and interferon-γ appear to inhibit EPO signaling and promoting cell death of erythroblasts. TNF-α could induce apoptosis or retard proliferation (84). TNF-β may reduce the number of progenitor cells by blocking proliferation and accelerating differentiation of erythroid progenitors (85). Interleukin-6 was found to prevent iron release from central macrophage thus blocking the supply of iron for erythropoiesis (86). Elevated interferon-γ was shown to upregulate in both macrophages and erythroblasts the expression and secretion of TNF-related apoptosis inducing ligand, which

inhibits differentiation of erythroblasts through activating p42/44 mitogen-activated protein kinase (MAPK) pathway (87).

1.1.2.2. Extracellular matrix: role of fibronectin and laminin

Interactions of receptors found on erythroblasts with extracellular matrix components, such as fibronectin and laminin, affect erythropoiesis by influencing terminal differentiation and migration of erythroid cells (88). It seems that the proliferation of erythroblasts is regulated by an EPO-dependent phase followed by an integrin/fibronectin dependent phase (88). Erythroblasts express fibronectin receptors α4β1 and α5β1. The expression of α5β1 gradually decreases during terminal differentiation that leaves α4β1 the sole fibronectin receptor on the late stage erythroblasts (89). The progressive loss of adherence to fibronectin facilitates the release of reticulocytes at the late stage of differentiation (90).

Various laminins localize to different regions in the bone marrow extracellular matrix. Among them, laminins10/11 presents in the subendothelial basement membrane of bone marrow sinusoids (91). As a receptor of laminin, Lutheran, which is present on the late stage erythroblasts, has a specific, high-affinity for laminins10/11 (92,93,94,95). It is speculated that the interaction between Lutheran and laminin may facilitate the movement of reticulocyte to sinusoids and subsequent egress into circulation (54).

1.1.2.3. Loss of organelles during terminal erythroblast differentiation

During development, erythroblasts progressively lose RNA, accumulate more hemoglobin and condense chromatin. The nucleus is finally extruded and exposes phosphatidylserine on its surface, which triggers phagocytosis by the central macrophage (38). In the circulation, some remnant of organelles, such as mitochondria, endocytic vesicles, ribosomes, Golgi cisternae and rough endoplasmic are retained within reticulocytes. During the process of maturation into erythrocytes, reticulocytes lose all the organelles (39,40). How the organelles are removed remains to be described. By using knockout mouse models, it was demonstrated that Nix, a BH3-only protein, plays a critical role in the mitochondrial

degradation in reticulocytes. Lack of this protein arrests terminal erythroid differentiation through inhibiting mitochondrial incorporation into autophagosomes and autophagosome maturation, resulting in an erythroid maturation defect (96,97,98). In contrast to Nix, Bim and PUMA, two other BH3-only proteins of the Bcl-2 family are not required for mitochondrial clearance in reticulocytes (97). In addition, ULK1, a ubiquitously expressed serine-threonine kinase, has been suggested to be involved in the organelle clearance (99). Autophagic activity was also found to be in the mechanism of exosome formation, finally reducing cell surface area and cell volume during maturation into erythrocytes. However, little is known about molecular mechanisms responsible for this process (100,101).

1.1.3. Hemoglobin switching and regulation

Primitive erythroid cells express ζ-globin, βH1-globin, and εγ-globin in addition to α1-globin, α2-globin, β1-globin and β2-globin, which are expressed in definitive erythroid cells in the mouse. During erythropoiesis, the expression of globin chains varies with the maturation stage in the primitive and definitive RBCs (102). Moreover, the hemoglobin content of primitive RBC was found to be a few times the amount in definitive erythrocytes (103). Gene expression analysis in primitive erythroid cells of early erythropoietic stages indicates that the initial expression of *ζ-globin*, *βH1-globin* genes is later switched to the *α1-globin*, *α2-globin* and *εγ-globin* genes, respectively, during the maturation process of primitive proerythroblasts to reticulocytes (104). Consequently, primitive RBCs express increasing levels of adult globins as gestation progresses, whereas definitive RBCs harbor only the adult protein variants (105). Some transcription factors are found to be essential in regulating the expression of globin in both primitive and definitive erythropoiesis. For example, the erythroid-specific kruppel like factor initially identified to regulate the adult *β-globin* genes was found to also play a role in the controlling of multiple erythroid-specific genes, including α-globin stabilizing protein and heme synthesis pathway proteins in the primitive erythropoieses as well (107,108). The deficiency of KLF2, a Kruppel-like transcript factor, has been found to decrease βH1-globin and εγ-globin expression level (106).

1.2. KEY FACTORS AFFECTING ERYTHROPOIESIS

Physiologically, the availability of nutritional factors, as well as status such as hypoxia represent key elements contributing to erythropoiesis. Although many questions still remain unanswered regarding the underlying molecular mechanisms that govern lineage-determining decisions toward the path of terminal maturation, specific signaling pathways and molecular networks have been identified to strictly regulate cell proliferation, prevent apoptosis, and coordinate cell-cycle arrest within terminal maturation (109).

1.2.1. Nutritional factors

1.2.1.1. Folate and vitamin B_{12}

Folate is present in both plant and animal tissues in the form of 5-methyl-THF (tetrahydrofolate, a reduced form of folate). In animals, 5-methyl-THF is absorbed in the jejunum after enzymatic cleavage to the monoglutamic form. Thus, in the circulation, folate is present as 5-methyl-TNF monoglutamate. Once folate is transported into cells, the folylpolyglutamate synthetase converts folate to the polyglutamyl form (110,111). Vitamin B_{12} is produced by microorganisms in the mammalian gut and was found to circulate as vitamin B_{12}-transcobalamin II complex, a functional carrier of vitamin B_{12} to the cells. As a coenzyme, it is involved in the transfer of a methyl group from 5-methyl-THF to homocysterin, thereby regenerating methionine. Thus a metabolic link exists between folate and vitamin B_{12} (112).

The deficiency of either folate or vitamin B_{12} cause megaloblastic anemia, characterized by pancytopenia with macrocytic erythrocytes, hypersegmented neutrophilic granulocytes and reticulocytopenia. Although affecting all hematopoietic lineages, megaloblastic anemia is most prominent in the erythroid lineage with an increased death rate of premature cells in the bone marrow, which leads to the appearance of increased numbers of large immature erythroblasts. Impaired DNA synthesis and its sequelae are key elements in the increased cell death that characterize this anemia. Impaired DNA synthesis would be expected to result in chromosomal breakage and possibly nuclear damage as indeed had been shown in the bone

marrow cells of patients with folate or vitamin B_{12} deficiency (113,114,115). The underlying mechanism is that folate or vitamin B_{12} deficiency decreases de novo synthesis of deoxynucleotides which in turn results in impaired synthesis and repair of DNA, and ultimately, in cell death (115,116,117).

In vivo and in vitro evidences document the morphological changes of ineffective erythropoiesis caused by folate or vitamin B_{12} deficiency. In vitro, the majority of erythroblasts undergo apoptosis in S-phase when cultured under folate-deficient conditions. The folate-deficient erythroid cells can be rescued from cell death by supplied in the medium containing sufficient amounts of both thymidine and purines or purine nucleosides to provide the necessary deoxynucleotides that permit DNA synthesis (118). In vivo, mice fed with folate- deficient diet develop a macrocytic anemia with decreased reticulocytes (119,120). As the folate-deficiency anemia progresses, the total number of nucleated cells decreases in the bone marrow erythroid cell population. In parallel, the size of the individual cells increases and cells undergo apoptosis. Although the absolute numbers of reticulocytes are decreased in folate-deficient mice, the absolute numbers of CFU-Es are increased in their bone marrow and spleen (119). It was postulated in folate-deficient mice, that EPO levels are elevated as a response to the anemia. More EPO responsive erythroid cells at early differentiation stages survive in an EPO-dependent manner. However, most of these early state erythroid cells fail to persist in the subsequent stages of differentiation, most often succumb to apoptosis while in S-phase of the cell cycle (120).

1.2.1.2. Iron

Iron is an essential component of many different proteins with vital function. Restriction of iron delivery to erythrocyte precursors limits erythropoiesis since most of the iron is used for the synthesis of hemoglobin in erythroid cells. Cellular iron acquisition and transportation depends on an array of proteins, among which, transferrin, transferrin receptor, and ferritin were considered to be the key players in iron metabolism (121).

Both heme-bound and elemental iron is absorbed through the brush border of the upper small intestine (122). Inorganic iron is first reduced from the oxidized form before being

absorbed by duodenal enterocytes via the divalent metal transporter1 (DMT1/SLC11A2) (123). Heme iron is absorbed by an unknown mechanism (124). Intracellularly, heme iron is released by inducible hemoxygenase 1 (HOX-1) (125). Cytosolic iron is then exported by ferroportin with the ferroxidase activity of hephaestin, facilitating the movement of iron across the enterocyte membrane to the circulation (126,127).

Physiologically, the iron absorption is affected by iron storage and rate of utilization (122). The 3`UTR of mRNA of DMT1 expressed in intestinal cells contains the iron responsive element (IRE). IREs are nucleotide sequences that is recognized by cytosolic IRE/iron regulatory proteins, known as IRP1 and IRP2. Diminished iron levels would result in the binding of IRP2 to IREs in 3`UTR and stabilizes the transcript, which leads to an increased DMT1 expression and subsequently iron absorption (128,129). Additionally, through an unknown mechanism, hypoxia can stimulate iron absorption independent of erythropoietic activity (130).

Iron is transported within the body in the form of plasma transferrin because under physiological conditions, iron exists as Fe^{3+}, which is virtually insoluble at neutral pH. Transferrin is a glycoprotein that binds Fe^{3+} very tightly but reversely. Most of the iron is used for the synthesis of hemoglobin in erythroid cells (131). Therefore, physiologically, erythroid precursors take up iron from transferrin. Delivery of iron to cells occurs after binding of transferrin to its receptors on the cell membrane (132,133). Upon entering cells, Fe^{3+} is released from transferrin by a process involving endosomal acidification. In erythroid cells, reduction of Fe^{3+} to Fe^{2+} occurs in the endosome, and then irons targets toward intracellular sites of use or storage in ferritin. Mitochondria are the main site of heme production by ferrochelatase, the enzyme that inserts Fe^{2+} into protoporphyrin IX (134).

Within erythroid cells, iron moves between various intracellular compartments. The intracellular iron is tightly controlled through regulating transferrin receptor and iron storage protein ferritin. The increase of cellular iron concentration stimulates ferritin synthesis and prevents the expression of transferrin receptor and vice versa. Iron dependent regulation of ferritin and transferrin receptors occurs post-transcriptionally. mRNAs of both proteins possess IREs. In ferritin, IREs are located in the 5` UTRs of the mRNA whereas similar IREs

are present in the 3`UTR of the transferring receptor mRNA. Binding of IRP1 to IREs in the 5`end of mRNA inhibits its translation. In contrast, binding of IRP2 to IREs in 3`UTR stabilizes the transcript. Iron storage expansion inactivates IRP1 and promotes degradation of IRP2, leading to increased ferritin levels and degradation of transferrin receptor mRNA. Visa versa, iron deficiency promotes cellular iron acquisition and decreases the cellular iron-storing protein (135).

Recycled hemoglobin iron by macrophage is the most important source of iron for daily erythropoiesis. In this process, senescent erythrocytes are phagocytosed by macrophages of the reticuloendothelial system where the heme moiety is split from hemoglobin and catabolized enzymatically via HOX-1. Thereafter, iron is freed from the protoporphyrin ring and exported by ferroportin to rejoin circulation (131).

The iron deficiency anemia results from insufficient supply of iron for heme synthesis and, consequently, hemoglobin formation in developing erythroid cells. Erythrocytes appear smaller than normal (microcytic) and contain reduced amounts of hemoglobin (hypochromic). The prevalence of anemia caused by iron deficiency is about a billion people worldwide. Patients with chronic disease such as infectious, inflammatory, or neoplastic disorders suffer from anemia caused by iron-deficient erythropoiesis and resultant defect in the recycling of hemoglobin iron in the reticuloendothelial system (136).

1.2.2. Erythropoietic cytokine: EPO

The production of hematopoietic cells is tightly regulated by hematopoietic cytokine superfamily. Each cytokine has multiple actions controlling the survival, proliferation, differentiation and maturation of the hematopoietic cells. HSCs and early progenitors possess the receptor c-kit of a stem cell factor (SCF), which is a powerful stimulus for the proliferation of these cells (137,138). During hematopoiesis, CSF is needed to stimulate granulocyte and macrophage colony formation (139,140,141,142,143). Interleukin-5 is a major regulator of eosinophil production (144). Leukemia inhibitory factor was found to stimulate the megakaryocyte colony formation (145). Interleukin-11 was proved to stimulate

megakaryocytopoiesis (146). Thrombopoietin strongly induces the megakaryocyte colony formation (147).

As a member of the hematopoietic cytokine superfamily, EPO is known as the predominant regulator of erythropoiesis. EPO is a glycoprotein with a molecular weight of 34-kDa and was first identified as a humoral erythropoietic factor in the 1950's (148,149). This glycoprotein hormone is produced mainly in the fetal liver hepatocytes and a subset of peritubular, interstitial cells in the adult renal cortex. Additionally, early-stage erythroid progenitors and neural cells were also found to express EPO (150,151,152,153). Under normal circumstances, only a few of interstitial cells produce EPO. Conditions that need to increase oxygen delivery, such as the residence at high altitude, pulmonary disease that results in decreased uptake of oxygen, admixture of venous to arterial blood through a right to left shunt and decreased renal blood flow stimulate EPO production. The number of interstitial cells that produce EPO increases exponentially in response to low oxygen tension (154,155). Conversely, inflammatory cytokines decrease EPO production. This is the primary cause of anemia of chronic inflammatory disease and the anemia of cancer (156,157).

1.2.2.1. Regulation of EPO production by HIF

The *EPO* gene is predominantly regulated by hypoxia-inducible factor (HIF) family (158,159). HIF was first identified as heterodimer consisting of an oxygen labile α-subunit and a constitutive β-subunit. All HIF-subunits are members of the Per-ARNT-Sim family of proteins (160,161). HIF-1α has a ubiquitous expression in tissues, whereas HIF-2α is restricted to certain cells types. Little is known about HIF-3α. All isoforms of HIF-α can form heterodimers with the β-subunit of HIF(162,163).

HIF was identified to target genes such as *EPO* that is essential for the hypoxic response through acting as a transcriptional activator (164,165). Under hypoxic conditions, HIF-2 stimulates the expression of EPO through binding to the hypoxia-response element enhancer region of the *EPO* gene promotor (166,167,168). Many more target genes of HIF have been subsequently found such as VEGF, glucose uptake transporter-1, transferrin, transferrin receptor, plasminogen activator inhibitor-1, aldolase C, and endothelin (169).

In accordance with the effects of hypoxia on serum EPO, the DNA-binding activity of HIF-α was found to be tightly regulated by cellular oxygen tension. Primary regulator of HIF stability is prolyl hydroxylase domain (PHD) enzymes that initiate the degradation of HIF via the von Hippel-Lindau tumor suppressor protein (VHL), a protein with ubiquitous expression. VHL is acting as the recognition component of a multiprotein ubiquitin ligase complex. Site-specific prolyl hydroxylation of HIF-α allows VHL binding and targeting for ubiquitin-mediated proteasomal degradation. This process is considered as the fundamental oxygen-sensitive step underlying the degradation of HIF-α. Thus, prolyl hydroxylation is the key element regulating the oxygen-sensitive turnover of HIF-α (170).

A family of three prolyl hydroxylases, PHD1, PHD2 and PHD3 has been identified. The isoforms of PHD have the tissue-specific expression. PHD1 is particularly expressed in testis. PHD2 could be found in more tissues and PHD3 is expressed at high levels in heart and skeletal muscle (171,172). Moreover, PHD2 and PHD3 are more cytoplasmic, whereas PHD1 is generally confined to nuclei (173,174). PHDs were also found to be regulated by HIF-α activity during hypoxia because the genes of PHD2 and PHD3 are targeted by HIF following hypoxic stimulation. Thus, a putative feedback loop also exits in HIF regulation (175,176).

1.2.2.2. EPO/EPOR signaling

The receptor of EPO, EPOR, is expressed in erythroid progenitors but also by a number of other tissues including cardiovascular system, kidney, placenta, macrophage, retinal cells and brain (171). The EPOR expression is stimulated by SCF , interleukin-1α and inhibited by interferon-1γ, ionomycin and phorbol ester phorbol-12-myristate-13-acetate (172,177,178).

In erythropoietic cells, EPOR starts to appear on late CFU-Es and proerythroblasts (179). In the bone marrow, EPO acts upon erythroid progenitors in the stages from CFU-E to the earliest basophilic erythroblasts. These cells are EPO responsive cells. Progenitor cells at these stages are dependent on widely varying amounts of EPO to promote proliferation, differentiation, and survival of erythroid precursors (180,181,182). Upon EPO binding to its receptor, the receptor undergoes a conformational change that activates a prebound, cytoplasmic, tyrosine kinase, Janus kinase 2 (JAK2) (183,184,185,186,187). Subsequently,

JAK2 phosphorylates several cytoplasmic tyrosine residues in the cytoplasmic tail of the EPOR that act as docking sites for proteins that contain Src-homology 2 domains. Consequently, multiple pathways mediating the cell proliferation and survival are activated, including signal transducer and activator of transcription 5, PI-3K/AKT, and MAPK (186,187).

Abnormal signaling pathways of the EPO-receptor occur for human erythropoietic disorders (188,189). For example, the prototypical erythropoietic disease, polycythemia vera is caused by various mutations of JAK2 (190,191,192) or Bcl-xL expression, which result in EPO-independent erythroblast growth (193,194,195,196).

1.3. STRESS ERYTHROPOIESIS

During normal erythropoiesis, as seen in healthy subject at sea level, the production of red cells equals the removal of senescent erythrocytes. In response to certain physiological or pathological stimuli, the red cell production increases dramatically, a process named stress erythropoiesis. Stress erythropoiesis is essential to adapt the mammalian organism to conditions resulting in low tissue oxygen tension, including cardiac or pulmonary diseases, blood loss, etc. In mice, stress erythropoiesis occurs in adult spleen and liver and during fetal development in the fetal liver. Growing evidence has suggests that stress erythropoiesis is more than a process simply enhancing steady-state erythropoiesis but a process requiring distinct quantitative and qualitative changes of cytokine pattern to stimulate erythropoiesis from unique progenitor cells (197,198,199,200).

Conditions of reduced arterial oxygen content (hypoxia) result in increased EPO plasma levels as a consequence of stimulated synthesis and secretion from kidney cells. In parallel, EPOR expression is found on a broader progenitor spectrum as compared to basal erythropoiesis, enabling EPO to exert its effect also on early hematopoietic progenitors, such as HSCs additionally to the EPOR expression in steady status that is restricted to progenitors such as CFU-Es. Moreover, bone marrow progenitors migrate to the spleen and subsequently differentiate into stress BFU-E under the influence of Hedgehog signaling and bone morphogenetic protein 4 (201). Consequently, erythropoiesis is enhanced by 10-100 fold

increase in the number of BFU-E and CFU-E in mouse spleen (202,203,204,205). In contrast to bone marrow BFU-Es, cultured spleen BFU-Es have been identified to produce erythroid colonies when exposed to high EPO concentration without addition of SCF or interleukin-3 (206).

The link between steady-state erythropoiesis and stress erythropoiesis remains variable. The deficiency of GAS6 or conditional deletion of focal adhesion kinase has affected stress erythropoiesis rather than homeostasis (82,207,208). On the other hand, stress erythropoiesis in the splenic microenvironment can be successful in the mice with a deficiency of Rac1 and Rac2 GTPases although these mice suffer from pathologic erythropoiesis under steady state conditions (208).

1.4. SENESCENCE AND CLEARANCE OF RBC

Matured mammalian RBCs circulate as anucleate biconcave cell with concentrated hemoglobin solution packed within protein-stabilized lipid bilayers. In the circulation, RBC life span varies with species and little is known about what factors determine the inter species RBC life span. A consensus exists that the life and death of RBCs are well regulated despite their lack of ability for protein synthesis (209).

Experimental evidence suggests that there are various mechanisms underlying the senescence of RBCs. The life span of erythrocytes is influenced by many factors such as metabolic rate, oxidative stress etc. Oxidative damage is likely to be one of the most important cause of RBC senescence and the exposure of senescence-associated ligands phosphatidylserine on the RBC surface (210,211,212,213). The gradual increase of oxidative damage was generally believed to result in calcium-triggered apoptosis although RBCs lack a nucleus and mitochondria (214,215). Thus, this process was termed eryptosis (216,217). In human, erythrocytes have a lifespan of 120 days and the senescent RBCs are removed from circulations mainly by the Kupffer cells in the liver. In other species, most notably rat and mouse, phagocytosis may also occur in spleen (209,218, 233).

1.4.1. Recognition of senescent erythrocytes

Recognition of senescent red cells by macrophages is the key mechanism in the removal of erythrocytes from the circulation. Phagocytosis of senescent erythrocytes by macrophages is believed to be a highly regulated process balanced between signaling through prophagocytic receptors and inhibitory receptors (214,215). Several molecular alterations on the surface of senescent RBCs had been found to serve as ligands to be recognized by macrophages. These alterations include modifications in protein carbohydrate moieties (219), loss of plasma membrane phospholipid asymmetry (210,211,220), and/or clustering of band 3 with subsequent binding of complement or antibodies (221). The recognition could be direct or through bridging proteins that may interact with RBC ligands (222,223,224,225,226,227). Following ligation of receptors such as Fcγ receptors, complement receptors, or scavenger receptors, phagocytosis by macrophages is induced (228,229,230).

1.4.1.1. Autologous immunoglobulin G (IgG)

In physiological circumstances, after the initial phase of reticulocyte maturation, erythrocytes gradually lose cell volume and hemoglobin, accompanied by an increase in cell density prior to being removed by macrophage. The removal of these senescent erythrocytes could be initiated by binding of autologous IgG. In physiological conditions, this is an efficient process since relatively small numbers (100-500 molecules IgG/cell) of these autoantibodies are sufficient to trigger phagocytosis and significant IgG binding does not occur until the last phase of erythrocyte life span (231,232). However, characterization of this IgG has not led to an unambiguous view (234).

Many in vitro and in vivo data had shown that binding of denatured hemoglobin to cytoplasmic domains of band 3 causes its oligomerization, which results in the formation of neoantigens that are recognized by specific IgGs (231,234). Band 3 is the Cl^-/bicarbonate anion exchanger and also the main integral membrane protein. The C-terminal part of the protein is an integral membrane domain that facilitates the transport of CO_2 through the body by the exchange of Cl^- and HCO_3^- across the erythrocyte membrane (243). The N-terminal

cytoplasmic domain of band 3 provides the main anchorage site for the cytoskeleton to the lipid bilayer through ankyrin-mediated binding of the spectrin-actin network. In addition, the cytoplasmic domain has a high affinity for deoxyhemoglobin (244). The band 3 functions were found to change with aging, such as a decrease in sulphate transport capacity, changes in the binding characteristics of ankyrin and the binding of glyceraldehyde 3-phosphate dehydrogenase (GAPDH), a key enzyme of glycolysis. The association of band 3 and GAPDH inhibits its activity and thereby the rate of ATP production (245,246). Also, deoxyhemoglobin and especially denatured hemoglobin (hemichromes) has a high affinity for the cytoplasmic domain of band 3. Thus, band 3 is an important factor in the regulation of erythrocyte structure and function during aging (232).

Aging-associated breakdown of band 3 is indicated by immunoblot data obtained with antisera reactive with both the membrane domain and the cytoplasmic domain (214,245). This is also supported by the functional data showing the aging-related decrease in anion transport capacity (232). Band 3 clustering may be induced by binding of denatured hemoglobin in senescent erythrocytes, which causes subsequent IgG binding. However, whether the crucial changes resulting in senescent red cell antigen activity are caused by band 3 degradation, cross-linking remain to be described (221,245).

1.4.1.2. CD 47

CD47, also known as integrin-associated membrane protein, is a 47-52 kDa transmembrane glycoprotein expressed ubiquitously in human tissues including erythrocytes (236,237). The ligation of CD 47 with its natural ligand thrombospondin-1 induces programmed cell death in nucleated blood cells (238). The remodeling of cytoskeleton and the exposure of phosphatidylserine at the outer leaflet of the membrane are the common characteristics of this death pathway (239). CD47 has been identified as a molecule that may also be involved in recognition of senescent erythrocytes by macrophages (235). The expression level of CD47 was speculated to be a mechanism controlling the elimination of senescent red cells. In vivo, CD47 deficient RBCs are cleared rapidly from the bloodstream when transfused to normal mice. In vitro, binding of anti-CD47 antibody to normal mouse

RBCs was found to enhanced phagocytosis (240). Thus macrophages must have specific receptors capable of recognizing normal RBCs expressing CD47, which initiates signaling cascades to inhibit macrophage activation and phagocytosis. Experimentally, CD47 on normal RBC can bind to and activate signal regulatory proteinα (SIRPα) that makes CD47 be a "marker of self" by signaling through SIRPα against phagocytosis by macrophages. However, erythrocytes from animals heterozygous for CD 47 survived normally in wild-type mice, which argue against a gradual disappearance of CD47 as the sole mechanism that regulates erythrocyte survival. It is more likely that the absence of CD47 triggers other processes that lead to erythrocyte removal (235).

1.4.1.3. Phosphatidylserine exposure

Exposure of phosphatidylserine at the surface of erythrocytes is another trigger for the removal of senescent erythrocytes. In erythrocyte pathologies such as sickle cell anemia, thalassemia and spherocytosis, the decreased erythrocyte survival is associated with an increase in phosphatidylserine exposure (240,241). It is speculated the decrease in phospholipid asymmetry might be a normal consequence of physiological aging at the level of the membrane. Exposure of phosphatidylserine in conjunction with other signals could result in recognition and removal of senescent erythrocytes by phagocytes (242).

1.4.2. Vesiculation during erythrocyte aging

During aging, erythrocyte volume decreases by 30%, with 20% hemoglobin loss, resulting in an increased intracellular hemoglobin concentration (244). In parallel, the surface area and lipid content, mainly cholesterol and phospholipid, decrease as well, implying an irreversible loss of membrane and cell content by the formation of vesicles (247). These changes result in the increased osmotic fragility and reduced deformability of erythrocytes, despite an increase in the surface-to-volume ratio (248). A portion of these vesicles possess IgG at their surface and exposes phosphatidylserine, similar to the senescent erythrocyte. It was also found that band 3 is the major membrane protein of vesicles and the hemoglobin

composition of these vesicles resembles that of the oldest erythrocyte (249,250,251). Vesicles disappear rapidly, generally within minutes from the circulation in a rat model. The scavengers are mainly Kupffer cells through recognizing of phosphatidylserine exposed by the vesicles (247,251).

The vesicles are formed throughout the whole erythrocyte life span but the mechanisms by which they are generated are poorly understood. It has been proposed, that during the early life of the erythrocyte, protein modifications such as oxidation, glycation, carbamylation, nitrosylation or ubiquitinylation already occur (252). In this process, both band 3 and hemoglobin could be affected. On one hand, the modification of hemoglobin may result in the binding of denatured hemoglobin to the cytoplasmic domain of band 3 and subsequent breakdown of the band 3 membrane domains. In turn, this disturbs the organization of the cell membrane by loss of lipid anchorage and affects the mobility of lipids in successive layers (253,254), which could lead to vesicle formation whereas the cytoskeleton remains intact. In vivo, this has been indicated in the erythrocytes of band 3 knockout animals (255,256). On the other hand, band 3 breakdown could be caused by calcium activated proteases (257,258). Subsequently, hemoglobin binds to band 3 breakdown products. The band 3 fragments, could either be driven by aggregation of the associated hemichromes, or be excluded from the functional complex. Either will cause lateral diffusion and subsequent aggregation of band 3 breakdown products. Eventually, this process increases erythrocyte membrane curvature and induces vesiculation (259).

Concluded from the above, the vesicle formation caused by the presence of band 3 breakdown products explains the loss of both cell volume and hemoglobin content (232,244). The vesicles displayed the signal for the removal similar to aged erythrocytes (253,254). In erythrocytes, non-functional or toxic compound and bad membrane patches are eliminated by this way. At the end of erythrocyte life, the vesicle formation system appeared to be overburdened and due to the increasing accumulation of toxin that resulted from dysfunction cellular defense, the removal of the whole erythrocyte occurs (250).

1.5. RESEARCH PROJECT

1.5.1. Background

In homeostasis, erythrocytes are constantly renewed to ensure proper tissue oxygenation (158). In hematopoietic organs, EPO starts to exert its effect on erythroblasts at CFU-E stage (179,205). The red cell output can increase dramatically under stress erythropoiesis induced by decreased tissue oxygenation. In general, this is accompanied by an elevation of EPO plasma levels (168). It is known that the EI is the niche for erythropoiesis in both steady and stress state. The macrophage/erythroblast and erythroblast/erythroblast interactions are essential for survival and differentiation of erythroblasts. A diverse array of adhesion molecules has been characterized to mediate these cellular interactions, among which the importance of integrins has been established. The α4β1 integrin complex in erythroblasts was found to contribute to the erythroblast/macrophage interaction by binding to its counter receptor VCAM-1 on the central macrophage within islands (49). Most recently, macrophage αv integrin and erythroblast ICAM-4 had been identified to participate in island formation as well (50,51).

Integrin is a subfamily of heterodimeric transmembrane proteins composed of α and β subunits. Both subunits are type 1 membrane proteins, have large extracellular ectodomains and short cytoplasmic tails (260). In mammals, there are at least 18 α subunits and 9 β subunits, assembling into at least 24 distinct integrins. Integrin α and β subunits are totally structurally different, with no detectable homology between them. Whereas sequence identity among α subunits is about 30% and among β subunits it is 45% (261).

Integrins are expressed by a variety of cell types and tissues, e.g. αIIbβ3 on platelets, α6β4 on keratinocyts, αEβ7 on T cells, dendritic cells and mast cells in mucosal tissues,α4β1 on leukocytes, α4β7 on a subset of memory T cells, the β2 integrin family on leukocytes and αvβ3 on endothelial cells (262). Ligands for these integrin receptors are mainly extracellular matrix and cell-surface proteins. Some integrins possess the Arginine-Glycine-Aspartic acids binding site, which allows integrins to bind to extracellular matrix proteins such as laminins and fibronectin (263). Upon binding the extracellular ligands, integrins undergo a series of

conformational changes, generating intracellular signals that trigger many events such as gene expression, adhesion, differentiation and proliferation, as well as survival or death. Deletion of integrin subunits in mice causes defects in many processes including development, vasculogenesis, lymphangiogenesis, thrombus formation, etc. Some integrin antagonists have been employed as therapeutic drugs to target on interaction of integrins with their ligands. Abciximab, a humanized anti-β3 antibody that blocks the binding of platelet integrin αIIbβ3 to fibrinogen has been implied to prevent thrombosis clinically (264).

The β3 subfamily of integrins comprises αVβ3 and αIIbβ3 (260). αvβ3 consists of a 125 kDa αv subunit and a 105 kDa β3 subunits. The expression of αvβ3 could be found on many cell types, including platelets, macrophages, osteoclasts, fibroblasts, some metastatic melanomas and endothelial cells (265,266,267,268). αvβ3 was found to recognize a wide range of ligands, such as vitronectin, fibronectin, fibrinogen, osteopontin, that make it play important roles in several distinct processes, particularly osteoclast mediated bone resorption, angiogenesis and pathological neovascularisation, and tumor metastasis (269,270,271,272, 273). It was reported that knockout of the gene for β3 enhanced tumorigenesis, angiogenesis, wound healing, inflammation and atherosclerosis (274,275,276,277).

αIIbβ3 is expressed on platelets and megakaryocytes that make it essential for platelet aggregation (278). Upon stimulation, platelet surface αIIbβ3 will bind to fibrinogen and von Willebrand factor to form platelet aggregates. It was proposed that mice deficient of integrin β3 could be used as the animal model of the human bleeding disorder, Glanzmann thrombasthenia, resulting from defects in the genes for either the αIIb or the β3 subunit. It was also reported that occasionally placental defects occur in integrin β3 lacking mice leading to fetal mortality (278). Postnatally these mice suffer from hemorrhage that results in anemia and reduced life expectancy. In these animals, extramedullary erythropoiesis is stimulated and reticulocytes are presented in the peripheral blood (279).

Previously, the characteristics of transgenic mice with very high expression of human EPO (tg6) have been investigated. Tg6 exhibited increased red blood cells with a hematocrit levels as high as 0.9 (280). Plasma nitric oxide levels (280) and erythrocyte flexibility were altered as well (281). Moreover, in tg6 mice, erythrocyte turnover is increased. In line with

this, erythrocyte population in tg6 mice harbors characteristics of accelerated aging, such as increased band 4.1a to 4.1b ratio, signs of oxidative stress, or decreased surface CD47 and sialic acids. In vivo tracking of erythrocytes also revealed dramatically increased engulfment by their liver macrophages (282).

1.5.2. Objectives

The present study aimed to investigate the pathological characteristics of stress erythropoiesis in integrin β3 knockout mice in comparison to EPO overexpression mice and thus to delineate the role of integrin β3 in the formation and stabilization of EI. Specifically, it was investigated whether the absence of integrin β3 disturbs the adhesion of erythroblasts to the central macrophage, resulting in premature red cells from EIs into the circulation.

CHAPTER 2. OWN RESEARCH

PREFACE

This chapter contains a manuscript describing the results of the research project "Decreased stability of erythroblastic islands in integrin β3 deficient mice" under the supervision of Prof. Dr. med. Johannes Vogel. This manuscript was submitted for publication.

Decreased stability of erythropoietic islands in integrin β3 deficient mice

Zhenghui Wang[1], Olga Vogel[1], Gisela Kuhn[2], Max Gassmann[1,3], Johannes Vogel[1]

[1]Institute of Veterinary Physiology, Vetsuisse Faculty University of Zürich and Zürich Center for Integrative Human Physiology (ZIHP),
[2]Institute for Biomechanics, Swiss Federal Institute of Technology, Zürich, Switzerland
[3]Universidad Peruana Cayefano Heridia (UPCH), Lima, Peru

Running head: integrin β3 and erythropoietic islands

Abstract Word / Character (including spaces) counts: 200 / 1488

Address correspondence and reprint requests to:
Johannes Vogel
Institute of Veterinary Physiology
Vetsuisse Faculty University of Zürich
Winterthurerstr. 260
CH-8057 Zürich
Switzerland
Tel.: +41 44 6358806
Fax: +41 44 6358932
E-mail:jvogel@vetphys.uzh.ch

Summary

Erythroblasts proliferate and differentiate in hematopoietic organs within erythropoietic islands (EI) composed of erythropoietic progenitor cells attached to a central macrophage. This cellular interaction crucially involves the erythroid intercellular adhesion molecule-4 (ICAM-4) and αv integrin. Because integrins are biologically active as α/β heterodimers we asked whether β3 could be a heterodimerization partner of αv integrin in EIs. To this end we compared stress erythropoiesis of integrin β3 deficient ($\beta3^{-/-}$) mice that exhibit impaired hemostasis due to platelet dysfunction with that of systemically erythropoietin-overexpressing (tg6) mice. Despite having much less erythropoietic stimulation compared to tg6 mice, peripheral blood of $\beta3^{-/-}$ mice contained more erythrocytes of a lower maturity stage. Unexpectedly, membranes of peripheral erythrocytes from $\beta3^{-/-}$ mice contained calnexin, a chaperone that is normally completely lost during terminal differentiation of reticulocytes prior to their release into the circulation. In contrast to erythropoietin-overexpressing mice, the erythropoietic subpopulations representing orthochromatic erythroblasts and premature reticulocytes as well as the number of cells per EI were reduced in $\beta3^{-/-}$ bone marrow. In conclusion, absence of integrin β3 impairs adhesion of the latest erythroid developmental stage to the central macrophage of EIs resulting in preterm release of abnormally immature erythrocytes into the circulation.

Keywords

Stress erythropoiesis, bone marrow niche, erythroblastic island, erythroblast differentiation, integrins, chaperone, calnexin

Abbreviations

Epo: erythropoietin**; HIF-1**: hypoxia-inducible factor-1; **EI**: erythropoietic island; **PS**: phosphtidylserine; **Emp**: erythroblast marophage protein; **VCAM-1**: vascular cell adhesion molecule-1; **ICAM-4**: intercellular adhesion molecule-4

Introduction

Proliferating and differentiating erythroblasts require a specialized microenvironment termed erythroblastic island (EI) (Allen and Dexter 1982, Hanspal and Hanspal 1994, Mohandas and Prenant 1978), normally (for review see e.g. (An and Mohandas 2011, Manwani and Bieker 2008, Mohandas and Chasis 2010)) composed of a F4/80 expressing central macrophage surrounded by about 5-30 cells from nucleated proerythroblasts through multilobulated reticulocytes (Lee*, et al* 1988). During differentiation orthochromatic erythroblasts extrude their nucleus that is subsequently engulfed by the central macrophage, a mechanism crucially requiring macrophage – erythroblast interactions (Mohandas and Chasis 2010). Moreover, this interaction enhances proliferation of erythroblasts by speeding up the G0/G1 phase to complete more cell divisions per time unit and, thus, generating more reticulocytes (Hanspal and Hanspal 1994). In addition, erythroblast – erythroblast interactions regulate survival of erythroblasts through Fas – FasL interaction (Liu*, et al* 2006). In man the direct contact between erythroblasts is also essential for homotypic signaling between erythroblasts within the EI niche as a mechanism for regulating GATA-1 activity to complete terminal differentiation (De Maria*, et al* 1999).

The above-mentioned interactions are mediated by a diverse array of adhesion molecules. Erythroblast macrophage protein (Emp) was the first molecule described to be involved in the attachment of erythroblasts to the central macrophage and to neighboring erythroblasts (Hanspal and Hanspal 1994). Subsequently α4β1 integrin in erythroblasts and vascular cell adhesion molecule 1 (VCAM-1) in central macrophages (Sadahira*, et al* 1995) and erythroid intercellular adhesion molecule-4 (ICAM-4, also known as the

Landsteiner and Weiner (LW) blood group glycoprotein (Bailly, *et al* 1994)) as well as macrophage αv integrin was found to contribute to the erythroblast – macrophage interactions (Lee, *et al* 2006).

Since it has been shown that αIIbβ3 and αvβ3 integrins can interact with ICAM-4 on red blood cells (RBCs) (Hermand, *et al* 2004, Hermand, *et al* 2003), the present study aimed to compare characteristics of stress erythropoiesis in integrin β3 deficient mice with that of Epo overexpressing mice (tg6). Integrin β3 deficient mice resemble human Glanzmann thrombasthenia characterized by mild gastrointestinal and cutaneous hemorrhage due to impaired platelet aggregation (Hodivala-Dilke, *et al* 1999). Tg6 mice have independent of oxygen tension about 10-times elevated Epo plasma levels resulting in hematocrit values of 0.8-0.9 (Ruschitzka, *et al* 2000). Despite having less stimulated erythropoiesis than tg6 mice, peripheral blood of β3 deficient mice contained RBCs of a lower maturation stage. Surprisingly, erythrocytes from $\beta3^{-/-}$, but not from tg6 mice, contained calnexin, an endoplasmatic reticulum glycoprotein chaperone that is normally completely lost during terminal RBC differentiation (Patterson, *et al* 2009). Moreover, the erythropoietic subpopulation representing orthochromatic erythroblasts and premature reticulocytes as well as the number of cells per EI was reduced in $\beta3^{-/-}$ bone marrow. These findings suggest that β3 integrin could be involved in attachment of late developmental stages of RBCs to the EI.

Materials and Methods

Animals. Mice aged between 4 and 6 months were used and genotyped as described (Hodivala-Dilke*, et al* 1999, Ruschitzka*, et al* 2000). All experiments conformed governmental and institutional guidelines.

Analysis of peripheral blood. Hematological parameters were determined with standard techniques. Plasma erythropoietin concentrations were measured with EPO-Trac^{Tm} ^{125}I RIA kit (DiaSorin) and RBC osmotic fragility, flexibility and life-span as described (Bogdanova*, et al* 2007, Vogel*, et al* 2003). RBC membrane proteins analysis (Bogdanova*, et al* 2007) revealed for ß3$^{-/-}$ mice an additional band that was analyzed by mass spectrometry (Functional Genomics Center Zürich). Optical density ratios between bands 4.1a and 4.1b and the extra band and band 4.2 were determined as described (Gassmann*, et al* 2009). RBCs were also analyzed flowcytometrically (cf. below) for Annexin V-FITC binding (apoptosis detection kit, PromoKine), reticulocyte number (Retic-COUNT, BD Biosciences), remnants of endoplasmatic reticulum (ER-tracker®, Invitrogen) in reticulocytes (Retic-COUNT positive red cells) and CD71 and CD44 expression.

Fluorescence-Activated cell Sorting (FACS) and flow cytometry of hematopoietic tissues. Bone marrow and spleen single-cell suspensions were immunostained for Ter119, CD71, and CD44 and CD47 (all from BD Biosciences) after blocking cellular Fc receptors with 5% rat serum and analyzed using a flow cytometer (FACSCalibur or Gallios, Becton Dickinson) and the Winmdi or Kaluza software. Hematopoietic cells

labeled with CD44 and TER119 antibodies were also sorted (Aria III, 5L, Becton Dickinson), transferred onto slides and staining with May-Grunwald solution.

Histological analysis of hematopoietic tissues. Perfusion fixed (4% parformaldehyde, PBS) and decalcified bone and spleen sections were stained with Prussian blue, Hematoxylin and eosin or, after auto-fluorescence quenching (Schnell*, et al* 1999), with FITC-labeled anti mouse F4/80 (Abcam) and PE-labeled anti mouse Ter119 antibodies and 4′,6-Diamidino-2-phenylindole dihydrochloride (DAPI, Sigma) to identify EIs in bone marrow. EI density and Ter119 positive cells per EI were determined (cf. legend to fig. 5A) in 10 randomly selected, non-overlapping fields of bone marrow sections per mouse.

Other bone marrow sections were immunostained for fibronectin (rabbit anti-human fibronectin, ICN/Cappel; goat anti-rabbit IgG, DyLight 649 labeled, Jackson ImmunoResearch Lab.), coverslipped using a moviol-based (Calbiochem) embedding medium (Osborn and Weber 1982) containing 1,4-Diazobicyclo-[2.2.2]-Octan (Sigma) and hardened over night. After image acquisition (HPX 120 C, Axioimager.Z2, Axiocam HRm CCD camera, Axiovision software version 4.5, Zeiss) average optical density levels (oDL) of single bone marrow vessels were determined (MCID Analysis 7.0) by taking into account only pixels exceeding an oDL of 45 (20% above average background value) and excluding elements with a size below 10 pixels (cf. supplemental fig. 7B).

Analysis of bone structure. Cortical and trabecular microarchitecture of femurs was assessed by micro-computed tomography (MicroCT40 (Scanco Medical) scanner as described (Hildebrand*, et al* 1999, Hildebrand and Ruegsegger 1997, Kohler*, et al* 2007).

Statistics. Results are expressed as means ±SEM. Statistical significances were assessed using a 2-tailed Student t-test for unpaired samples with Bonferroni correction and labeled as * = $p<0.05$, ** = $p< 0.01$ or *** = $p<0.001$ when compared to the respective wt controls or as # = $p<0.05$, ## = $p< 0.01$ or ### = $p<0.001$ for comparison between $\beta3^{-/-}$ and tg6 mice.

Results

Erythropoiesis is mildly stimulated in integrin $\beta3^{-/-}$ mice. In line with our previous reports (Bogdanova*, et al* 2007, Ruschitzka*, et al* 2000, Vogel*, et al* 2003), average hematocrit of the tg6 mice used here was 0.83 whereas it was 12% lower in $\beta3^{-/-}$ but not $\beta3^{+/-}$ mice compared to wt littermates. (fig. 1A). Accordingly in four mice of each genotype, hemoglobin concentration (g/dl: wt: 16.05 ±0.15; $\beta3^{-/-}$: 12 ±0.7, $p < 0.05$) and red cell count ($*10^6/\mu l$: wt: 10.82 ±0.37; $\beta3^{-/-}$: 7.7 ±0.89, $p < 0.01$) was reduced in $\beta3^{-/-}$ mice. Erythrocyte parameters such as MCH (pg: 15 ±0.01; $\beta3^{-/-}$: 16 ±0.02, ns) and MCHC (g/dl: wt: 34 ±0.03; $\beta3^{-/-}$: 32 ±1, ns) were unchanged suggesting normal hemoglobin synthesis. RBC volume was increased in $\beta3^{-/-}$ mice (MCV (fL): wt: 44 ±1; $\beta3^{-/-}$: 49 ±2, $p < 0.05$) with a slightly higher scatter in $\beta3^{-/-}$ mice (RDW: wt: 20.9 ±0.7; $\beta3^{-/-}$: 21.3 ±1.1, ns).

The 1.5-fold and 5.5-fold splenic enlargement in $\beta3^{-/-}$ and tg6 mice, respectively, indicates stimulated extramedullary erythropoiesis that is, however, much stronger in the Epo-overexpressing mice (fig. 1B). Accordingly, plasma Epo levels were unaltered in $\beta3^{-/-}$ ($\beta3^{-/-}$: 20.49 ±1.45 U/L; wt: 20.35 ±0.85 U/L respectively, n = 10). Flow cytometric erythrocyte size determination and peripheral blood smears did not reveal morphological alterations in $\beta3^{-/-}$ mice (supplemental figs. 1A and 3). Prussian blue staining of bone marrow and spleen sections did not indicate altered iron storage in $\beta3^{-/-}$ mice (supplemental fig. 1B).

Red cell survival is normal in integrin $\beta3^{-/-}$ mice. In wt mice RBC half-life was within literature values (Manodori and Kuypers 2002), namely 21.6 ±0.67 days (n = 8). In integrin $\beta3^{-/-}$ mice half-life was slightly (17.9 ±2.96 days (n = 5)) but not significantly (p = 0.29) lower, maybe because of the higher data scatter in $\beta3^{-/-}$ mice compared to their wt littermates (coefficient of variation 36.93% vs. 8.99%). This just marginally reduced red cell survival together with limited splenomegaly and unaltered plasma Epo levels suggest mild erythropoietic stimulation in $\beta3^{-/-}$ mice.

Mechanical properties of erythrocytes from integrin $\beta3^{-/-}$ mice are normal. Mechanical properties of erythrocytes are age-dependent with young cells being more flexible and resistant to osmotic stress. Erythrocytes of tg6 mice were reported to be more flexible and having a higher osmotic resistance (Bogdanova*, et al* 2007, Vogel*, et al* 2003). Compared to wt littermates, $\beta3^{-/-}$ mice showed a trend towards increased erythrocyte flexibility at higher shear forces (supplemental fig. 2A) but unchanged

osmotic resistance (50% lysis of RBCs: wt: 0.5581%, $\beta3^{-/-}$: 0.5545%, supplemental fig. 2B).

Peripheral erythrocytes of integrin $\beta3^{-/-}$ mice show a higher degree of immaturity than those of tg6 mice. Compared to wt, reticulocyte counts were significantly and, more surprisingly, similarly increased in $\beta3^{-/-}$ and tg6 mice. Maturity of the peripheral red cells was therefore assessed by additional measurements (figs. 2 & 3).

The skewness of the intensity distribution directly impacts the geometric mean (cf. fig. 2B) that can be used to estimate reticulocyte age distribution (Wiczling and Krzyzanski 2007, Wiczling and Krzyzanski 2008). Average fluorescence intensity of Retic-COUNT® stained reticulocytes from $\beta3^{-/-}$ was significantly higher than of those of their wt littermates whereas tg6 reticulocytes had the same staining intensity as control mice. Accordingly, Brilliant-Kresyl blue stained blood smears revealed more chromatin in $\beta3^{-/-}$ than in wt or tg6 reticulocytes (supplemental fig. 3). Using flow cytometry, expression of the transferrin receptor CD71 was assessed because this protein diminishes with erythroblast maturation (Kina*, et al* 2000). Compared to wt controls a similar and significant increase in cells positive for CD71, was observed in $\beta3^{-/-}$ and tg6 mice. Next, we examined on RBCs expression of the adhesion molecule CD44 that might be more specific for late erythropoietic developmental stages (Chen*, et al* 2009). Compared to wt littermates as well as to tg6 mice $\beta3^{-/-}$ mice had significantly more CD44 positive RBCs. In contrast, RBCs of tg6 mice showed the same CD44 expression as their wt controls. Another sign of immaturity are remnants of the endoplasmatic reticulum (ER) that were considerably (+50%) more increased in $\beta3^{-/-}$ than in tg6 RBCs. Red cell aging, next to

other stresses, results in phosphatidylserine exposure. As reported previously (Foller, *et al* 2007) tg6 erythrocytes bound significantly more Annexin V whereas $\beta3^{-/-}$ RBCs showed unaltered Annexin V binding (fig. 2A). Tg6 erythrocytes express less CD47 (Bogdanova, *et al* 2007), a marker that declines with RBC aging (Oldenborg, *et al* 2000). In contrast to tg6 RBCs, $\beta3^{-/-}$ red cells displayed increased CD47 expression by about 42% compared to their wt littermates (fig. 2B).

Next, we determined the band 4.1a / 4.1b ratio of RBC ghost proteins that increases with RBC aging (Inaba and Maede 1988). Figure 3A shows examples of silver stained SDS-polyacrylamide gel electrophoresis (SDS-PAGE). For both wt strains used the band 4.1a / 4.1b ratio was within the values reported previously for mice (Bogdanova, *et al* 2007, Inaba and Maede 1988). In line with our previous work the band 4.1a /4.1b ratio was increased in tg6 mice compared to their wt controls (fig. 3B), which had been interpreted as accelerated aging of the transgenic RBCs (Bogdanova, *et al* 2007). In contrast, in $\beta3^{-/-}$ mice the band 4.1a /4.1b ratio was dramatically reduced by about 75% suggesting a reduced average age of peripheral $\beta3^{-/-}$ RBCs.

Interestingly, silver-stained SDS-PAGE of RBC membrane extracts from $\beta3^{-/-}$ mice showed an extra band at around 90kD (fig. 3A), which was identified as calnexin with minor contamination with other proteins most likely from platelets (cf. supplemental fig. 4). Calnexin, an endoplasmatic reticulum glycoprotein chaperone, is normally completely lost before reticulocytes are released into the circulation (Patterson, *et al* 2009) was absent in tg6 RBC membrane preparations (fig. 3A & 3C) implying even abnormal immaturity of the peripheral RBCs from $\beta3^{-/-}$ mice. These data suggest a reduced stability of the erythropoietic niche in β3 deficient mice.

The latest erythroid developmental stage is reduced in bone marrow of $\beta3^{-/-}$ mice. Using the flow cytometric assay developed by Liu et al. (Liu, *et al* 2006), we next examined the erythroblast differentiation stages in hematopoietic tissues. Based on Ter119 and CD71 expression, bone marrow and spleen cells were classified as proerythroblast (ProE) and cells expressing high levels of Ter119 (cf. supplemental fig. 5).

Splenic erythroblasts (Ter119 positive cells) were significantly increased in both genetically modified mouse lines (n = 8, all in %: $\beta3^{+/+}$: 10.7 ±2.56; $\beta3^{-/-}$: 28.6 ±4.85, $p<0.01$ vs. $\beta3^{+/+}$; BL6: 7.2 ±2.65; tg6: 66.7 ±2.74, $p<0.001$ vs. BL6) but not in bone marrow (n = 8, all in %: $\beta3^{+/+}$: 34.8 ±2.31; $\beta3^{-/-}$: 42 ±3.86; BL6: 49.2 ±2.16; tg6: 50.5 ±2.11). The proportion of the different erythroblast subsets Ery.A, Ery.B and Ery.C in bone marrow was clearly different between $\beta3^{-/-}$ and tg6 mice. Whereas compared to their respective wt controls the percentage of ProE and Ery.A was similar in $\beta3^{-/-}$ and tg6 mice, the percentage of Ery.B was increased in $\beta3^{-/-}$ but lower in tg6 mice. Conversely, the percentage of the most mature erythroblast subset Ery.C that represents orthochromatic erythroblasts as well as premature reticulocytes (Liu, *et al* 2006) was reduced in $\beta3^{-/-}$ but increased in tg6 mice (fig. 4A). This finding is in line with more immature peripheral red blood cells we found in $\beta3^{-/-}$ mice. Interestingly, the high increase of Ery.C in tg6 mice compared to their wt controls might suggest delayed RBCs release from the bone marrow, which fits to our previous report that tg6 RBCs share features of young and aged erythrocytes (Bogdanova, *et al* 2007). In the spleen of tg6 mice the increase of ProE was

much more pronounced compared to $\beta3^{-/-}$ mice (11-fold vs. 4.8-fold) but no other differences between both mouse lines were found in this organ (fig. 4B).

A study using cultured splenic proerythroblasts and bone marrow cells obtained from mice infected with the anemia-inducing strain of Friend leukemia virus (FVA) suggests that later erythropoietic developmental stages may resolve better when stained with antibodies against CD44 (Chen*, et al* 2009). Therefore, we also analyzed the expression of CD44 on bone marrow and spleen cells of our mice. Compared to Chen et al. (Chen*, et al* 2009) our flow-cytometrically obtained pattern looked differently. Consequently, we sorted the cells and identified their morphology after May-Grunwald staining (cf. supplemental fig. 6). In CD44 and TER119 stained mouse bone marrow cells four erythropoietic subopulations could be distinguished. Subpopulation I corresponded to ProE and Ery.A, II to EryA, III to some EryB and mainly Ery.C as defined by Liu et al. (Liu*, et al* 2006) and IV mainly to reticulocytes but also some erythrocytes similar to the definition from Chen et al. (Chen*, et al* 2009). In spleen cells however subpopulations I and II could not be separated reliably. Whereas the proportion of splenic erythropoietic stages in spleens of $\beta3^{-/-}$ and tg6 mice was similarly altered compared to their respective wt control (fig. 4D), clear differences were found in the bone marrow. As for CD71 the most striking differences between both genetically modified mouse lines were found in the last erythroid stage (IV, fig. 4C). Compared to their non-transgenic littermates the fraction of population IV was reduced to about 40% in $\beta3^{-/-}$ mice whereas in tg6 mice in was increased by about 30%. Moreover subpopulation III was increased in $\beta3^{-/-}$ mice but reduced in tg6 mice although this did not reach the level of statistical significance (fig. 4C). Note that erythropoietic stimulation resulted in an inversion of the ratio between

subpopulation III (or Ery.B) and IV (or Ery.C) only in $\beta3^{-/-}$ but not in tg6 (cf. fig. 4A & C and also supplemental fig. 6).

$\beta3^{-/-}$ EIs contain less erythroblasts. Our above-mentioned flow-cytometric data prompted us to next visualize bone marrow EIs with ani-F4/80 and anti-Ter119 antibodies (fig 5A). Compared to respective wt controls, EI density in femur marrow was unchanged in $\beta3^{-/-}$ mice but significantly increased in tg6 mice. However, significantly less (-30%) erythroblasts per island were observed in $\beta3^{-/-}$ whereas in tg6 mice it was comparable to wt controls (fig. 5B).

Fibronectin immunoreactivity of bone marrow is increased in $\beta3^{-/-}$ and decreased in tg6 mice. Quantitative immunofluorescence of fibronectin staining in the bone marrow revealed quite stable measurements. Compared to their respective wt controls vessel-associated fibronectin staining intensity was significantly increased in $\beta3^{-/-}$ mice but decreased in tg6 mice (fig. 6, supplemental fig. 7).

Three dimensional bone structure of $\beta3^{-/-}$ mice is not altered. Epo induces indirectly trabecular bone loss (Singbrant*, et al* 2011) to free marrow space for erythroid cell expansion. Mice lacking β3 were reported non-quantitatively to have more but dysfunctional osteoclasts resulting in increased cortical and trabecular bone mass (McHugh*, et al* 2000). In contrast, we quantified the three-dimensional structure of the femurs using micro-computed tomography imaging (Hildebrand*, et al* 1999). Using this technique we did not observe significant changes in the cortical bone in none of our mice.

However, trabecula of tg6 bones showed reduced numbers, increased spacing but unaltered thickness (supplemental fig. 8B). In contrast, $\beta3^{-/-}$ mice displayed a slight non-significant trend towards reduced trabecular spacing and increased trabecular number in line with McHugh et al. (McHugh*, et al* 2000). Hematoxylin and eosin stained bone sections showed no obvious differences regarding the trabecular or cortical bone structure in $\beta3^{-/-}$ mice (supplemental fig. 8C).

Discussion

Despite having only mildly stimulated erythropoiesis (unaltered plasma Epo values, unchanged EI density in bone marrow, minor splenic enlargement, normal RBC life-span) integrin β3 deficient mice exhibit peripheral RBCs of a lower maturity grade (more intense RNA staining in reticulocytes, increased CD44 and CD47 expression, increased band 4.1a / 4.1b ratio) in comparison to tg6 mice with maximally stimulated erythropoiesis. Of note, $\beta3^{-/-}$ mice retain calnexin in their peripheral erythrocytes indicating even abnormal immaturity. Moreover, in bone marrow from β3 deficient but not erythropoietin overexpressing mice the late stage erythroblasts are reduced. Together with the finding of reduced numbers of erythroblasts per EI in β3 deficient mice these observations suggest that integrin β3 might play a role in the stabilization of the erythopoietic islands, most likely during the late maturation stage just before reticulocyte release.

Central macrophages of EIs express αv integrin and erythroid ICAM-4 (LW glycoprotein) that is critical for EI formation (Lee*, et al* 2006). However, integrins,

ligands for ICAMs, are functional only as heterodimers composed of one α and one β subunit. Whereas β subunits combine with different α subunits, α subunits bind only one β subunit with the exception of αv, α4 and α6 (Hynes 1992). Thus, the question remained as to the binding partner of αv integrin on the central macrophage of EIs. A hint to answer this question was the observation that the red cell ICAM-4 can bind αIIbβ3 as well as αvβ3 integrin heterodimers, both present on platelets (Hermand*, et al* 2004, Hermand*, et al* 2003). Genetic deficiency of αIIb and β3 integrins results in a bleeding disorder known as Glanzmann thromboplasthenia (Coller*, et al* 1987) as in the β3 integrin deficient mice used here (Hodivala-Dilke*, et al* 1999). In contrast, ICAM-4 deficient animals do not show alterations in hemostasis, hematocrit or hemoglobin levels (Lee*, et al* 2006), probably because during hemostasis platelet integrins bind to extracelluar matrix molecules such as fibrinogen, fibronectin, von Willebrand factor, thrombospondin and vitronectin (Felding-Habermann and Cheresh 1993, Hynes 1992) and not ICAM-4. However, binding of RBCs to the forming thrombus requires interaction of ICAM-4 with αIIbβ3 and/or αvβ3 integrins (Hermand*, et al* 2004, Hermand*, et al* 2003) although this has not yet been proven in vivo (Lee*, et al* 2006). Our present data suggest an additional function of integrin β3, namely, stabilizing EIs as heterodimerization partner of αv integrin on central macrophages. This is concluded from the observation that in contrast to tg6 mice with much higher erythropoietic stimulation β3 integrin deficient mice exhibit abnormally immature peripheral RBCs (figs. 2, 3 and supplemental figs. 3 & 4), EI's with significantly less Ter119 positive cells (fig. 5B) and a reduced erythroid bone marrow population representing orthochromatic erythroblasts and premature reticulocytes (figs. 4C, 4E).

It could be shown that different hematopoietic cell lines bind to ICAM-4, which involves α4β1 integrin and αv-family integrins but β3 and αv integrin specific antibodies failed to reduce binding of these hematopoietic cell lines to ICAM-4 (Spring*, et al* 2001). Maybe the stable cell lines used in the latter study do not entirely reflect the dynamic in vivo situation, an interpretation in line with the fact that the same study also shows that only 6 out of 12 tested hematopoietic cell lines bound ICAM-4 (Spring*, et al* 2001). Moreover, the same group showed later that the αv integrin is indeed involved in binding of erythroblasts to the central macrophage (Lee*, et al* 2006). However, the whole picture might be more complex as α4β1 integrin can in addition to ICAM-4 (Spring*, et al* 2001) also interact with the vascular cell adhesion molecule-1 (VCAM-1) within EIs (Sadahira*, et al* 1995). In this case, α4β1 integrin is expressed on erythroblasts and VCAM-1 on the central macrophage (Sadahira*, et al* 1995). Another hint for the importance of the integrin – ICAM-4 – interaction for RBC production suggests expression and secretion of a soluble ICAM-4 isoform by erythroblasts (Lee*, et al* 2003) that could compete with the membrane bound ICAM-4 for integrin counterreceptors and thus play a role for the final detachment of reticulocytes from the central macrophage. If one heterodimerization partner of αv integrin is missing, e.g. β3 as we suggest, ICAM-4 dependent EI stability could be weakened and, thus, lower concentrations of soluble ICAM-4 could result in a preterm release of late stage erythroblasts or premature reticulocytes from the EI. Moreover, our data suggest that strong erythropoietic stimuli *per se* such as massive systemic Epo overexpression in tg6 mice do not trigger preterm release of reticulocytes (figs. 3, 4C, 5 and supplemental fig. 3).

Adhesion of the whole EI to the extracellular matrix might be important as well. Maturating EIs migrate towards the bone marrow sinusoids where young RBCs are released into the circulation (Yokoyama*, et al* 2003). Whereas in early developmental stages Epo plays the predominant role, interactions of differentiating RBCs with the extracellular matrix e.g. fibronectin are crucially important for the second phase of maturation (Eshghi*, et al* 2007) and might even provide proliferative stimuli for hematopoietic cells (Vuillet-Gaugler*, et al* 1990, Weinstein*, et al* 1989). The fibronectin dependent late phase of RBC maturation correlates with the migration of the EIs towards the sinusoids and both mechanisms might be regulated by interplay between integrin β1 and β3 (Danen*, et al* 2002). Using quantitative immunofluorescence we found in $\beta3^{-/-}$ mice compared to their wt controls bone marrow fibronectin to be increased whereas in tg6 mice it was decreased (fig. 6). In $\beta3^{-/-}$ mice increased fibronectin expression could be a compensatory mechanism to enhance binding of the premature RBCs, erythroblasts or the whole EI to the extracellular matrix to prevent the release of cells of even lower maturity into the circulation. Moreover, this compensatory mechanism could in $\beta3^{-/-}$ mice enhance also the second phase of erythroid maturation that requires fribronectin interaction with α4β1 integrin (Eshghi*, et al* 2007), which should not be altered in $\beta3^{-/-}$ mice. This interpretation fits to the significant higher fraction of Ery.B in the bone marrow of $\beta3^{-/-}$ mice (fig. 4A). In parallel, more fibronectin could facilitate migration of EIs towards the sinusoids resulting in reduced Ery.C (or group IV) population as observed in $\beta3^{-/-}$ bone marrow (fig. 4A & C). Conversely, bone marrow fibronectin staining intensity was decreased in tg6 mice. Tg6 mice need to fight against the uncontrolled RBC production. Because they cannot escape the early stage of erythroid

differentiation and expansion due to transgenic Epo production reduced fibronectin expression in tg6 mice could represent a compensatory mechanism for decelerating / inhibiting the fibronectin-dependent but Epo-independent second phase of erythroid differentiation (Eshghi*, et al* 2007) and migration of the EIs towards the sinusoids. This would keep the young erythrocytes longer than normal in the bone marrow. Indeed, we previously demonstrated that RBCs from tg6 mice share features of young as well as senescent red cell (Bogdanova*, et al* 2007), which fits to this interpretation.

Bone remodeling to reduce trabecular volume density is crucial for erythropoiesis and inhibition of osteoclasts blunts the erythropoietic response to Epo (Singbrant*, et al* 2011). Accordingly, in tg6 mice bone marrow volume was increased on cost of trabecular number with increased trabecular spacing (supplemental fig. 8), an observation in line with our previous findings (Heinicke*, et al* 2006). In contrast, integrin β3 deficient mice were reported to have impaired bone remodeling as shown by an enhanced density of tailbones that, however, contain mainly yellow marrow (Lee and Rosse 1979) and histological examples of distal femora suggesting an increased bone mass (McHugh*, et al* 2000). In addition, this latter study shows in $\beta3^{-/-}$ mice more osteoclasts that appear dysfunctional although they retain resorptive capacity when cultured on whale dentin. Unfortunately, no quantifications of these observations are provided. Quantitative micro-computed tomography based analysis of femora, however, did not reveal significant signs for osteosclerosis in $\beta3^{-/-}$ mice (supplemental fig. 8B). On the other hand, altered bone remodeling should affect the EI density (Singbrant*, et al* 2011) (that was unchanged in $\beta3^{-/-}$ mice) rather than the number of erythroid progenitors per island (that was reduced in

β3$^{-/-}$ mice). Thus, it is unlikely that the probably marginally disturbed bone remodeling in β3$^{-/-}$ mice could be causal for the observed instability of their EIs.

In conclusion, by comparing stress erythropoiesis of Epo overexpressing mice and integrin β3$^{-/-}$ mice we discovered a new functional role of integrin β3 for stabilization of erythropoietic islands. Our findings suggest that integrin β3 is important during the very late stage of red cell production by delaying release of premature reticulocytes.

Acknowledgements

The authors would like to thank R.O. Hynes for sharing his integrin β3$^{-/-}$ mice with us, B. Grenacher for performing plasma Epo measurements, J. Goede for help with the morphological evaluation of bone marrow cells and the Functional Genomics Center Zürich for analyzing the extra band.

Funding

This study was supported in part by the Swiss National Science Foundation (310030_120321 to JV).

Authorship

ZW performed most experiments except for blood smear analysis, fibronectin staining (done by OV), ectacytomertry, RBC life span measurements (done by JV), μCT and

analysis of bone structure (done by GK). MG generated tg6 mice and revised the article text and data presentation. JV designed the study and wrote the manuscript together with ZW.

Conflict-of-interest disclosure

The authors declare no competing financial interests.

References

Allen, T.D. & Dexter, T.M. (1982) Ultrastructural aspects of erythropoietic differentiation in long-term bone marrow culture. *Differentiation,* **21,** 86-94.

An, X. & Mohandas, N. (2011) Erythroblastic islands, terminal erythroid differentiation and reticulocyte maturation. *Int J Hematol,* **93,** 139-143.

Bailly, P., Hermand, P., Callebaut, I., Sonneborn, H.H., Khamlichi, S., Mornon, J.P. & Cartron, J.P. (1994) The LW blood group glycoprotein is homologous to intercellular adhesion molecules. *Proc Natl Acad Sci U S A,* **91,** 5306-5310.

Bogdanova, A., Mihov, D., Lutz, H., Saam, B., Gassmann, M. & Vogel, J. (2007) Enhanced erythro-phagocytosis in polycythemic mice overexpressing erythropoietin. *Blood.,* **110,** 762-769.

Chen, K., Liu, J., Heck, S., Chasis, J.A., An, X. & Mohandas, N. (2009) Resolving the distinct stages in erythroid differentiation based on dynamic changes in membrane protein expression during erythropoiesis. *Proc Natl Acad Sci U S A,* **106,** 17413-17418.

Coller, B.S., Seligsohn, U. & Little, P.A. (1987) Type I Glanzmann thrombasthenia patients from the Iraqi-Jewish and Arab populations in Israel can be differentiated by platelet glycoprotein IIIa immunoblot analysis. *Blood,* **69,** 1696-1703.

Danen, E.H., Sonneveld, P., Brakebusch, C., Fassler, R. & Sonnenberg, A. (2002) The fibronectin-binding integrins alpha5beta1 and alphavbeta3 differentially modulate RhoA-GTP loading, organization of cell matrix adhesions, and fibronectin fibrillogenesis. *J Cell Biol,* **159,** 1071-1086.

De Maria, R., Zeuner, A., Eramo, A., Domenichelli, C., Bonci, D., Grignani, F., Srinivasula, S.M., Alnemri, E.S., Testa, U. & Peschle, C. (1999) Negative regulation of erythropoiesis by caspase-mediated cleavage of GATA-1. *Nature,* **401,** 489-493.

Eshghi, S., Vogelezang, M.G., Hynes, R.O., Griffith, L.G. & Lodish, H.F. (2007) Alpha4beta1 integrin and erythropoietin mediate temporally distinct steps in erythropoiesis: integrins in red cell development. *J Cell Biol,* **177,** 871-880.

Felding-Habermann, B. & Cheresh, D.A. (1993) Vitronectin and its receptors. *Curr Opin Cell Biol,* **5,** 864-868.

Foller, M., Kasinathan, R.S., Koka, S., Huber, S.M., Schuler, B., Vogel, J., Gassmann, M. & Lang, F. (2007) Enhanced susceptibility to suicidal death of erythrocytes from transgenic mice overexpressing erythropoietin. *Am J Physiol Regul Integr Comp Physiol,* **293,** R1127-1134.

Gassmann, M., Grenacher, B., Rohde, B. & Vogel, J. (2009) Quantifying Western blots: pitfalls of densitometry. *Electrophoresis,* **30,** 1845-1855.

Hanspal, M. & Hanspal, J.S. (1994) The association of erythroblasts with macrophages promotes erythroid proliferation and maturation: a 30-kD heparin-binding protein is involved in this contact. *Blood,* **84,** 3494-3504.

Heinicke, K., Baum, O., Ogunshola, O.O., Vogel, J., Stallmach, T., Wolfer, D.P., Keller, S., Weber, K., Wagner, P.D., Gassmann, M. & Djonov, V. (2006) Excessive erythrocytosis in adult mice overexpressing erythropoietin leads to hepatic, renal, neuronal, and muscular degeneration. *Am. J. Physiol. Regul. Integr. Comp. Physiol.,* **291,** R947-R956.

Hermand, P., Gane, P., Callebaut, I., Kieffer, N., Cartron, J.P. & Bailly, P. (2004) Integrin receptor specificity for human red cell ICAM-4 ligand. Critical residues for alphaIIbbeta3 and alphaVbeta3 binding. *Eur J Biochem,* **271,** 3729-3740.

Hermand, P., Gane, P., Huet, M., Jallu, V., Kaplan, C., Sonneborn, H.H., Cartron, J.P. & Bailly, P. (2003) Red cell ICAM-4 is a novel ligand for platelet-activated alpha IIbbeta 3 integrin. *J Biol Chem,* **278,** 4892-4898.

Hildebrand, T., Laib, A., Muller, R., Dequeker, J. & Ruegsegger, P. (1999) Direct three-dimensional morphometric analysis of human cancellous bone: microstructural data from spine, femur, iliac crest, and calcaneus. *J. Bone. Miner. Res.,* **14,** 1167-1174.

Hildebrand, T. & Ruegsegger, P. (1997) A new method for the model-independent assessment of thickness in three-dimensional images. *J Microsc,* **185,** 67-75.

Hodivala-Dilke, K.M., McHugh, K.P., Tsakiris, D.A., Rayburn, H., Crowley, D., Ullman-Cullere, M., Ross, F.P., Coller, B.S., Teitelbaum, S. & Hynes, R.O. (1999) Beta3-integrin-deficient mice are a model for Glanzmann thrombasthenia showing placental defects and reduced survival. *J Clin Invest,* **103,** 229-238.

Hynes, R.O. (1992) Integrins: versatility, modulation, and signaling in cell adhesion. *Cell,* **69,** 11-25.

Inaba, M. & Maede, Y. (1988) Correlation between protein 4.1a/4.1b ratio and erythrocyte life span. *Biochim Biophys Acta,* **944,** 256-264.

Kina, T., Ikuta, K., Takayama, E., Wada, K., Majumdar, A.S., Weissman, I.L. & Katsura, Y. (2000) The monoclonal antibody TER-119 recognizes a molecule associated with glycophorin A and specifically marks the late stages of murine erythroid lineage. *Br J Haematol,* **109,** 280-287.

Kohler, T., Stauber, M., Donahue, L.R. & Muller, R. (2007) Automated compartmental analysis for high-throughput skeletal phenotyping in femora of genetic mouse models. *Bone,* **41,** 659-667.

Lee, G., Lo, A., Short, S.A., Mankelow, T.J., Spring, F., Parsons, S.F., Yazdanbakhsh, K., Mohandas, N., Anstee, D.J. & Chasis, J.A. (2006) Targeted gene deletion demonstrates that the cell adhesion molecule ICAM-4 is critical for erythroblastic island formation. *Blood,* **108,** 2064-2071.

Lee, G., Spring, F.A., Parsons, S.F., Mankelow, T.J., Peters, L.L., Koury, M.J., Mohandas, N., Anstee, D.J. & Chasis, J.A. (2003) Novel secreted isoform of adhesion molecule ICAM-4: potential regulator of membrane-associated ICAM-4 interactions. *Blood,* **101,** 1790-1797.

Lee, M.Y. & Rosse, C. (1979) Replacement of fatty marrow by active granulocytopoietic bone marrow following transplantation of mammary carcinoma into mice. *Anat Rec,* **195,** 31-46.

Lee, S.H., Crocker, P.R., Westaby, S., Key, N., Mason, D.Y., Gordon, S. & Weatherall, D.J. (1988) Isolation and immunocytochemical characterization of human bone marrow stromal macrophages in hemopoietic clusters. *J Exp Med,* **168,** 1193-1198.

Liu, Y., Pop, R., Sadegh, C., Brugnara, C., Haase, V.H. & Socolovsky, M. (2006) Suppression of Fas-FasL coexpression by erythropoietin mediates erythroblast expansion during the erythropoietic stress response in vivo. *Blood,* **108,** 123-133.

Manodori, A.B. & Kuypers, F.A. (2002) Altered red cell turnover in diabetic mice. *J. Lab. Clin. Med.,* **140,** 161-165.

Manwani, D. & Bieker, J.J. (2008) The erythroblastic island. *Curr Top Dev Biol,* **82,** 23-53.

McHugh, K.P., Hodivala-Dilke, K., Zheng, M.H., Namba, N., Lam, J., Novack, D., Feng, X., Ross, F.P., Hynes, R.O. & Teitelbaum, S.L. (2000) Mice lacking beta3 integrins are osteosclerotic because of dysfunctional osteoclasts. *J Clin Invest,* **105,** 433-440.

Mohandas, N. & Chasis, J.A. (2010) The erythroid niche: molecular processes occurring within erythroblastic islands. *Transfus Clin Biol,* **17,** 110-111.

Mohandas, N. & Prenant, M. (1978) Three-dimensional model of bone marrow. *Blood,* **51,** 633-643.

Oldenborg, P.A., Zheleznyak, A., Fang, Y.F., Lagenaur, C.F., Gresham, H.D. & Lindberg, F.P. (2000) Role of CD47 as a marker of self on red blood cells. *Science.,* **288,** 2051-2054.

Osborn, M. & Weber, K. (1982) Immunofluorescence and immunocytochemical procedures with affinity purified antibodies: tubulin-containing structures. *Methods Cell Biol,* **24,** 97-132.

Patterson, S.T., Li, J., Kang, J.A., Wickrema, A., Williams, D.B. & Reithmeier, R.A. (2009) Loss of specific chaperones involved in membrane glycoprotein biosynthesis during the maturation of human erythroid progenitor cells. *J Biol Chem,* **284,** 14547-14557.

Ruschitzka, F.T., Wenger, R.H., Stallmach, T., Quaschning, T., de Wit, C., Wagner, K., Labugger, R., Kelm, M., Noll, G., Rulicke, T., Shaw, S., Lindberg, R.L., Rodenwaldt, B., Lutz, H., Bauer, C., Luscher, T.F. & Gassmann, M. (2000) Nitric oxide prevents cardiovascular disease and determines survival in polyglobulic mice overexpressing erythropoietin. *Proc. Natl. Acad. Sci. U. S. A.,* **97,** 11609-11613.

Sadahira, Y., Yoshino, T. & Monobe, Y. (1995) Very late activation antigen 4-vascular cell adhesion molecule 1 interaction is involved in the formation of erythroblastic islands. *J Exp Med,* **181,** 411-415.

Schnell, S.A., Staines, W.A. & Wessendorf, M.W. (1999) Reduction of lipofuscin-like autofluorescence in fluorescently labeled tissue. *J Histochem Cytochem,* **47,** 719-730.

Singbrant, S., Russell, M.R., Jovic, T., Liddicoat, B., Izon, D.J., Purton, L.E., Sims, N.A., Martin, T.J., Sankaran, V.G. & Walkley, C.R. (2011) Erythropoietin couples erythropoiesis, B-lymphopoiesis, and bone homeostasis within the bone marrow microenvironment. *Blood,* **117,** 5631-5642.

Spring, F.A., Parsons, S.F., Ortlepp, S., Olsson, M.L., Sessions, R., Brady, R.L. & Anstee, D.J. (2001) Intercellular adhesion molecule-4 binds alpha(4)beta(1) and alpha(V)-family integrins through novel integrin-binding mechanisms. *Blood,* **98,** 458-466.

Vogel, J., Kiessling, I., Heinicke, K., Stallmach, T., Ossent, P., Vogel, O., Aulmann, M., Frietsch, T., Schmid-Schonbein, H., Kuschinsky, W. & Gassmann, M. (2003) Transgenic mice overexpressing erythropoietin adapt to excessive erythrocytosis by regulating blood viscosity. *Blood.,* **102,** 2278-2284.

Vuillet-Gaugler, M.H., Breton-Gorius, J., Vainchenker, W., Guichard, J., Leroy, C., Tchernia, G. & Coulombel, L. (1990) Loss of attachment to fibronectin with terminal human erythroid differentiation. *Blood,* **75,** 865-873.

Weinstein, R., Riordan, M.A., Wenc, K., Kreczko, S., Zhou, M. & Dainiak, N. (1989) Dual role of fibronectin in hematopoietic differentiation. *Blood,* **73,** 111-116.

Wiczling, P. & Krzyzanski, W. (2007) Method of determination of the reticulocyte age distribution from flow cytometry count by a structured-population model. *Cytometry A,* **71,** 460-467.

Wiczling, P. & Krzyzanski, W. (2008) Flow cytometric assessment of homeostatic aging of reticulocytes in rats. *Exp Hematol,* **36,** 119-127.

Yokoyama, T., Etoh, T., Kitagawa, H., Tsukahara, S. & Kannan, Y. (2003) Migration of erythroblastic islands toward the sinusoid as erythroid maturation proceeds in rat bone marrow. *J Vet Med Sci,* **65,** 449-452.

Figure legends

Fig 1. *Comparison of the strength of erythropoietic stimulation in integrin β3 deficient and Epo overexpressing (tg6) mice.* (A) In homozygous β3 deficient mice the hematocrit is slightly but significantly decreased. Systemic overexpression of Epo results in extreme hematocrit values as high as 82% in line with our previous reports (Bogdanova*, et al* 2007, Ruschitzka*, et al* 2000, Vogel*, et al* 2003) ($n \geq 5$). (B) Stimulation of erythropoiesis results in splenic enlargement in both genetically modified mouse lines that is, however, stronger in tg6 mice ($n \geq 5$).

Fig 2. *Analysis of peripheral RBCs in integrin $\beta3^{-/-}$ and tg6 mice.* (A) This bar graph shows for both genetically modified mouse lines the fold changes of the parameters in relation to their respective wt controls (set to 1). Reticulocyte counts were significantly and similarly increased in both $\beta3^{-/-}$ and tg6 mice but only β3 deficient mice showed a significantly higher reticulocyte staining intensity ($n \geq 6$, cf. also supplemental fig. 3). The percentage of CD71 positive RBCs was similarly increased in $\beta3^{-/-}$ and tg6 mice ($n \geq 6$) whereas the CD44 positive fraction was significantly increased only in $\beta3^{-/-}$ mice ($n = 5$). Accordingly, the ER-tracer dye positive reticulocyte faction was higher in $\beta3^{-/-}$ mice ($n = 5$). Binding of annexin V to RBCs, marking the eryptotic RBC fraction, did not differ significantly between β3 deficient mice and their wt controls. In contrast, according to our previous findings (Foller*, et al* 2007) annexin V binding was significantly increased on tg6 erythrocytes ($n = 6$). (B) In addition, RBCs from $\beta3^{-/-}$ displayed increased immunoreactivity for CD47 on their surface as evident from right-shift of the population (image) that is quantified by the geometric mean (bar graph, $n = 4$).

Fig 3. *Silver-stained SDS–polyacrylamide gel electrophoresis of erythrocyte membrane proteins.* (A) In β3 deficient mice an additional band was detected that was identified as calnexin using mass spectroscopy (cf. supplemental fig. 4). (B) Quantification of the band 4.1a/4.1b ratio revealed in β3 deficient mice a reduction whereas in accordance with our previous study (Bogdanova*, et al* 2007) this ratio was increased in tg6 ($n \geq 5$). (C) Quantification of the calnexin band intensity in relation to the band 4.2 intensity revealed practically no signal in tg6 mice whereas it was clearly detectable in $\beta3^{-/-}$ mice ($n \geq 5$).

Fig 4. *Analysis of erythroblast subsets in bone marrow and spleen.* (A) In the bone marrow ProE were significantly increased to a similar extend in both $\beta3^{-/-}$ and tg6 mice. Ery.A were not altered whereas Ery.B were significantly increased in $\beta3^{-/-}$ mice but decreased in tg6 mice. The Ery.C population, representing orthochromatic erythroblasts and premature reticulocytes, was significantly decreased in $\beta3^{-/-}$ but increased in tg6 mice ($n = 5$). (B) In the spleen no differences between $\beta3^{-/-}$ and tg6 mice were found regarding the fraction of the different erythroblast subpopulations ($n = 5$).

Panel (C) and (D) show the different erythroblast subpopulations (definition see text and supplemental fig. 5) after staining with FITC-conjugated anti-CD44 and PE-conjugated anti-Ter119 antibodies. (C) In line with the findings obtained with CD71 the most obvious difference between $\beta3^{-/-}$ and tg6 mice was the marked decrease in the latest erythropoietic developmental stage (subpopulation IV) in $\beta3^{-/-}$ but an increase in tg6 bone marrow compared to wt controls. Also the pattern of the other subpopulations was

comparable to that observed with CD71. (D) As for CD71, in the spleen there was no difference between $\beta3^{-/-}$ and tg6 mice regarding the erythropoietic subpopulations.

Fig 5. *Analysis of EIs in bone marrow.* (A) Representative image of a bone marrow EI with the macrophage labeled with an antibody directed against F4/80 (green) and the erythroblasts labeled with an antibody against TER119 (red). Original magnification 1000x. Only those TER119 positive cells were considered to be associated with a central macrophage that were 25% or less of the cell diameter distant from a F4/80 positive cell (4 gray squares = cell diameter, yellow square: 25% of the diameter of that cell). (B) Quantification of the EI density per 10 fields of view per animal and the number of erythroblasts attached to a macrophage. Compared to wt controls there was no difference in $\beta3^{-/-}$ mice regarding EI density whereas in tg6 mice it was significantly increased (left panel). In $\beta3^{-/-}$ mice there was a significant reduction of cells per EI whereas tg6 mice did not show a difference compared to their wt controls regarding this parameter (right panel, n = 10).

Fig 6. *Assessment of local fibronectin expression in bone marrow.* Examples of images and quantification procedure cf. methods and supplemental fig. 7. Vessel-associated fibronectin staining intensity (8-bit optical density level: 0 = black, 255 = white) was increased in $\beta3^{-/-}$ mice but reduced in tg6 mice compared to their wt controls (n = 4). No difference was detected between both wt strains used.

Figure 1

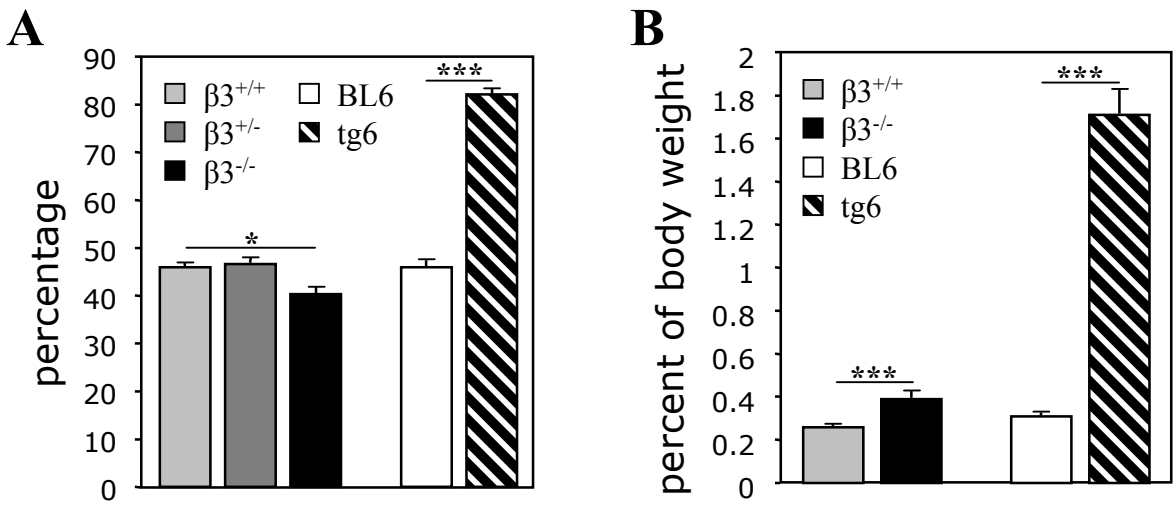
A
percentage
90
80
70
60
50
40
30
20
10
0
β3+/+
β3+/-
β3-/-
BL6
tg6
*
***
B
percent of body weight
2
1.8
1.6
1.4
1.2
1
0.8
0.6
0.4
0.2
0
β3+/+
β3-/-
BL6
tg6
***
***

Figure 2

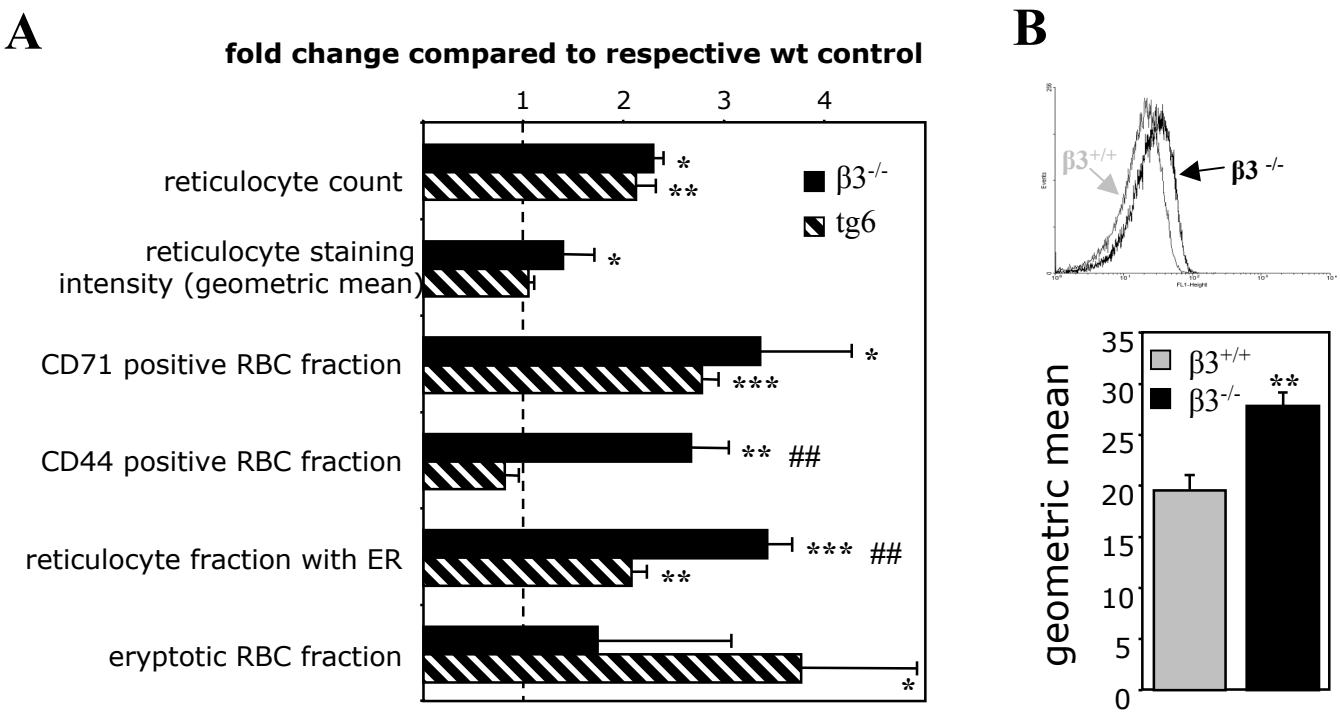
A
fold change compared to respective wt control
1
2
3
4
reticulocyte count
reticulocyte staining intensity (geometric mean)
CD71 positive RBC fraction
CD44 positive RBC fraction
reticulocyte fraction with ER
eryptotic RBC fraction
β3-/-
tg6
B
β3+/+
β3 -/-
geometric mean
35
30
25
20
15
10
5
0
β3+/+
β3-/-

Figure 3

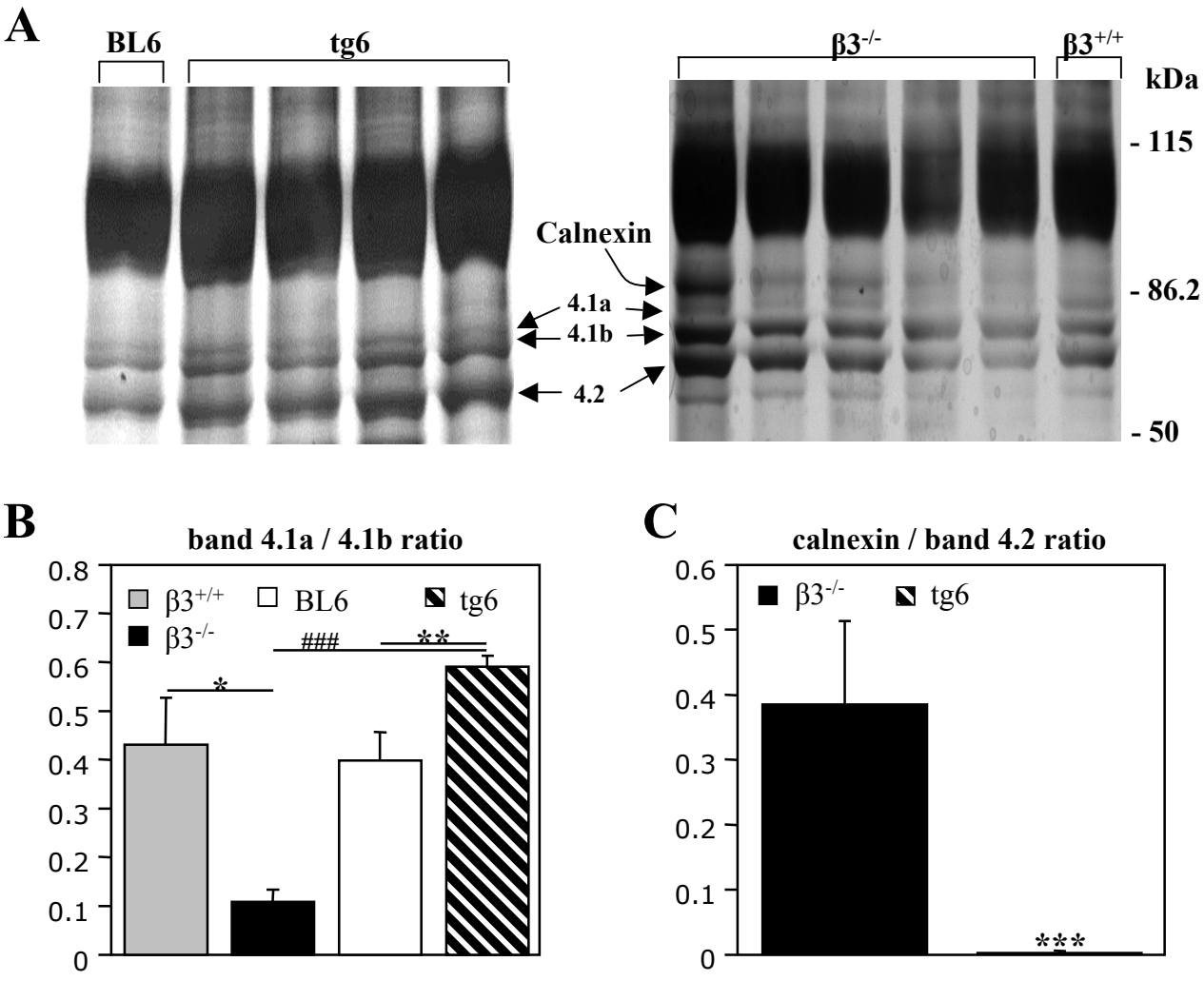
A
BL6
tg6
β3-/-
β3+/+
kDa
- 115
- 86.2
- 50
Calnexin
4.1a
4.1b
4.2
B
band 4.1a / 4.1b ratio
β3+/+
BL6
tg6
β3-/-
###
**
*
0.8
0.7
0.6
0.5
0.4
0.3
0.2
0.1
0
C
calnexin / band 4.2 ratio
β3-/-
tg6
***
0.6
0.5
0.4
0.3
0.2
0.1
0

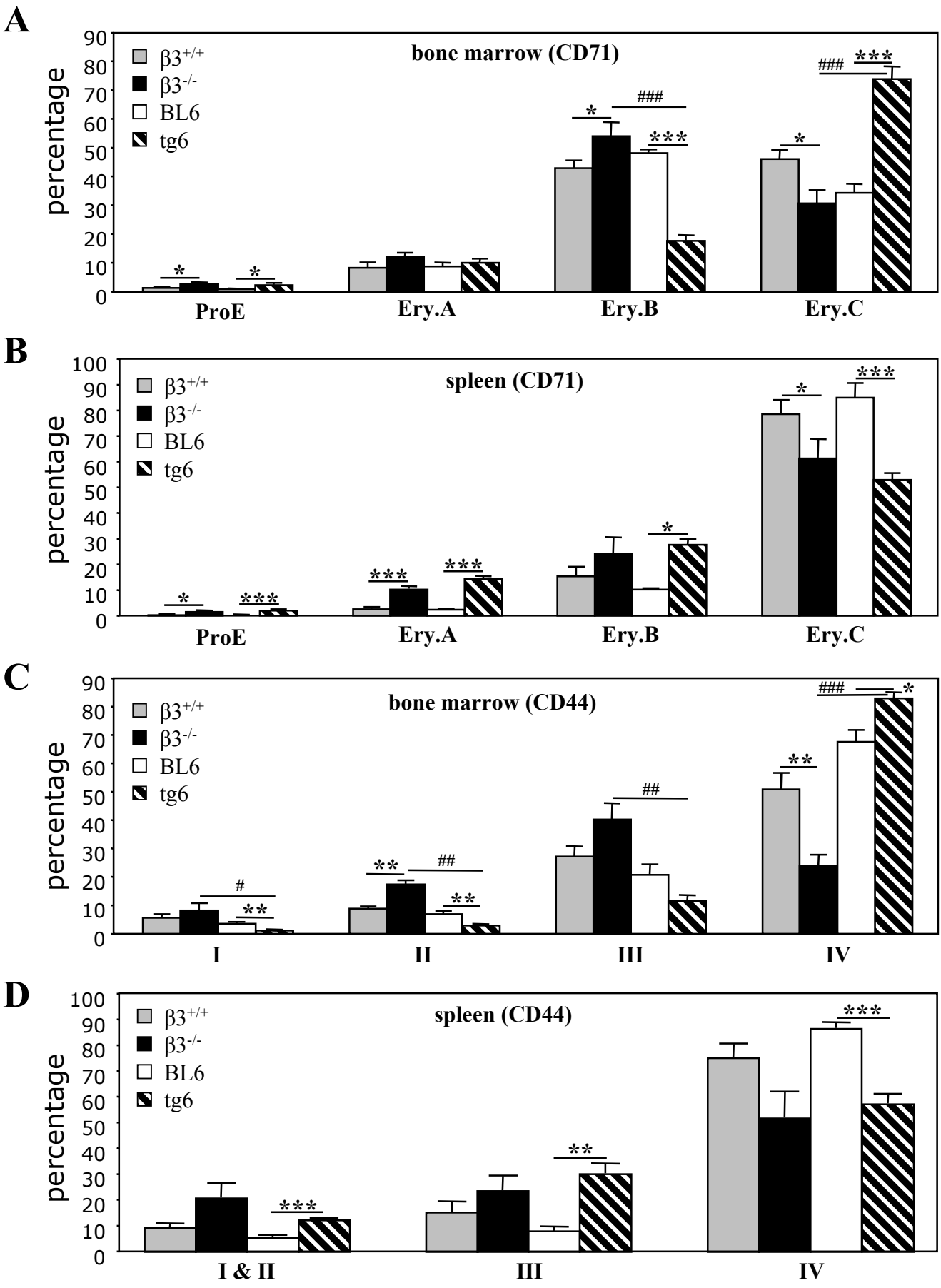
A
bone marrow (CD71)
β3+/+
β3-/-
BL6
tg6
percentage
ProE
Ery.A
Ery.B
Ery.C
B
spleen (CD71)
C
bone marrow (CD44)
I
II
III
IV
D
spleen (CD44)
I & II

Figure 5

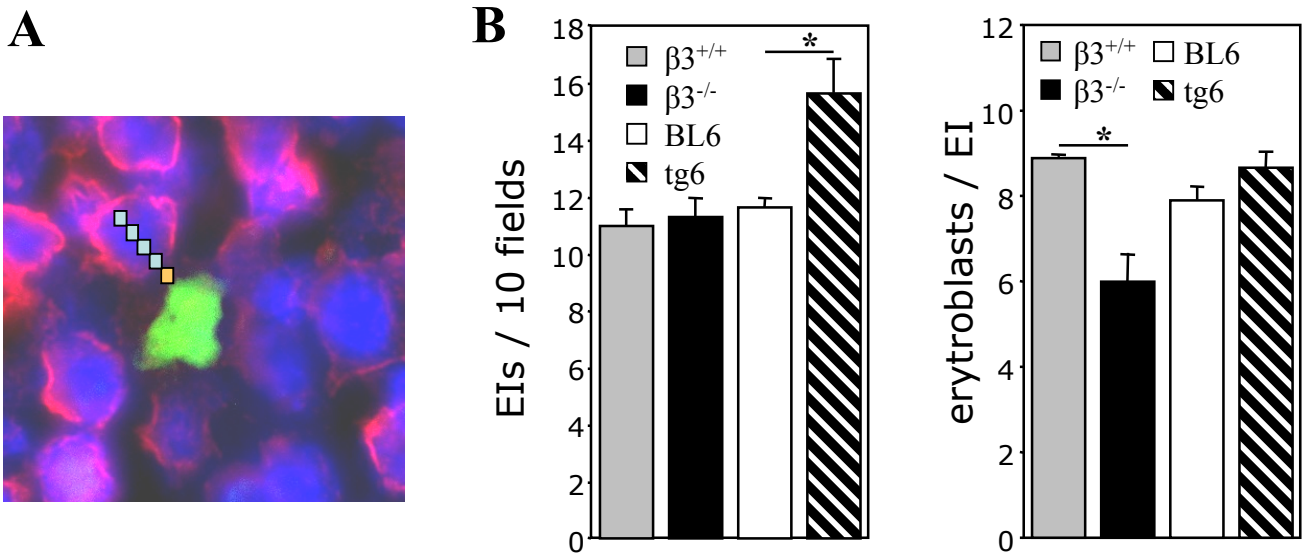

Figure 6

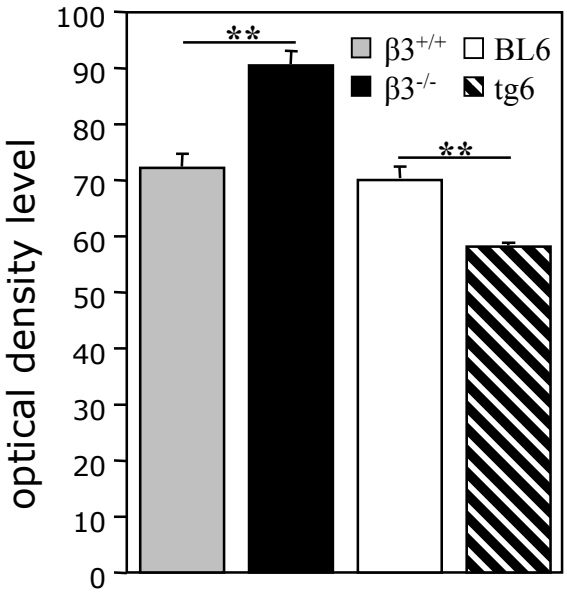
optical density level
100
90
80
70
60
50
40
30
20
10
0
**
**
β3+/+
BL6
β3-/-
tg6

Supplement to "Decreased stability of erythropoietic islands in integrin β3 deficient mice"

Zhenghui Wang, et al.

Supplemental figures

S-fig 1. (A) Size (left panel, n = 18) and gross morphology of erythrocytes (original magnification 400x, right panel) were not altered in $\beta3^{-/-}$ mice (cf. also supplementary fig. 3). (B) Prussian blue staining (original magnification 400x) revealed compared to wt controls no difference in iron deposition neither in bone marrow nor in spleens of $\beta3^{-/-}$ mice.

S-fig 2. (A) Mechanical properties of $\beta3^{-/-}$ erythrocytes were not significantly altered as assessed by recording elongation of the erythrocytes at shear stresses between 0.13 and 25.25 s^{-1} (10.1 mPa*s, solution #1) or 0.29 and 58.5 s^{-1} (23.4 mPa*s, solution #2). Higher shear stresses revealed a trend towards increased flexibility in $\beta3^{-/-}$mice (n = 6). (B) Osmotic fragility of $\beta3^{-/-}$ RBCs was indistinguishable from that of their wt controls ($n \geq 6$).

S-fig 3. Blood smears were stained with Brillian-Kresyl blue to visualize reticulocytes. Shown are selected fields containing an amassment of reticulocytes (labeled with green arrowheads). Reticulocytes from $\beta3^{-/-}$ mice showed more and denser staining. Original magnification 1000x.

S-fig 4. (A) MASCOT's probability based Mowse scores of the proteins identified in the additional 90kD band found in the gels from $\beta 3^{-/-}$ peripheral RBC membrane preparations (cf. fig. 3A). Scores >52 indicate identity or extensive homology ($p < 0.05$; green hatched area indicates non-significant results). Calnexin has a score of 291 indicating that the probability that this protein is not present in the extra band is smaller than 10^{-29} %. 16 peptide query matches and 9.5% sequence coverage were obtained and mass accuracy for all peptides was better than 20.5 ppm. Marked are also all other significant protein hits from mice found in the extra band. (B) The whole amino acid sequence of calnexin is shown with the identified peptide fragments marked (bold and underlined).

S-fig 5. Bone marrow and spleen cells (shown here: bone marrow) were classified based on Ter119 and CD71 expression as proerythroblast (ProE) and cells expressing high levels of Ter119. The population pattern was similar for bone marrow and spleen. The whole population of $Ter119_{high}$ cells, representing later stages of erythroblast development, was further subdivided according to its CD71 expression level and forward scatter (FSC). The resulting three subpopulations were identified as Ery.A ($Ter119_{high}$ $CD71_{high}$ FSC_{high}), Ery.B ($Ter119_{high}$ $CD71_{high}$ FSC_{low}) and Ery.C ($Ter119_{high}$ $CD71_{low}$ FSC_{low}), corresponding to basophilic, polychromatic and orthochromatic erythroblasts and reticulocytes, respectively.

S-fig 6. Flow cytometric analysis of bone marrow (A) and spleen cells (B) after staining with fluorescence labeled antibodies against CD44 (FL1) and TER119 (FL2) and

definition of subpopulations (C). (A) In TER119 positive bone marrow cells four distinct subpopulations could be distinguished based on CD44 staining intensity and forward scatter (FL1 INT vs. FS INT plots). These populations are labeled I, II, III and IV. Note that only in $\beta3^{-/-}$ mice more cells are found in population III than IV (arrows, cf. also to fig. 4C). In contrast, in spleen cells (B) only three subpopulations could be distinguished with the CD44 and TER119 antibodies. The population labels correspond to those in (A). (C) Cells found primarily in May-Grunwald stained cytospin preparations of the subpopulations defined in (A) and (B) after FACS. Subpopulation I corresponded to ProE and Ery.A, II to EryA, III to some EryB and mainly Ery.C as defined by Liu et al. (Liu*, et al* 2006) and IV mainly to reticulocytes but also some erythrocytes similar to the definition from Chen et al. (Chen*, et al* 2009).

S-fig 7. (A) Examples of immunofluorescence against fibronectin (original magnification 200x). (B) Illustration of the quantification procedure. Using an image analyzing system a threshold 20% above the average background optical density level (oDL, 0 = black, 255 = white) was defined. A circular sample tool was used to measure each single vessel in the images separately. The threshold procedure defined the pixels representing each single vessel (red). Then the average oDL (8-bit grayscale, 0 = black and 255 = white) of each vessel was calculated.

S-fig 8. (A) Representative µCT images of the distal femur of all mouse lines investigated. Trabecular bone (red) had been detected user independently by software (cf. methods). Note the reduced volume density of the trabecular bone in the tg6 mouse. (B)

Quantification of the trabecular bone structure. Trabecular thickness was the same among all mouse lines. Tg6 mice showed a significantly decreased trabecular number, which resulted in increased trabecular spacing. This suggests expanded space for erythopoietic cells ($n \geq 3$). (C) Examples of hematoxylin and eosin stained bone sections. No differences regarding the trabecular or cortical bone structure were found in $\beta 3^{-/-}$ mice. Bone marrow in tg6 mice appeared to contain more cells than wt controls.

Supplemental References

Chen, K., Liu, J., Heck, S., Chasis, J.A., An, X. & Mohandas, N. (2009) Resolving the distinct stages in erythroid differentiation based on dynamic changes in membrane protein expression during erythropoiesis. *Proc Natl Acad Sci U S A,* **106,** 17413-17418.

Liu, Y., Pop, R., Sadegh, C., Brugnara, C., Haase, V.H. & Socolovsky, M. (2006) Suppression of Fas-FasL coexpression by erythropoietin mediates erythroblast expansion during the erythropoietic stress response in vivo. *Blood,* **108,** 123-133.

A

Erythrocyte FSC height

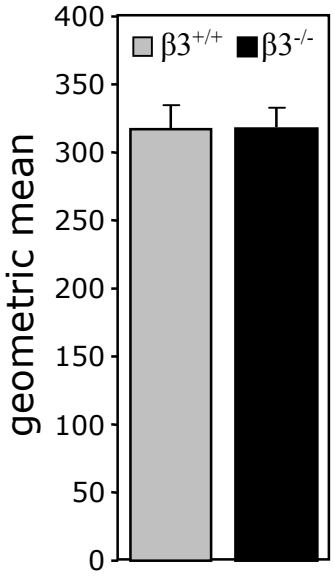

representative blood smear of a β3$^{-/-}$ mouse

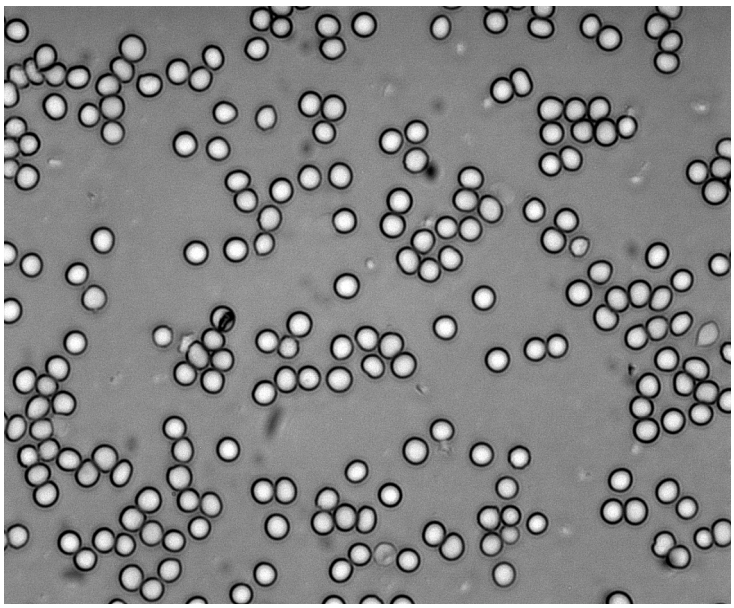

B

Prussian blue staining

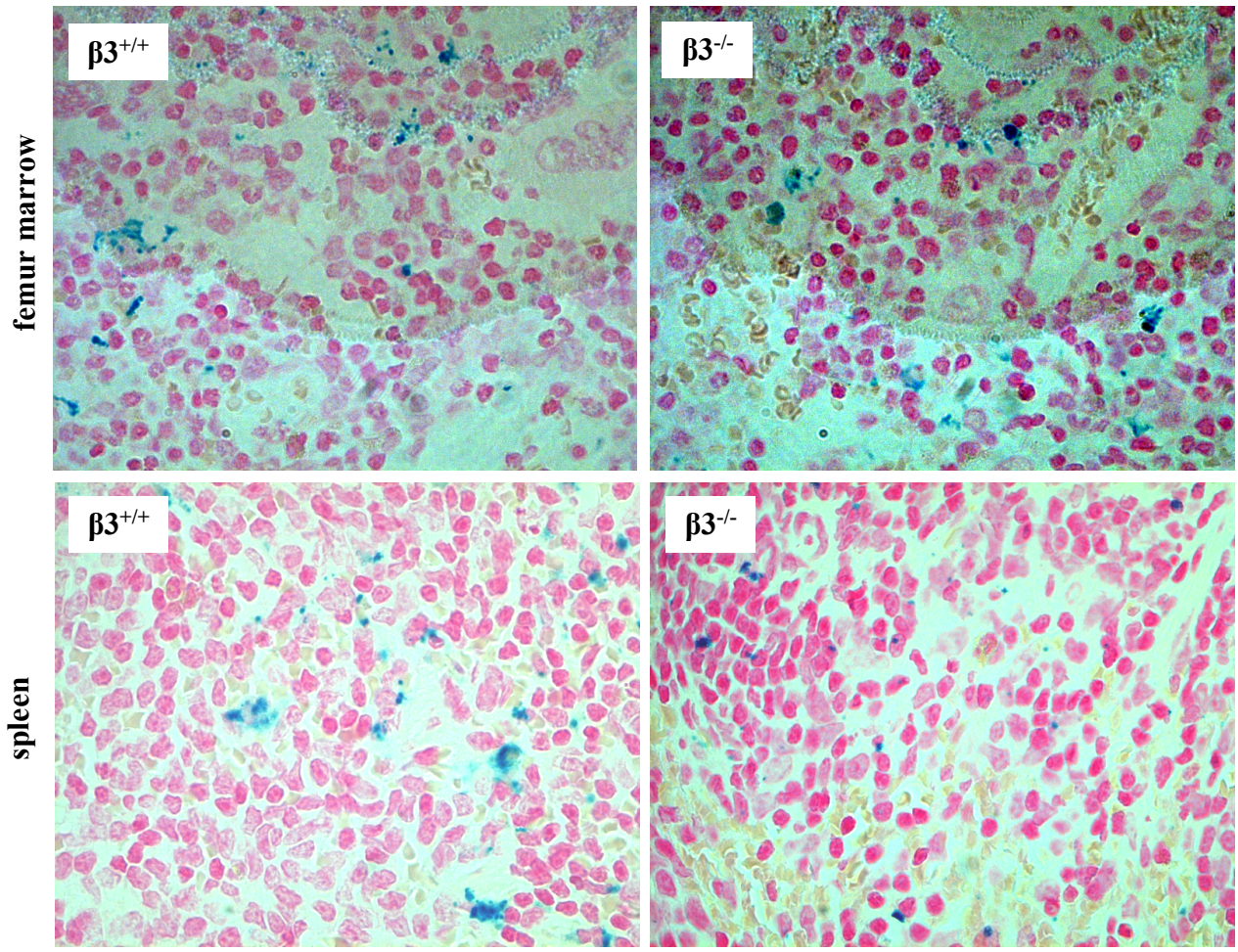

A

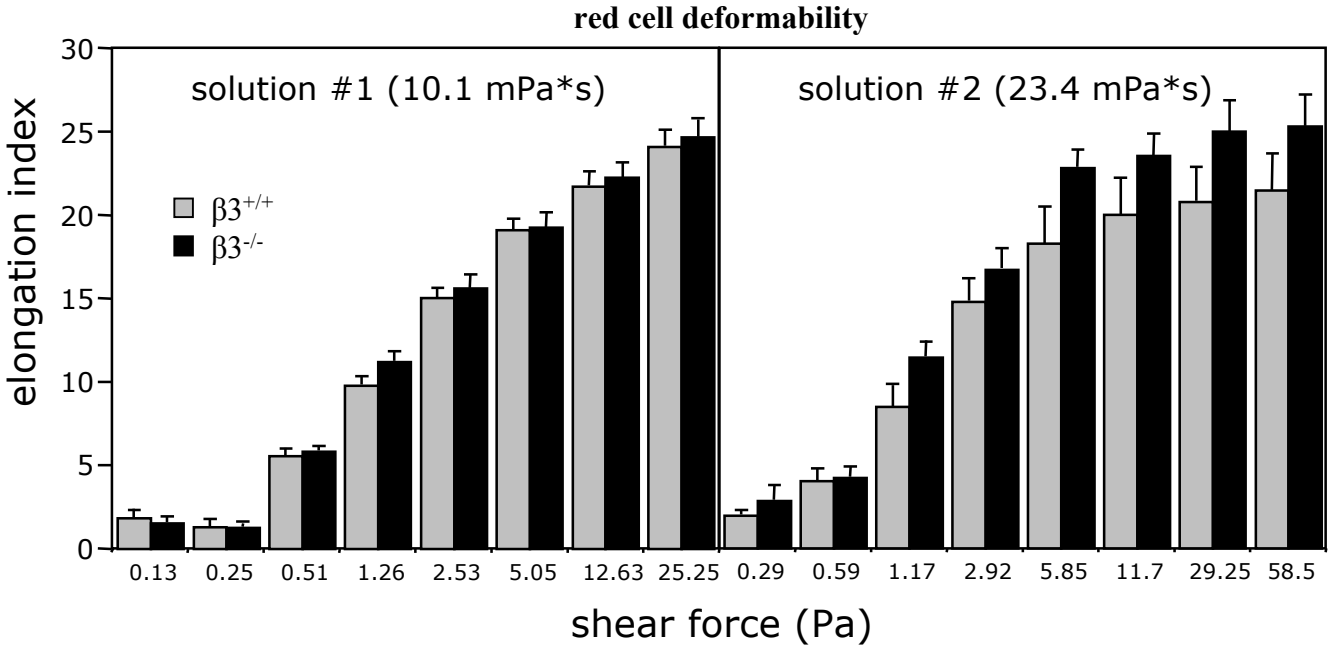
red cell deformability
solution #1 (10.1 mPa*s)
solution #2 (23.4 mPa*s)
β3+/+
β3-/-
elongation index
0
5
10
15
20
25
30
0.13
0.25
0.51
1.26
2.53
5.05
12.63
25.25
0.29
0.59
1.17
2.92
5.85
11.7
29.25
58.5
shear force (Pa)

B

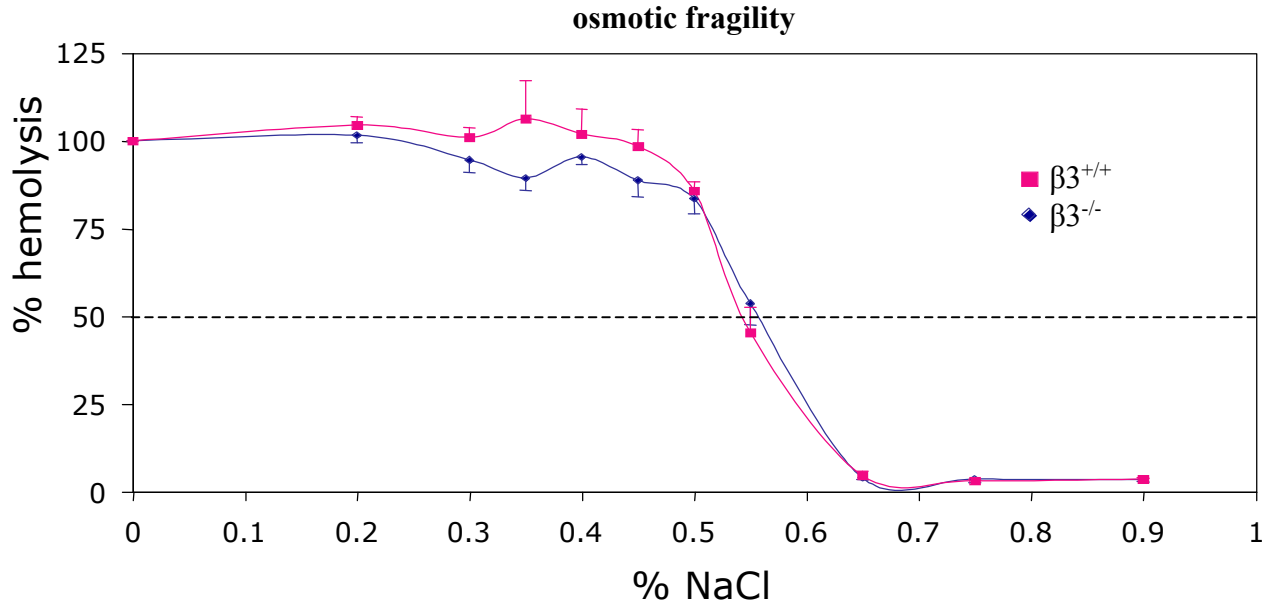
osmotic fragility
β3+/+
β3-/-
% hemolysis
0
25
50
75
100
125
0
0.1
0.2
0.3
0.4
0.5
0.6
0.7
0.8
0.9
1
% NaCl

Suppl. figure 3

Brilliant-Kresyl blue staining of blood smears

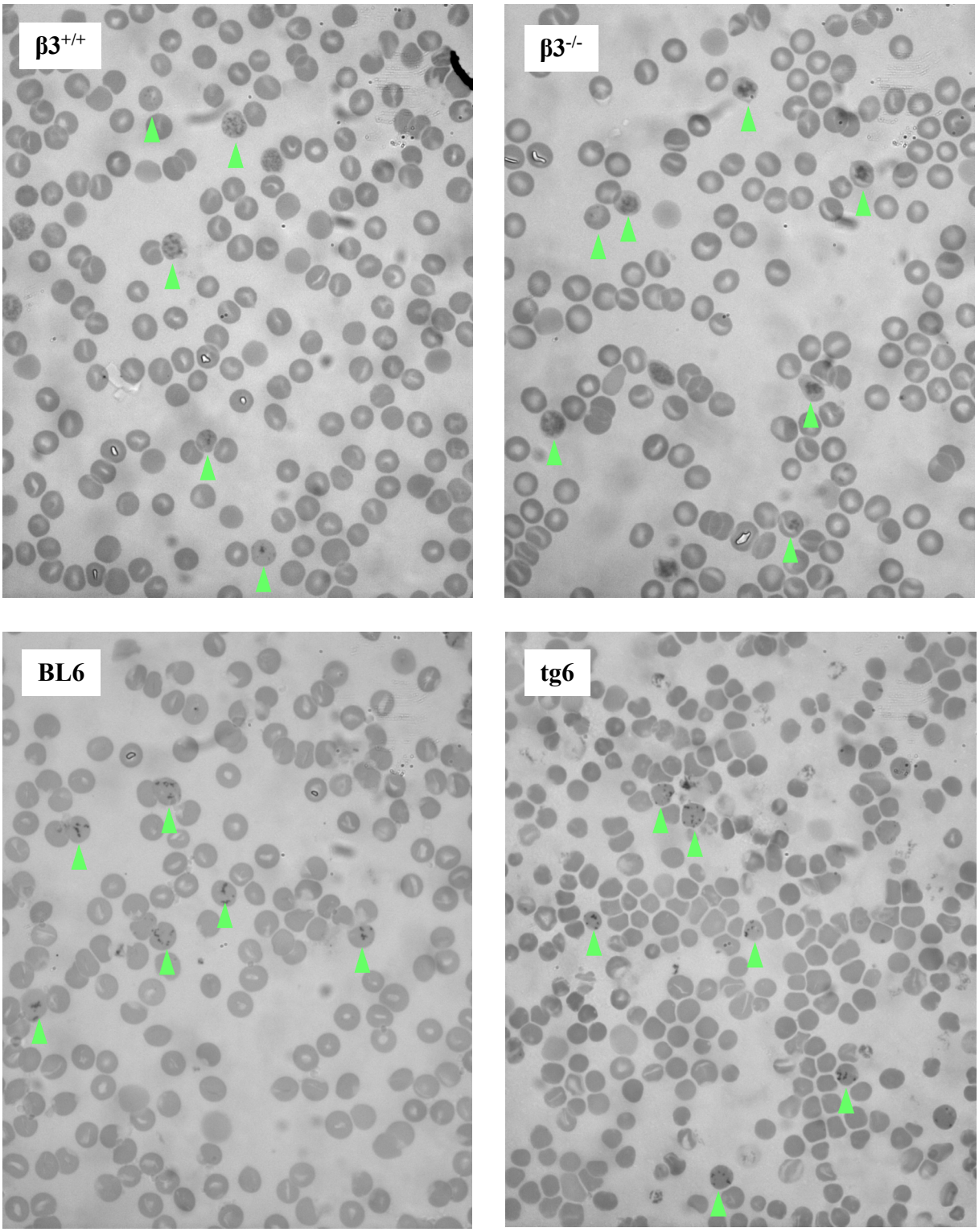

A

LC/ESI/MS/MS analysis of the extra band seen in fig. 3A

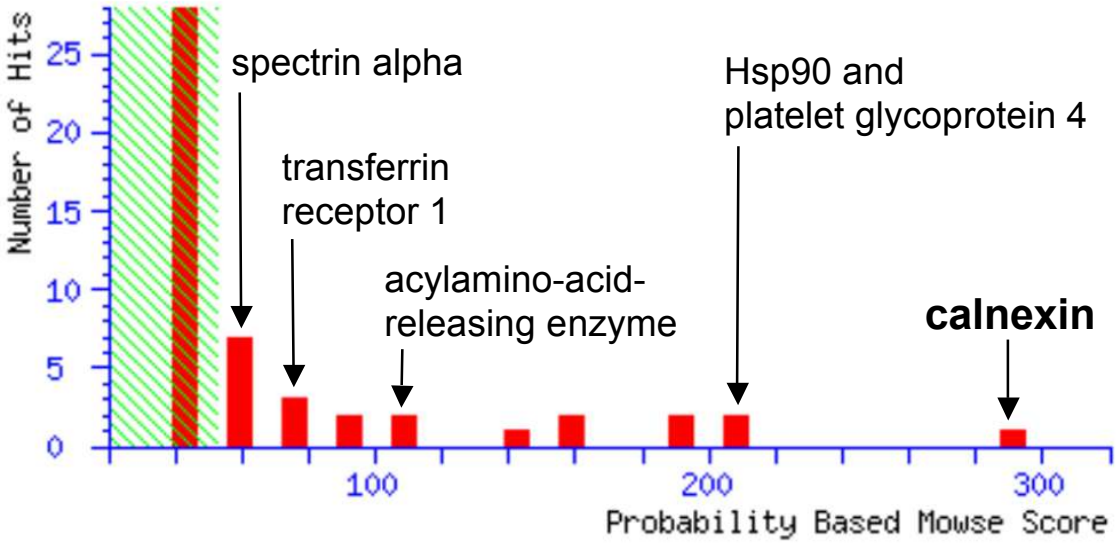

B

peptide matches for calnexin

```
1   megkwllcll lvlgtaavea hdghdddaid ieddlddvie evedsksksd astppspkvt
61  ykapvptgev yfadsfdrgs lsgwilskak kddtddeiak ydgkwevdem ketklpgdkg
121 lvlmsrakhh aisaklnkpf lfdtkplivq yevnfqngie cggayvklls ktaelsldqf
181 hdktpytimf gpdkcgedyk lhfifrhknp ktgvyeekha krpdadlkty ftdkkthlyt
241 lilnpdnsfe ilvdqsvvns gnllndmtpp vnpsreiedp edrkpedwde rpkiadpdav
301 kpddwdedap skipdeeatk pegwlddepe yipdpdaekp edwdedmdge weapqianpk
361 cesapgcgvw qrpmidnpny kgkwkppmid npnyqgiwkp rkipnpdffe dlepfkmtpf
421 saiglelwsm tsdiffdnfi isgdrrvvdd wandgwglkk aadgaaepgv vlqmleaaee
481 rpwlwvvyil tvalpvflvi lfccsgkkqs nameykktda pqpdvkdeeg keeeknkrde
541 eeeeekleek qksdaeedgv tgsqdeedsk pkaeedeiln rsprnrkprr e
```

Suppl. figure 5

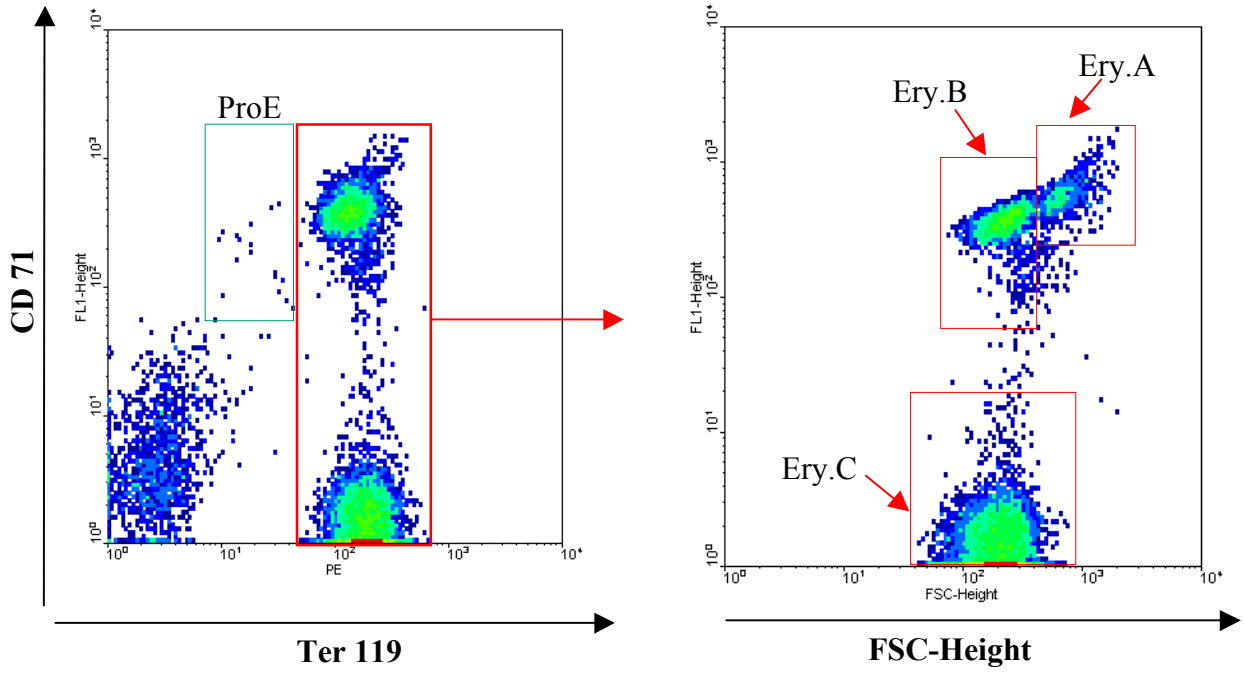

A

Flow cytometry of CD44 (FL1) and TER119 (FL2) stained bone marrow cells

β3$^{+/+}$

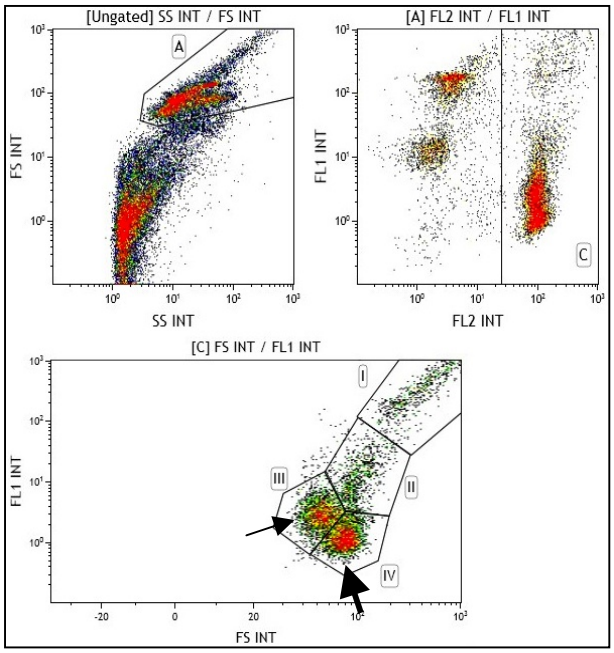

β3$^{-/-}$

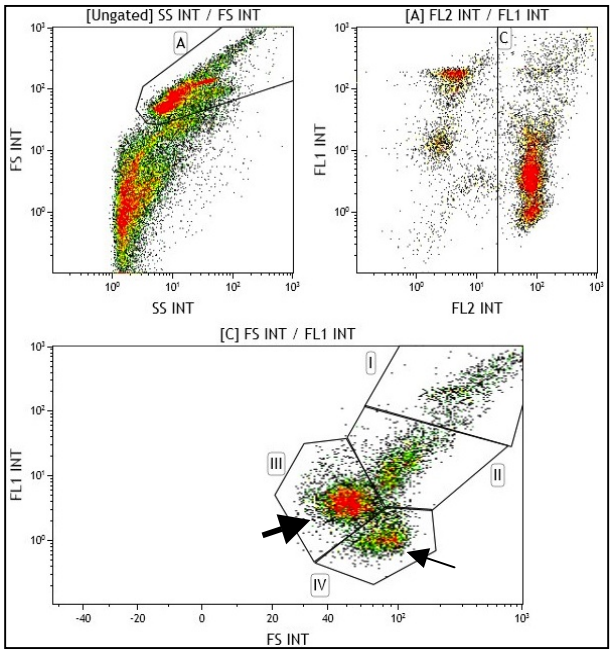

BL6

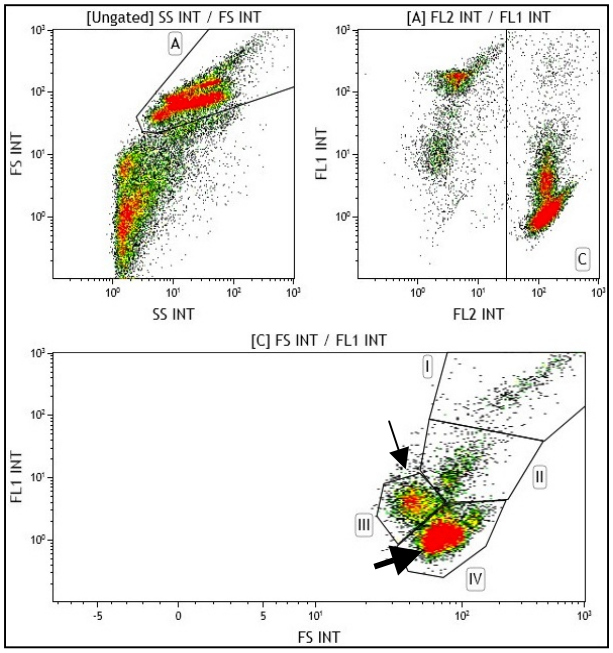

tg6

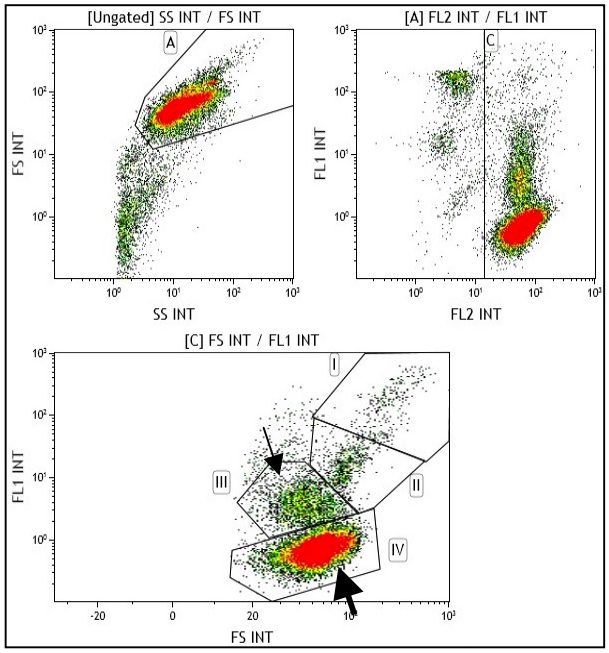

B

Flow cytometry of CD44 (FL1) and TER119 (FL2) stained spleen cells

β3$^{+/+}$

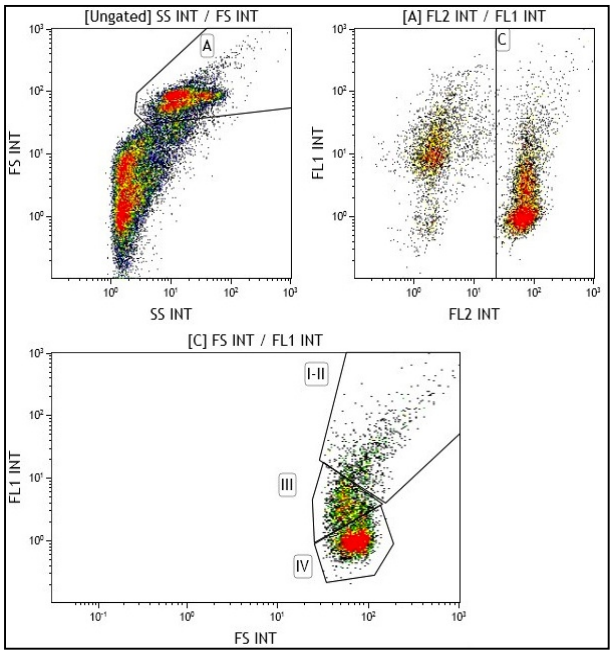

β3$^{-/-}$

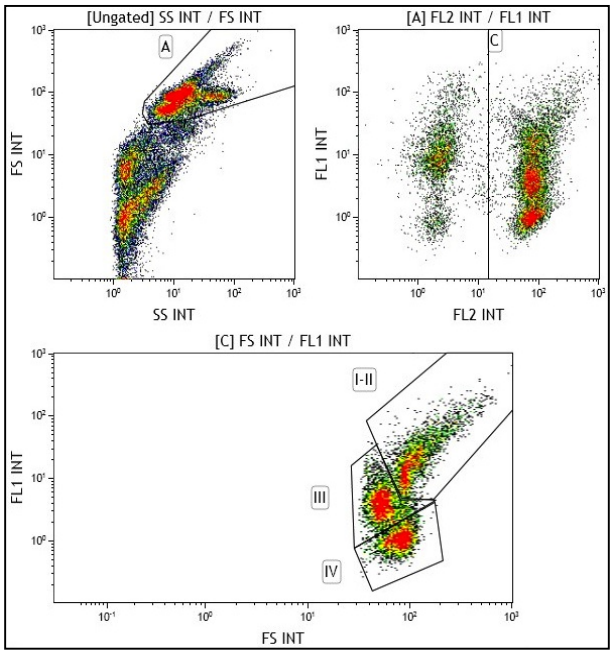

BL6

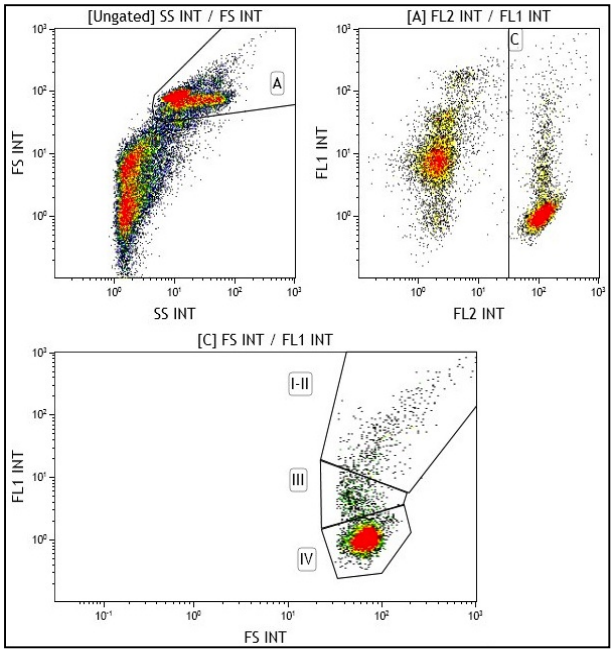

tg6

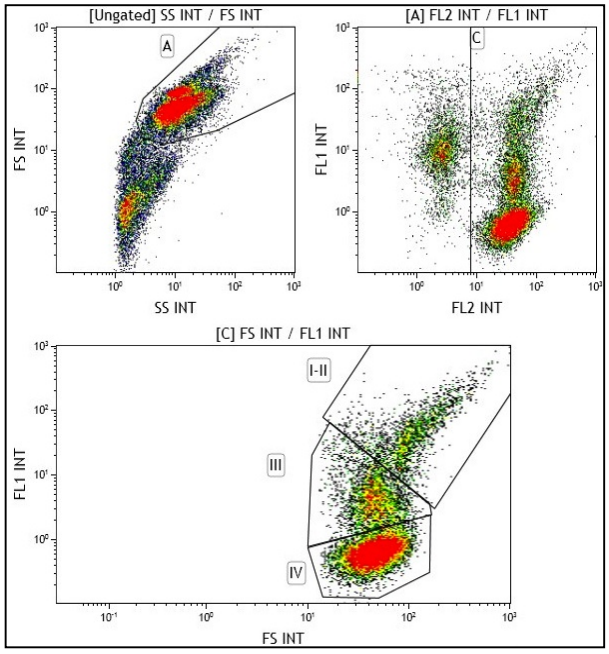

C

group I
(proerythroblasts and
basopholic erythroblasts)

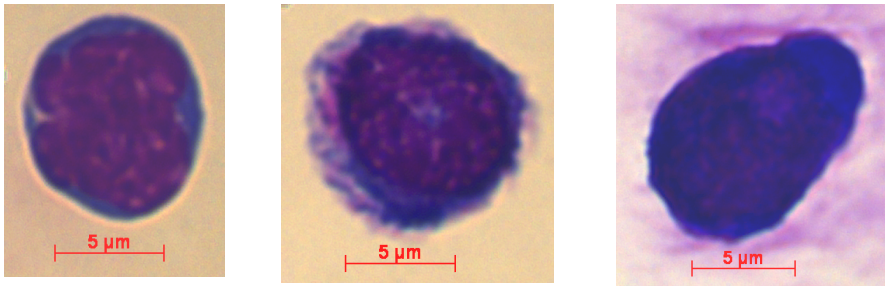

group II
(polychomatic erythroblasts)

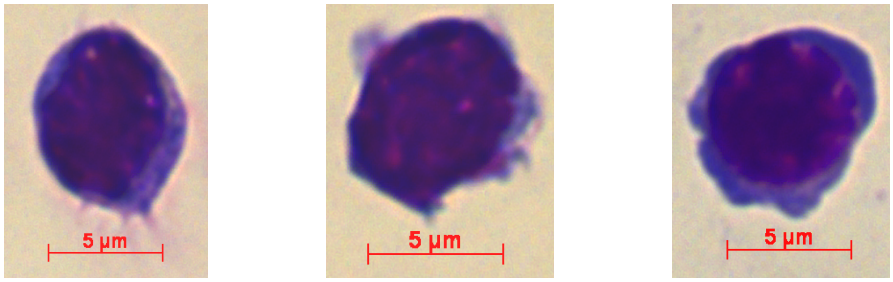

group III
(orthochomatic erythroblasts)

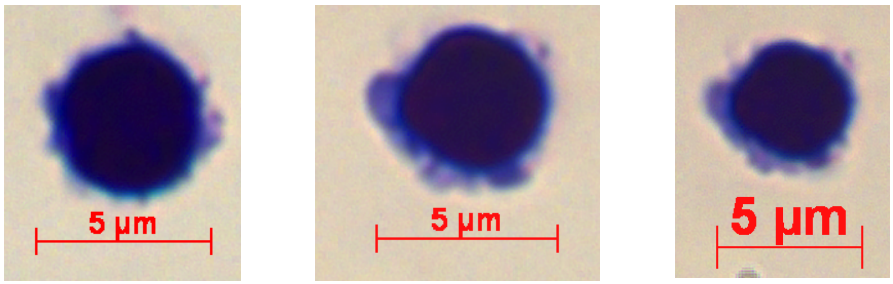

group IV
(reticulocytes

and

erythrocytes)

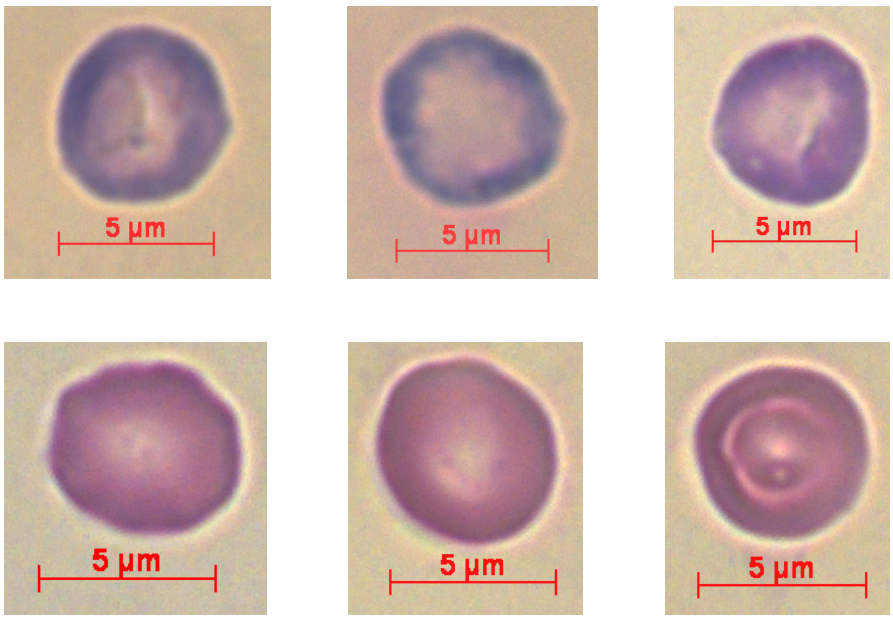

A

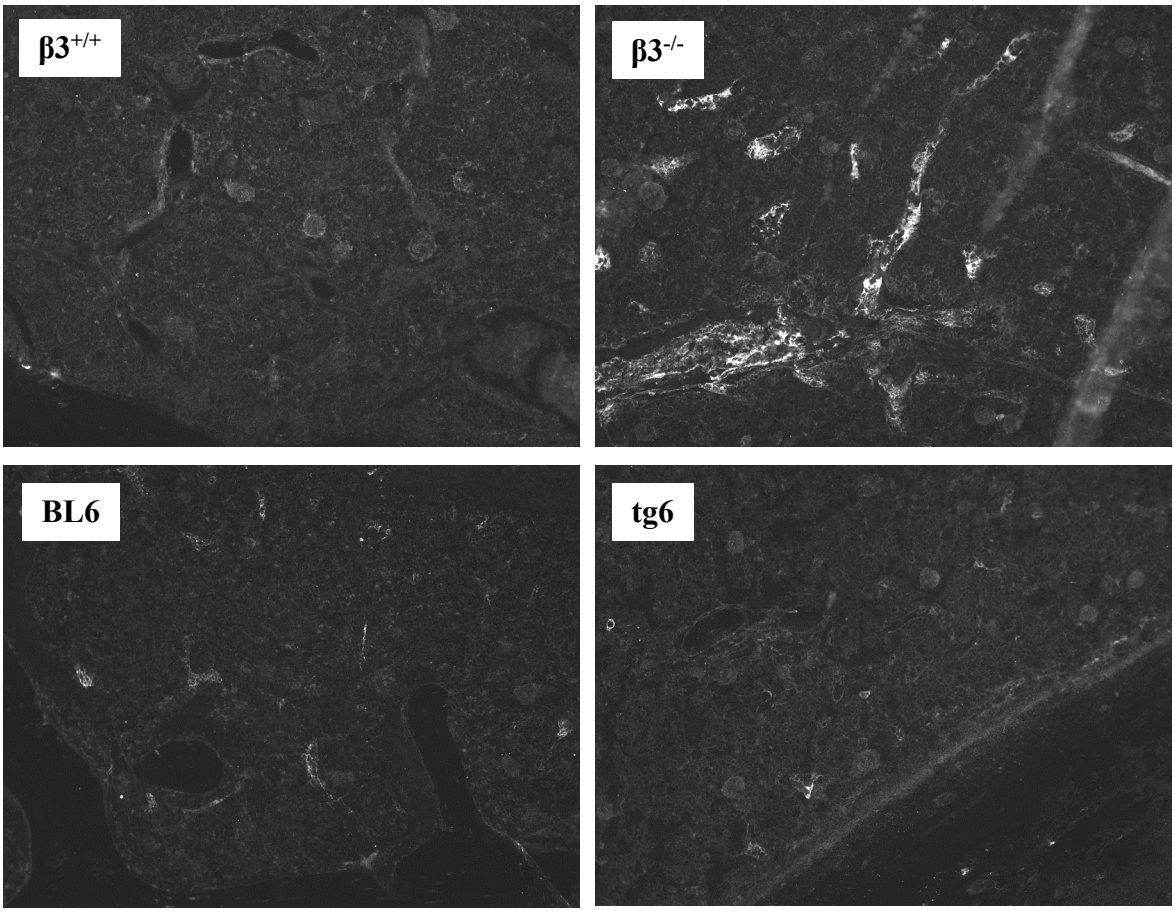

B

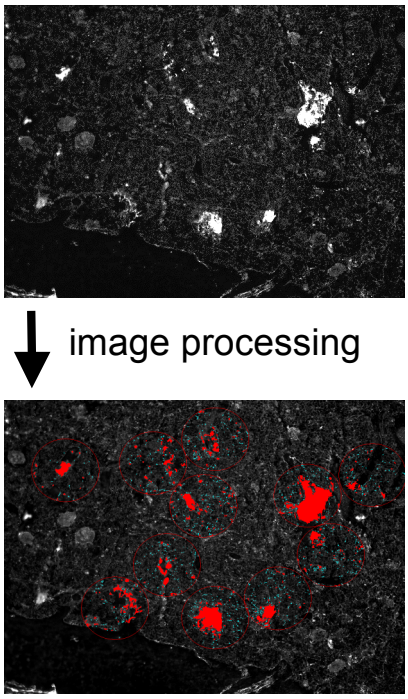

A

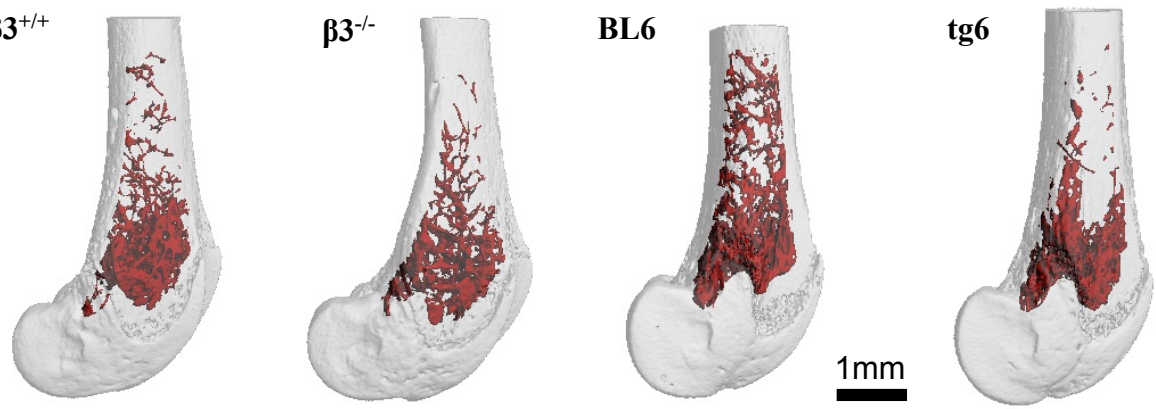
β3+/+
β3-/-
BL6
tg6
1mm

B

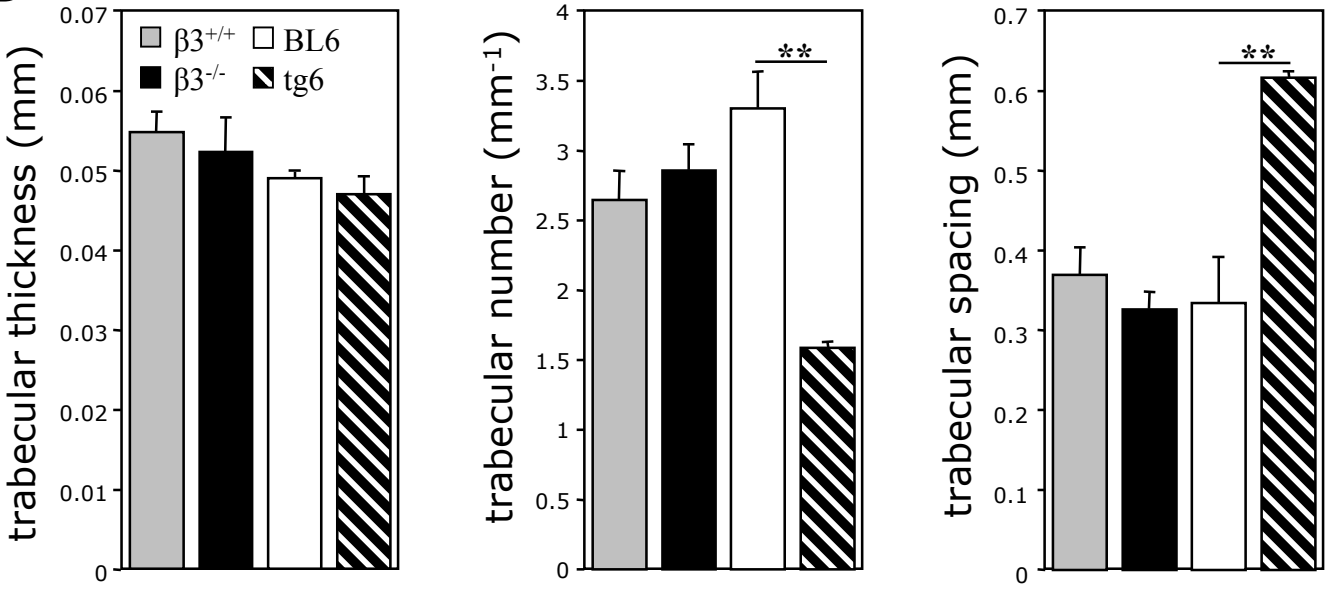
trabecular thickness (mm)
0.07
0.06
0.05
0.04
0.03
0.02
0.01
0
β3+/+
BL6
β3-/-
tg6
trabecular number (mm-1)
4
3.5
3
2.5
2
1.5
1
0.5
0
**
trabecular spacing (mm)
0.7
0.6
0.5
0.4
0.3
0.2
0.1
0
**

C

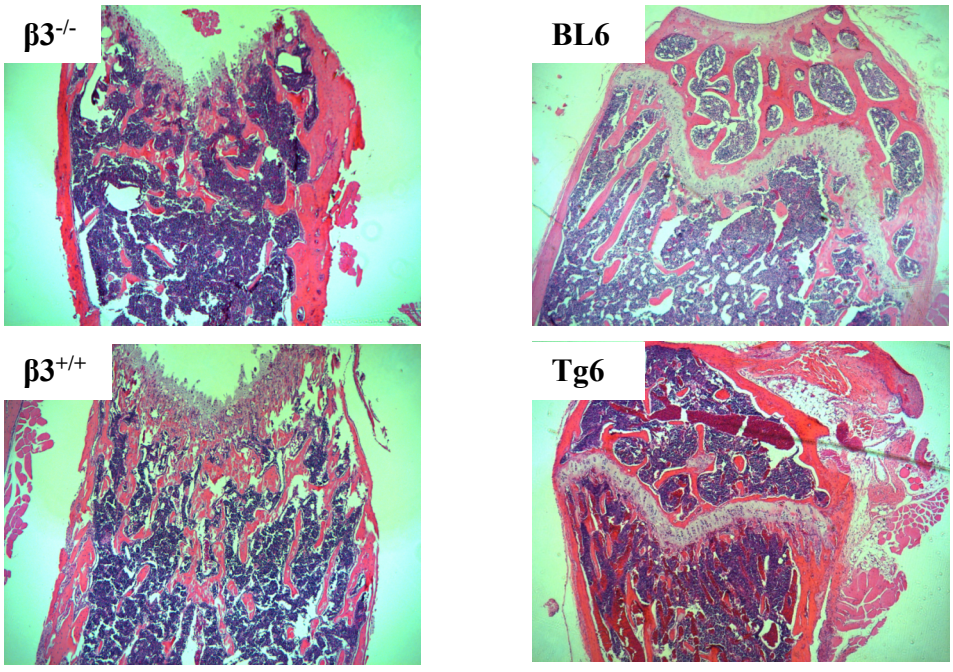
β3-/-
BL6
β3+/+
Tg6

CHAPTER 3. CONCLUSION AND PERSPECTIVES

Normal erythropoiesis takes place mainly in specialized microanatomical niches termed EI that are composed of a central macrophage with erythroblasts and premature reticulocytes attached (43). This close association of erythroblasts with the central macrophage is necessary for the maturation of erythroblasts (42) and crucially dependent on molecules contributing to the interaction of macrophage and erythroblasts. Many different molecules mediating both erythroblast/erythroblast and erythroblast/macrophage interactions have been identified, such as EMP, ICAM-4, VCAM-1 and integrins. Of specific interest for the present study was the fact that red cell ICAM-4 is important for the formation and stability of EIs (51) but also that the counterreceptor on the central macrophage was not well defined yet. In vitro, αv integrin was found to be expressed in macrophages isolated from EI and the ICAM-4/αv interactions is critical for EI integrity. However, since integrins are only functional as heterodimers composed of an α and a β subunit (261), we asked, what could be the heterodimerization partner of αv integrin on central macrophages mediating attachment of erythroblasts.

Previously, ICAM-4 on red cells was found to be the receptor of αvβ3 and αIIbβ3 integrin heterodimers, both present on platelets (283). Furthermore, critical amino acids in the binding sites of human cell ICAM-4 with αvβ3 integrins have been identified (283). These previous observations suggested that integrin β3 may contribute to the interaction with ICAM-4 also in EIs. Thus, the lack of integrin β3 could disturb the stabilization of erythroblastic island. This question was addressed in the present study using integrin $\beta3^{-/-}$ mice in comparison to mice constitutively overexpressing EPO, which results in hematocrit values of up to 90%.

Despite being reported to suffer from chronic gastrointestinal bleeding due to impaired thrombocyte function (279), hematocrit, spleen size, plasma EPO level and RBC lifespan were rather marginally altered in $\beta3^{-/-}$ mice suggesting that erythropoiesis is only mildly stimulated in these mice. Flow cytometric measurement of erythrocyte size and peripheral blood smears did not indicate any morphological abnormality of erythrocytes in $\beta3^{-/-}$ mice.

Furthermore, β3 lacking mice did in contrast to tg6 mice no show reduced bone mass as assessed by quantitative μCT analysis of the trabecular bone. Thus, these data indicate less erythropoietic stimulation in β3 lacking mice compared to EPO overexpressing ones (tg6) that exhibit maximally stimulated erythropoiesis as shown previously (280, 281,282).

However, when analyzing peripheral blood of $\beta3^{-/-}$ and tg6 mice regarding reticulocyte staining intensity, CD47 expression and, band 4.1a / 4.1b ratio we found that peripheral blood of integrin β3 lacking mice contains more immature peripheral erythrocytes than that of tg6 mice. Of note, in contrast to tg6 mice peripheral red cells of $\beta3^{-/-}$ mice even retained calnexin, a protein that is normally completely lost during maturation of the reticulocytes before they are released to the circulation. In addition, flow cytometric measurements of erythroblast developmental stages in bone marrow from β3 lacking but not from EPO overexpressing tg6 mice revealed a reduced percentage of latest stage erythroblasts. Moreover, in β3 lacking but not tg6 mice the number of erythroblasts per EI was also reduced. These data led to the conclusion that integrin β3 might play an important role for the stabilization of EIs and that the lack of β3 integrin could result in preterm release of immature reticulocytes into circulation.

Taken together, by comparing stress erythropoiesis in two genetically modified animals ($\beta3^{-/-}$ and tg6 mice), we discovered a new functional role of integrin β3 for stabilization of erythropoietic islands. β3 integrin appears to be important especially during the very late stage of red cell maturation by delaying release of premature reticulocytes. Interestingly, neoplastic diseases of the erythroid linage are characterized by abnormally immature peripheral red cells, which might be due to a disturbed expression pattern of adhesion molecules in the neoplastic cells resulting in decreased EI stability. Whether this is indeed the case and whether tests regarding calnexin expression on peripheral erythrocytes or staining intensity of reticulocytes might be useful in detecting early stages of neoplasias of the erythroid linage should be addressed in future studies.

REFERENCES

1. Palis J. Ontogeny of erythropoiesis. Curr Opin Hematol. 2008; 15:155-61.

2. Orlic D, Wu JM, Carmichael RD, et al. Increased erythropoiesis and 2′5′—A polymerase activity in the marrow and spleen of phenylhydrazine-injected rats. Exp Hematol. 1982; 10:478-85.

3. Broudy VC, Lin NL, Priestely GV, et al. Interaction of Stem Cell Factor and its receptor c-kit mediates lodgment and acute expansion of hematopoietic cells in the murine spleen. Blood. 1996; 88:75-81.

4. Ou LC, Kim D, Layton Jr WM, et al. Splenic erythropoiesis in polycythemic response of the rat to high-altitude exposure. J Appl Physiol.1980; 48:857-61.

5. Vannucchi AM, Paoletti F, Linari S, et al. Identification and characterization of a bipotent (erythroid and megakaryocytic) cell precursor from the spleen of phenylhydrazine-treated mice. Blood. 2000; 95:2559-68.

6. Sabin FR. Studies on the origin of blood-vessels and red blood-corpuscles as seen in the living blastoderm of chicks during the second day of incubation. Contr Embryol. 1920; 9:215-62.

7. Haar JL, Ackerman GA. Ultrastructural changes in mouse yolk sac associated with the initiation of vitelline circulation. Anat Rec. 1971; 170:437-56.

8. Haar JL, Ackerman GA. A phase and electron microscopic study of vasculogenesis and erythropoiesis in the yolk sac of the mouse. Anat Rec.1971; 170:199-223.

9. Ferkowicz MJ, Yoder MC. Blood island formation: longstanding observations and modern interpretations. Exp Hematol. 2005; 33:1041-9.

10. Baron MH. Embryonic origins of mammalian hematopoiesis. Exp Hematol. 2003; 31:1160 -9.

11. Choi K. The hemangioblast: a common progenitor of hematopoietic and endothelial cells. J Hematother Stem Cell Res. 2002; 11:91-101.

12. Oostendorp RA, Harvey KN, Kusadasi N, et al. Stromal cell lines from mouse aorta - gonad - mesonephros subregions are potent supporters of hematopoietic stem cell activity. Blood. 2002; 99:1183-9.

13. Palis J, Robertson S, Kennedy M, et al. Development of erythroid and myeloid progenitors in the yolk sac and embryo proper of the mouse. Development. 1999; 126:5073-84.

14. Yokomizo T, Takahashi S, Mochizuki N, et al. Characterization of GATA-1(+) hemangioblastic cells in the mouse embryo. EMBO J. 2007; 26:184-96.

15. Tsai FY, Keller G, Kuo FC, et al. An early haematopoietic defect in mice lacking the transcription factor GATA-2. Nature. 1994; 371:221-6.

16. Tsai F-Y, Orkin SH. Transcription factor GATA-2 is required for proliferation/ survival of early hematopoietic cells and mast cell formation, but not for erythroid and myeloid terminal differentiation. Blood. 1997; 89:3636-43.

17. Weiss MJ, Orkin SH. Transcription factor GATA-1 permits survival and maturation of erythroid precursors by preventing apoptosis. Proc Natl Acad Sci USA. 1995; 92:9623-27.

18. Gregory T, Yu C, Ma A, et al. GATA-1 and erythropoietin cooperate to promoter erythroid cell survival by regulating bcl-xl expression. Blood. 1999; 94:87-96.

19. Lugus JJ, Chung YS, Mills JC, et al. GATA2 functions at multiple steps in hemangioblast development and differentiation. Development 2007; 134:393-405.

20. Perlingeiro RC. Endoglin is required for hemangioblast and early hematopoietic development. Development. 2007; 134:3041-8.

21. McGrath KE, Koniski AD, Malik J, et al. Circulation is established in a step-wise pattern in the mammalian embryo. Blood. 2003; 101:1669-76.

22. Lucitti JL, Jones EA, Huang C, et al. Vascular remodeling of the mouse yolk sac requires hemodynamic force. Development. 2007; 134:3317-26.

23. Ji RP , Phoon CK , Aristiz á bal O , et al. Onset of cardiac function during early mouse embryogenesis coincides with entry of primitive erythroblasts into the embryo proper. Circ Res. 2003; 92:133-5.

24. Kingsley PD, Malik J, Fantauzzo K, et al. Yolk sac-derived primitive erythroblasts enucleate during mammalian embryogenesis. Blood. 2004; 104:19-25.

25. Fantoni A, de la Chapelle A, Marks PA. Synthesis of embryonic hemoglobins during erythroid cell development in fetal mice. J Biol Chem. 1969; 244:675-81.

26. McGrath KE, Kingsley PD, Koniski AD, et al. Enucleation of primitive erythroid cells generates a transient population of "pyrenocytes" in the mammalian fetus. Blood. 2008; 111:2409-17.

27. Skutelsky E, Danon D. An electron microscopic study of nuclear elimination from the late erythroblast. J Cell Biol. 1967; 33:625-35.

28. Wong PMC, Chung SW, Chui DHK, et al. Properties of the earliest clonogenic hemopoietic precursors to appear in the developing murine yolk sac. Proc Natl Acad Sci USA. 1986; 83:3851-4.

29. Kurata H, Mancini GC, Alespieti G, et al. Stem cell factor induces proliferation and differentiation of fetal progenitor cells in the mouse. Br J Haematol. 1998; 101:676-87.

30. Emerson SG, Shanti T, Ferrara JL, et al. Developmental regulation of erythropoiesis by hematopoietic growth factors: analysis on populations of BFU-E from bone marrow, peripheral blood, and fetal liver. Blood. 1989; 74:49-55.

31. Migliaccio AR, Migliaccio G. Human embryonic hemopoiesis: control mechanisms underlying progenitor differentiation in vitro. Dev Biol. 1988; 125:127-34.

32. Rich IN, Kubanek B. Erythroid colony formation in foetal liver and adult bone marrow and spleen from the mouse. Blood. 1976; 33:171-80.

33. Koury MJ, Bondurant MC. The molecular mechanism of erythropoietin action. Eur J Biochem. 1992; 210:649-63.

34. Koury MJ, Sawyer ST, Brandt SJ. New insights into erythropoiesis. Curr Opin Hematol. 2002; 9:93-100.

35. Iscove NN, Sieber F, Winterhalter KH. Erythroid colony formation in cultures of mouse and human bone marrow: analysis of the requirement for erythropoietin by gel filtration and affinity chromatography on agarose-concanavalin A. J Cell Physiol. 1974; 83:309-20.

36. Stephenson JR, Axelrad AA, McLeod DL, et al. Induction of colonies of hemoglobin-synthesizing cells by erythropoietin in vitro. Proc Natl Acad Sci USA. 1971; 68:1542-6.

37. Chasis JA. Erythroblastic islands: specialized microenvironmental niches for erythropoiesis. Curr Opin Hematol. 2006; 13:137-41.

38. Yoshida H, Kawane K, Koike M, et al. Phosphatidylserine-dependent engulfment by macrophages of nuclei from erythroid precursor cells. Nature. 2005; 437:754- 8.

39. Gronowicz G, Swift H, Steck TL. Maturation of the reticulocyte in vitro. J Cell Sci. 1984; 71:177-97.

40. Koury MJ, Koury ST, Kopsombut P, et al. In vitro maturation of nascent reticulocytes to erythrocytes. Blood. 2005; 105:2168-74.

41. Bessis M. L'ilot erythroblastique. Unite functionelle de la moelle osseuse. Rev Hematol. 1958; 13:8-11.

42. Bessis MC, Breton-Gorius J. Iron metabolism in the bone marrow as seen by electron microscopy: a critical review. Blood. 1962; 19:635-63.

43. Bessis M, Mize C, Prenant M. Erythropoiesis: comparison of in vivo and in vitro amplification. Blood Cells. 1978; 4:155-74.

44. Austyn JM, Gordon S. F4/80, a monoclonal antibody directed specifically against the mouse macrophage. Eur J Immunol. 1981; 11:805-15.

45. Hume DA, Robinson AP, MacPherson GG, et al. The mononuclear phagocyte system of the mouse defined by immunohistochemical localization of antigen F4/80. Relationship between macrophages, Langerhans cells, reticular cells, and dendritic cells in lymphoid and hematopoietic organs. J Exp Med. 1983; 158:1522-36.

46. Hanspal M, Hanspal JS. The association of erythroblasts with macrophages promotes erythroid proliferation and maturation: a 30-kD heparin-binding protein is involved in this contact. Blood. 1994; 84:3494-504.

47. Hanspal M, Smockova Y, Uong Q. Molecular identification and functional characterization of a novel protein that mediates the attachment of erythroblasts to macrophages. Blood. 1998; 92:2940-50.

48. Soni S, Bala S, Gwynn B, et al. Absence of erythroblast macrophage protein (Emp) leads to failure of erythroblast nuclear extrusion. J Biol Chem. 2006; 281:20181-9.

49. Sadahira Y, Yoshino T, Monobe Y. Very late activation antigen 4-vascular cell adhesion molecule 1 interaction is involved in the formation of erythroblastic islands. J Exp Med. 1995; 181:411-5.

50. Lee G, Lo AJ, Short S, et al. Adhesion molecule ICAM-4 participates in erythroblastic island formation. Blood. 2004; 104:168a.

51. Lee G, Lo AJ, Short S, et al. Targeted gene deletion demonstrates that adhesion molecule ICAM-4 is critical for erythroblastic island formation. Blood. 2005; 106:474a.

52. Seki M, Shirasawa H. Role of the reticular cells during maturation process of the erythroblast. 3. The fate of phagocytized nucleus. Acta Pathol Jpn. 1965; 15:387- 405.

53. Skutelsky E, Danon D. On the expulsion of the erythroid nucleus and its phagocytosis. Anat Rec. 1972; 173:123-6.

54. Chasis JA, Mohandas N. Erythroblastic islands: niches for erythropoiesis. Blood. 2008; 112:470-8.

55. Lee JC, Gimm JA, Lo AJ, et al. Mechanism of protein sorting during erythroblaste nucleation: role of cytoskeletal connectivity. Blood. 2004; 103:1912-9.

56. Kawane K, Fukuyama H, Kondoh G, et al. Requirement of DNase II for definitive erythropoiesis in the mouse fetal liver. Science. 2001; 292:1546-9.

57. Leimberg MJ, Prus E, Konijn AM, et al. Macrophages function as a ferritin iron source for cultured human erythroid precursors. J Cell Biochem. 2008; 103:1211- 8.

58. Lee EY, Chang CY, Hu N, et al. Mice deficient for Rb are nonviable and show defects in neurogenesis and haematopoiesis. Nature. 1992; 359:288−94.

59. Clarke AR, Maandag ER, van Roon M, et al. Requirement for a functional Rb-1 gene in murine development. Nature. 1992; 359:328-30.

60. Spike BT, Dibling BC, Macleod KF. Hypoxic stress underlies defects in erythroblast islands in the Rb-null mouse. Blood. 2007; 110:2173-81.

61. Clark AJ, Doyle KM, Humbert PO. Cell-intrinsic requirement for pRb in erythropoiesis. Blood. 2004; 104:1324-6.

62. Mohandas N, Chasis JA. The erythroid niche: molecular processes occurring within erythroblastic islands. Transfus Clin Biol. 2010; 17:110-1.

63. Sadahira Y, Mori M. Role of the macrophage in erythropoiesis. Pathol Int. 1999; 49:841-5.

64. Yokoyama T, Kitagawa H, Takeuchi T, et al. No apoptotic cell death of erythroid cells of erythroblastic islands in bone marrow of healthy rats. J Vet Med Sci. 2002; 64:913-9.

65. Rhodes MM, Kopsombut P, Bondurant MC, et al. Adherence to macrophages in erythroblastic islands enhances erythroblast proliferation and increases erythrocyte production by a different mechanism than erythropoietin. Blood. 2008; 111:1700-8.

66. Inada T, Iwama A, Sakano S, et al. Selective expression of the receptor tyrosine kinase, HTK, on human erythroid progenitor cells. Blood. 1997; 89:2757-65.

67. Suenobu S, Takakura N, Inada T, et al. A role of EphB4 receptor and its ligand, ephrin-B2, in erythropoiesis. Biochem Biophys Res Commun. 2002; 293:1124- 31.

68. Muta K, Krantz SB, Bondurant MC, et al. Stem cell factor retards differentiation of normal human erythroid progenitor cells while stimulating proliferation. Blood. 1995; 86:572-80.

69. Matsushima T, Nakashima M, Oshima K, et al. Receptor binding cancer antigen expressed on SiSo cells, a novel regulator of apoptosis of erythroid progenitor cells. Blood. 2001; 98:313-21.

70. De Maria R, Testa U, Luchetti L, et al. Apoptotic role of Fas/Fas ligand system in the regulation of erythropoiesis. Blood. 1999; 93:796-803.

71. Liu Y, Pop R, Sadegh C, et al.Suppression of Fas-FasL coexpression by erythropoietin mediates erythroblast expansion during the erythropoietic stress response in vivo. Blood. 2006; 108:123-33.

72. Pevny L, Lin CS, D'Agati V, et al. Development of hematopoietic cells lacking transcription factor GATA-1. Development. 1995; 121:163-72.

73. Pevny L, Simon MC, Robertson E, et al. Erythroid differentiation in chimaeric mice blocked by a targeted mutation in the gene for transcription factor GATA-1. Nature. 1991; 349:257-60.

74. Weiss MJ, Keller G, Orkin SH. Novel insights into erythroid development revealed through in vitro differentiation of GATA-1 embryonic stem cells. Genes Dev. 1994; 8:1184-97.

75. Fujiwara Y, Browne CP, Cunniff K, et al. Arrested development of embryonic red cell precursors in mouse embryos lacking transcription factor GATA-1. Proc Natl Acad Sci USA. 1996; 93:12355-8.

76. Whyatt D, Lindeboom F, Karis A, et al. An intrinsic but cell-nonautonomous defect in GATA-1-overexpressing mouse erythroid cells. Nature. 2000; 406:519- 24.

77. Whyatt DJ, Karis A, Harkes IC, et al. The level of the tissue-specific factor GATA-1 affects the cell-cycle machinery. Genes Funct. 1997; 1:11-24.

78. Gutiérrez L, Lindeboom F, Langeveld A, et al. Homotypic signalling regulates Gata1 activity in the erythroblastic island. Development. 2004; 131:3183-93.

79. Kurtz A, Hartl W, Jelkmann W, et al. Activity in fetal bovine serum that stimulates erythroid colony formation in fetal mouse livers is insulinlike growth factor I. J Clin Invest. 1985; 76:1643-8.

80. Porter P, Ogawa M. Erythroid burst promoting activity (BPA). In: Dunn CDR, ed. Current Concepts in Erythropoiesis. New York: Wiley; 1983:81.

81. Sawada K, Krantz SB, Dessypris EN, et al. Human colony-forming units- erythroid do not require accessory cells, but do require direct interaction with insulin-like growth factor I and/or insulin for erythroid development. J Clin Invest. 1989; 83:1701-9.

82. Angelillo-Scherrer A, Burnier L, Lambrechts D et al. Role of Gas6 in erythropoiesis and anemia in mice. J Clin Invest. 2008; 118:583-96.

83. Tordjman R, Delaire S, Plouet J, et al. Erythroblasts are a source of angiogenic factors. Blood. 2001; 97:1968-74.

84. Dai C, Chung IJ, Jiang S, et al. Reduction of cell cycle progression in human erythroid progenitor cells treated with tumour necrosis factor alpha occurs with reduced CDK6 and is

partially reversed by CDK6 transduction. Br J Haematol. 2003; 121:919-27.

85. Zermati Y, Fichelson S, Valensi F, et al. Transforming growth factor inhibits erythropoiesis by blocking proliferation and accelerating differentiation of erythroid progenitors. Exp Hematol. 2000; 28:885-94.

86. Nemeth E, Ganz T. Regulation of iron metabolism by hepcidin. Annu Rev Nutr. 2006; 26:323-42.

87. Secchiero P, Melloni E, Heikinheimo M, et al. TRAIL regulates normal erythroid maturation through an ERK-dependent pathway. Blood. 2004; 103:517-22.

88. Eshghi S, Vogelezang MG, Hynes RO,et al. Alpha4beta1 integrin and erythropoietin mediate temporally distinct steps in erythropoiesis: integrins in red cell development. J Cell Biol. 2007; 177: 871-8

89. Rosemblatt M, Vuillet-Gaugler MH, Leroy C, et al. Coexpression of two fibronectin receptors, VLA-4 and VLA-5, by immature human erythroblastic precursor cells. J Clin Invest. 1991; 87:6-11.

90. Vuillett-Gaugler MH, Breton-Gorius Vainchenker W, Guichard J, et al. Loss of attachement to fibronectin with terminal erythroid differentiation. Blood. 1990; 75:865-73.

91. Gu Y, Sorokin L, Durbeej M, et al. Characterization of bone marrow laminins and identification of alpha5-containing laminins as adhesive proteins for multipotent hematopoietic FDCP-Mix cells. Blood. 1999; 93:2533-42.

92. Zen Q, Cottman M, Truskey G, et al. Critical factors in basal cell adhesion molecule/lutheran-mediated adhesion to laminin. J Biol Chem. 1999; 274:728-34.

93. Udani M, Zen Q, Cottman M, et al. Basal cell adhesion molecule/lutheran protein: The receptor critical for sickle cell adhesion to laminin. J Clin Invest. 1998; 101:2550-8.

94. El Nemer W, Gane P, Colin Y, et al. The lutheran blood group glycoproteins, the erythroid receptors for laminin, are adhesion molecules. J Biol Chem. 1998; 273:16686-93.

95. Parsons SF, Lee G, Spring FA, et al. Lutheran blood group glycoprotein and its newly characterized mouse homologue specifically bind alpha5 chain-containing human laminin with high affinity. Blood. 2001; 97:312-20.

96. Diwan A, Koesters AG, Odley AM, et al. Unrestrained erythroblast development in Nix-/- mice reveals a mechanism for apoptotic modulation of erythropoiesis. Proc Natl Acad Sci USA. 2007; 04:6794-9.

97. Schweers RL, Zhang J, Randall MS, et al. NIX is required for programmed mitochondrial clearance during reticulocyte maturation. Proc Natl Acad Sci USA. 2007; 104:19500-5.

98. Sandoval H, Thiagarajan P, Dasgupta SK, et al. Essential role for Nix in autophagic maturation of erythroid cells. Nature. 2008; 454:232-6.

99. Kundu M, Lindsten T, Yang CY, et al. Ulk1 plays a critical role in the autophagic clearance of mitochondria and ribosomes during reticulocyte maturation. Blood. 2008; 112:1493-502.

100. Fader CM, Colombo MI. Multivesicular bodies and autophagy in erythrocyte Maturation. Autophagy. 2006; 2:122-5.

101. Yousefi S, Simon HU. Autophagy in cells of the blood. Biochim Biophys Acta. 2009; 9:1461-4.

102. Trimborn T, Gribnau J, Grosveld F, et al. Mechanisms of developmental control of transcription in the murine [alpha]- and [beta]-globin loci. Genes Dev. 1999; 13:112-24.

103. Palis J, Yoder MC. Yolk - sac hematopoiesis: the first blood cells of mouse and man. Exp Hematol. 2001; 29:927-36.

104. Kingsley PD, Malik J, Emerson RL, et al. “Maturational” globin switching in primary primitive erythroid cells. Blood. 2006; 107:1667-72.

105. Jane SM, Cunningham JM . Molecular mechanisms of hemoglobin switching . Intl J Biochem Cell Biol. 1996; 28:1197-209.

106. Basu P, Morris PE, Haar JL, et al. KLF2 is essential for primitive erythropoiesis and regulates the human and murine embryonic beta-like globin genes in vivo. Blood. 2005; 106:2566-71.

107. Hodge D, Coghill E, Keys J, et al. A global role for EKLF in definitive and primitive erythropoiesis. Blood. 2006; 107:3359-70.

108. Nilson DG, Sabatino DE, Bodine DM, et al. Major erythrocyte membrane protein genes in EKLF-deficient mice. Exp Hematol. 2006; 34:705-12.

109. Kim SI, Bresnick EH. Transcriptional control of erythropoiesis: emerging mechanisms and principles. Oncogene. 2007; 26:6777-94.

110. Gregory JF 3rd. Case study: folate bioavailability. J Nutr. 2001; 131:376S-82S.

111. Halsted CH. The intestinal absorption of dietary folates in health and disease. J Am Coll Nutr. 1989; 8:650-8.

112. Seetharam B, Bose S, Li N. Cellular import of cobalamin (vitamin B-12). J Nutr. 1999 129:1761-64.

113. Shane B, Stokstad ELR. 1985. Vitamin B12-folate interrelationships. Annu Rev Nutr. 1985; 5:115-41.

114. Heath CW. Cytogenetic observations in vitamin B12 and folate deficiency. Blood. 1966; 27:800-15.

115. Menzies RC, Crossen PE, Fitzgerald PH, et al. Cytogenetic and cytochemical studies on marrow cells in B12 and folate deficiency. Blood. 1966; 28:581-94.

116. Wickramasinghe SN, Cooper EH, Chalmers DG. A study of erythropoiesis by combined morphologic, quantitative cytochemical and autoradiographic methods. Blood. 1968; 31:304-13.

117. Yoshida Y, Todo A, Shirakawa S, et al. Proliferation of megaloblasts in pernicious anemia as observed from nucleic acid metabolism. Blood. 1968; 31:292-303.

118. Koury MJ, Price JO, Hicks GG. Apoptosis in megaloblastic anemia occurs during DNA synthesis by a p53-independent, nucleoside-reversible mechanism. Blood. 2000; 96:3249-55.

119. Bills ND, Koury MJ, Clifford AJ, et al. Ineffective hematopoiesis in folate- deficient mice. Blood. 1992; 79:2273-80.

120. Koury MJ, Horne DW, Brown ZA, et al. 1997. Apoptosis of late stage erythroblasts in megaloblastic anemia: association with DNA damage and macrocyte production. Blood. 1997; 89:4617-23.

121. Koury MJ, Ponka P. New insights into erythropoiesis: the roles of folate, vitamin B12, and iron. Annu Rev Nutr. 2004; 24:105-31.

122. Miret S, Simpson RJ, McKie AT. Physiology and molecular biology of dietary iron absorption. Annu Rev Nutr. 2003; 23:283-301.

123. Gunshin H, Mackenzie B, Berger UV, et al. Cloning and characterization of a mammalian proton-coupled metal-ion transporter. Nature. 1997; 388: 482-8.

124. Qiu A, Jansen M, Sakaris A, et al. Identification of an intestinal folate transporter and the molecular basis for hereditary folate malabsorption. Cell. 2006; 127: 917- 28.

125. Ferris CD, Jaffrey SR, Sawa A, et al. Haem oxygenase-1 prevents cell death by regulating cellular iron. Nat Cell Biol. 1999; 1:152-7.

126. Donovan A, Brownlie A, Zhou Y, et al. Positional cloning of zebrafish ferroportin1 identifies a conserved vertebrate iron exporter. Nature. 2000; 403:776-81.

127. Vulpe CD, Kuo YM, Murphy TL, et al. Hephaestin, a ceruloplasmin homologue implicated in intestinal iron transport, is defective in the sla mouse. Nat Genet. 1999; 21:195-9.

128. Canonne-Hergaux F, Gruenheid S, Ponka P, et al.Cellular and subcellular localization of the Nramp2 iron transporter in the intestinal brush border and regulation by dietary iron. Blood. 1999; 93:4406-17.

129. Rolfs A, Bonkovsky HL, Kohlroser JG, et al. Intestinal expression of genes involved in iron absorption in humans. Am J Physiol Gastrointest Liver Physiol. 2002; 282:598-607.

130. Lee PL, Gelbart T, West C, et al. The human Nramp2 gene: characterization of the gene structure, alternative splicing, promoter region and polymorphisms. Blood Cells Mol Dis. 1998; 24:199-215.

131. Maines MD. The heme oxygenase system: a regulator of second messenger gases. Annu Rev Pharmacol Toxicol. 1997; 37:517-54.

132. Ponka P, Lok CN. The transferrin receptor: role in health and disease. Int Biochem Cell Biol. 1999; 31:1111-37.

133. Richardson DR, Ponka P. The molecular mechanisms of the metabolism and transport

of iron in normal and neoplastic cells. Biochim Biophys Acta. 1997; 1331:1-40.

134. Ponka P. Tissue-specific regulation of iron metabolism and heme synthesis: distinct control mechanisms in erythroid cells. Blood. 1997; 89:1-25.

135. Mikulits W, Schranzhofer M, Beug H, et al. Post-transcriptional control via iron-responsive elements: the impact of aberrations in hereditary disease. Mutat Res. 1999; 437:219-30.

136. Spivak JL. Iron and the anemia of chronic disease. Oncology. 2002; 16:25-33.

137. Williams DE, Eisenman J, Baird A, et al. Identification of a ligand for the c-kit proto-oncogene. Cell. 1990; 63:167-74.

138. Nocka K, Tan JC, Chui E, et al. Molecular bases of dominant negative and loss of function mutations at the murine c-kit/white spotting locus: W37, Wv, W41 and W. EMBO J. 1990; 9:1805-13.

139. Stanley ER, Heard PM. Factors regulating macrophage production and growth: purification and some properties of the colony stimulating factor from medium conditioned by mouse L cells. J Biol Chem. 1977; 252:4305-12.

140. Burgess AW, Camakaris J, Metcalf D. Purification and properties of colony-stimulating factor from mouse lung-conditioned medium. J Biol Chem. 1977; 252:1998-2003.

141. Nicola NA, Metcalf D, Matsumoto M, et al. Purification of a factor inducing differentiation in murine myelomonocytic leukemia cells: identification as granulocyte colony-stimulating factor. J Biol Chem. 1983; 258:9017-23.

142. Metcalf D, Nicola NA. Proliferative effects of purified granulocyte colony- stimulating factor (G-CSF) on normal mouse hemopoietic cells. J Cell Physiol. 1983; 116:198-206.

143. Ihle JN, Keller J, Henderson L, et al. Procedures for the purification of interleukin 3 to homogeneity. J Immunol. 1982; 129:2431-6.

144. Lopez AF, Begley CG, Williamson DJ, et al. Murine eosinophil differentiation factor: an eosinophil-specific colony-stimulating factor with activity for human cells. J Exp Med. 1986; 163:1085-99.

145. Metcalf D. The unsolved enigmas of leukemia inhibitory factor. Stem Cells. 2003;

21:5-14.

146. Paul SR, Bennett F, Calvetti JA, et al. Molecular cloning of a cDNA encoding interleukin 11, a stromal cell-derived lymphopoietic and hematopoietic cytokine. Proc Natl Acad Sci USA. 1990; 87:7512-6.

147. Wendling F, Maraskovsky E, Debili N, et al. cMpl ligand is a humoral regulator of megakaryocytopoiesis. Nature. 1994; 369: 571-4.

148. Reissman K. Studies on the mechanism of erythropoietic stimulation in parabiotic rats during hypoxia. Blood. 1950; 5:372-80.

149. Erslev A. Humoral regulation of red cell production. Blood. 1953; 8:349-57.

150. Stopka T, Zivny JH, Stopkova P, et al. Human hematopoietic progenitors express erythropoietin. Blood. 1998; 91:3766-72.

151. Tong Z, Yang Z, Patel S, et al. Promoter polymorphism of the erythropoietin gene in severe diabetic eye and kidney complications. Proc Natl Acad Sci USA. 2008; 105:6998-7003.

152. Tam BY, Wei K, Rudge JS, et al. VEGF modulates erythropoiesis through regulation of adult hepatic erythropoietin synthesis. Nat Med. 2006; 12:793-800.

153. Weidemann A, Kerdiles YM, Knaup KX, et al. The glial cell response is an essential component of hypoxia-induced erythropoiesis in mice. J Clin Invest 2009; 119:3373-83.

154. Koury ST, Koury MJ, Bondurant MC, et al. Quantitation of erythropoietin- producing cells in kidneys of mice by in situ hybridization: correlation with hematocrit, renal erythropoietin mRNA and serum erythropoietin concentration. Blood. 1989; 74:645-51.

155. Smith TG, Robbins PA, Ratcliffe PJ. The human side of hypoxia-inducible factor. Br J Hematol. 2008; 141:325-34.

156. Jelkmann WE, Fandrey J, Frede S, et al. Inhibition of erythropoietin production by cytokines. Implications for the anemia involved in inflammatory states. Ann N Y Acad Sci. 1994; 718:300-9.

157. Krantz SB. Pathogenesis and treatment of the anemia of chronic disease. Am J Med Sci. 1994; 307:353-4.

158. Jelkmann W. Molecular biology of erythropoietin. Intern Med. 2004; 43:649 -59.

159. Rogers HM, Yu X, Wen J, et al. Hypoxia alters progression of the erythroid program. Exp Hematol. 2008; 36:17-27.

160. Ema M, Taya S, Yokotani N, et al. A novel bHLH-PAS factor with close sequence similarity to hypoxia-inducible factor 1α regulates the VEGF expression and is potentially involved in lung and vascular development. Proc Natl Acad Sci USA. 1997; 94:4273-8.

161. Gu YZ, Moran SM, Hogenesch JB, et al. Molecular characterization and chromosomal localization of a third α-class hypoxia inducible factor. Gene Expr.1998; 7:205-13.

162. Wiesener MS, Jurgensen JS, Rosenberger C, et al. Widespread hypoxia-inducible expression of HIF-2α in distinct cell populations of different organs. FASEB J. 2003; 17:271-3.

163. Stroka DM, Burkhardt T, Desbaillets I, et al. HIF-1 is expressed in normoxic tissue and displays an organ-specific regulation under systemic hypoxia. FASEB J. 2001; 15:2445-53.

164. Chowdhury R, Hardy A, Schofield CJ. The human oxygen sensing machinery and its manipulation. Chem Soc Rev. 2008; 37:1308-19.

165. Gordan JD, Simon MC. Hypoxia-inducible factors: central regulators of the tumor phenotype. Curr Opin Genet Dev. 2007; 17:71-7.

166. Semenza GL. Regulation of mammalian O2 homeostasis by hypoxia-inducible factor 1. Annu Rev Cell Dev Biol. 1999; 15:551-78.

167. Semenza G, Wang G. A nuclear factor induced by hypoxia via de novo protein synthesis binds to the human erythropoietin gene enhancer at a site required for transcriptional activation. Mol Cell Biol. 1992; 12 5447-54.

168. Wang GL, Semenza GL. Purification and characterization of HIF-1. J Biol Chem. 1995; 270:1230-7.

169. Semenza GL, Nejfelt MK, Chi SM, et al. Hypoxia-inducible nuclear factors bind to an enhancer element located 3' to the human erythropoietin gene. Proc Natl Acad Sci USA. 1991; 88:5680-4.

170. Bruick RK, McKnight SL. A conserved family of prolyl-4-hydroxylases that modify

HIF. Science. 2001; 294:1337-40.

171. D'Andrea AD, Lodish HF, Wong GG. Expression cloning of the murine erythropoietin receptor. Cell. 1989; 57:277-85.

172. Sato T, Watanabe S, Ishii E, et al. Induction of the erythropoietin receptor gene and acquisition of responsiveness to erythropoietin by stem cell factor in HML/SE, a human leukemic cell line. J Biol Chem. 1998; 273:16921-6.

173. Freeman RS, Hasbani DM, Lipscomb EA, et al. SM-20, EGL-9, and the EGLN family of hypoxia-inducible factor prolyl hydroxylases. Mol Cells. 2003; 16:1-12.

174. Oehme F, Ellinghaus P, Kolkhof P, et al. Overexpression of PH-4, a novel putative proline 4-hydroxylase, modulates activity of hypoxia-inducible transcription factors. Biochem Biophys Res Commun. 2002; 296:343-9.

175. Huang J, Zhao Q, Mooney SM, et al. Sequence determinants in hypoxia- inducible factor-1α for hydroxylation by the prolyl hydroxylases PHD1, PHD2, and PHD3. J Biol Chem. 2002; 277:39792-800.

176. Aprelikova O, Chandramouli GV, Wood M, et al. Regulation of HIF prolyl hydroxylases by hypoxia-inducible factors. J Cell Biochem. 2004; 92:491-501.

177. Winter SS, Howard T, Ware RE. Regulation of expression of the human erythropoietin receptor gene. Blood Cells Mol Dis. 1996; 22:214-24.

178. Taniguchi S, Dai CH, Price JO, et al. Interferon gamma downregulates stem cell factor and erythropoietin receptors but not insulin-like growth factor-I receptors in human erythroid colony-forming cells. Blood. 1997; 90: 2244-52.

179. Broudy VC, Lin N, Brice M, et al. Erythropoietin receptor characteristics on primary human erythroid cells. Blood. 1991; 15:2583-90.

180. Koury MJ, Bondurant MC. Erythropoietin retards DNA breakdown and prevents programmed death in erythroid progenitor cells. Science. 1990; 248:378-81.

181. Wu H, Liu X, Jaenisch R, et al. Generation of committed erythroid BFU-E and CFU-E progenitors does not require erythropoietin or the erythropoietin receptor. Cell. 1995; 83:59-67.

182. Kelley LL, Koury MJ, Bondurant MC, et al. Survival or death of individual proerythroblasts results from differing erythropoietin sensitivities: a mechanism for controlled rates of erythrocyte production. Blood. 1993; 82:2340-52.

183. Witthuhn BA, Quelle FW, Silvennoinen O, et al. JAK2 associates with the erythropoietin receptor and is tyrosine phosphorylated and activated following stimulation with erythropoietin. Cell. 1993; 74:227-36.

184. Miura O, Nakamura N, Quelle FW, et al. Erythropoietin induces association of the JAK2 protein tyrosine kinase with the erythropoietin receptor in vivo. Blood. 1994; 84:1501-7.

185. Elliott S, Pham E, Macdougall IC. Erythropoietins: a common mechanism of action. Exp Hematol. 2008; 36:1573-84.

186. Richmond TD, Chohan M, Barber DL. Turning cells red: signal transduction mediated by erythropoietin. Trends Cell Biol. 2005; 15:146-55.

187. Tong W, Zhang J, Lodish HF. Lnk inhibits erythropoiesis and Epo-dependent JAK2 activation and downstream signaling pathways. Blood. 2005; 105:4604-12.

188. Ang SO, Chen H, Gordeuk VR, et al. Endemic polycythemia in Russia: mutation in the VHL gene. Blood Cells Mol Dis. 2002; 28:57-62.

189. Schafer AI. Molecular basis of the diagnosis and treatment of polycythemia vera and essential thrombocythemia. Blood. 2006; 107:4214-22.

190. James C, Ugo V, Le Couedic JP, et al. A unique clonal JAK2 mutation leading to constitutive signalling causes polycythaemia vera. Nature. 2005; 434:1144-8.

191. Scott LM, Tong W, Levine RL, et al. JAK2 exon 12 mutations in polycythemia vera and idiopathic erythrocytosis. N Engl J Med. 2007; 356:459-68.

192. Kralovics R, Passamonti F, Buser AS, et al. A gain-of-function mutation of JAK2 in myeloproliferative disorders. N Engl J Med. 2005; 352:1779-90.

193. Silva M, Richard C, Benito A, et al. Expression of Bcl-x in erythroid precursors from patients with polycythemia vera. N Engl J Med. 1998; 338:564-71.

194. Cheng EH, Wei MC, Weiler S, et al. BCL-2, BCL-X(L) sequester BH3 domain-only

molecules preventing BAX- and BAK-mediated mitochondrial apoptosis. Mol Cell. 2001; 8:705-11.

195. Lindsten T, Ross AJ, King A, et al. The combined functions of proapoptotic Bcl-2 family members bak and bax are essential for normal development of multiple tissues. Mol Cell. 2000; 6:1389-99.

196. Wei MC, Zong WX, Cheng EH, et al. Proapoptotic BAX and BAK: a requisite gateway to mitochondrial dysfunction and death. Science. 2001; 292:727-30.

197. Lenox LE, Shi L, Hegde S, et al. Extramedullary erythropoiesis in the adult liver requires BMP-4/Smad5-dependent signaling. Exp Hematol. 2009; 37:549-58.

198. Ploemacher RE, van Soest PL. Morphological investigation on phenylhydrazine-induced erythropoiesis in the adult mouse liver. Cell Tissue Res. 1977; 178: 435-61.

199. Ploemacher RE, van Soest PL, Vos O. Kinetics of erythropoiesis in the liver induced in adult mice by phenylhydrazine. Scand J Haematol. 1977; 19:424-34.

200. Porayette P, Paulson RF. BMP4/Smad5 dependent stress erythropoiesis is required for the expansion of erythroid progenitors during fetal development. Dev Biol. 2008; 317:24-35.

201. Perry JM, Harandi OF, Paulson RF. BMP4, SCF, and hypoxia cooperatively regulate the expansion of murine stress erythroid progenitors. Blood. 2007; 109:4494-502.

202. Broudy VC, Lin NL, Priestley GV, et al. Interaction of stem cell factor and its receptor c-kit mediates lodgment and acute expansion of hematopoietic cells in the murine spleen. Blood. 1996; 88:75-81.

203. Hara H, Ogawa M. Erthropoietic precursors in mice with phenylhydrazine- induced anemia. Am J Hematol. 1976; 1:453-8.

204. Wickrema A, Bondurant MC, Krantz SB. Abundance and stability of erythropoietin receptor mRNA in mouse erythroid progenitor cells. Blood. 1991; 78:2269-75.

205. Wickrema A, Krantz SB, Winkelmann JC, et al. Differentiation and erythropoietin receptor gene expression in human erythroid progenitor cells. Blood. 1992; 80:1940-9.

206. Lenox LE, Perry JM, Paulson RF. BMP4 and Madh5 regulate the erythroid response to acute anemia. Blood. 2005; 105:2741-8.

207. Vemula S, Ramdas B, Hanneman P, et al. Essential role for focal adhesion kinase in regulating stress hematopoiesis. Blood. 2010; 116:4103-15.

208. Kalfa TA, Pushkaran S, Zhang X, et al. Rac1 and Rac2 GTPases are necessary for early erythropoietic expansion in the bone marrow but not in the spleen. Haematologica. 2010; 95:27-35.

209. Vacha J. Red cell life span. In: Agar NS, Board PG, eds. Red blood cells of domestic mammals. New York: Elsevier, 1983; 67-132.

210. Boas FE, Forman L, Beutler E. Phosphatidylserine exposure and red cell viability in red cell aging and in hemolytic anemia. Proc Natl Acad Sci USA. 1998; 95:3077-81.

211. Connor J, Pak CC, Schroit AJ. Exposure of phosphatidylserine in the outer leaflet of human red blood cells: relationship to cell density, cell age, and clearance by mononuclear cells. J Biol Chem.1994; 269:2399-404.

212. Beppu M, Mizukami A, Nagoya M, et al. Binding of anti-band 3 autoantibody to oxidatively damaged erythrocytes: formation of senescent antigen on erythrocyte surface by an oxidative mechanism. J Biol Chem.1990; 265:3226-33.

213. Kiefer CR, Snyder LM. Oxidation and erythrocyte senescence. Curr Opin Hematol. 2000; 7:113-6.

214. Bosman CJCGM , Willekens FLA, Were JM. Erythrocyte aging: a more than superficial resemblance to apoptosis? Cell Physiol Biochem. 2005; 16:1-8.

215. Lang F, Lang KS, Lang PA, et al. Mechanisms and significance of eryptosis. Antioxid Redox Signal. 2006; 8:1183-92.

216. Lang KS, Lang PA, Bauer C, et al. Mechanisms of suicidal erythrocyte death. Cell Physiol Biochem. 2005; 15:195-202.

217. Bratosin D, Estaquier J, Petit F, et al. Programmed cell death in mature erythrocytes: a model for investigating death effector pathways operating in the absence of mitochondria. Cell Death Differ. 2001; 8:1143-56.

218. Bratosin D, Mazurier J, Tissier JP, et al. Cellular and molecular mechanisms of senescent erythrocyte phagocytosis by macrophages: a review. Biochimie. 1998; 80:173-95.

219. Vaysse J, Gattegno L, Bladier D, et al. Adhesion and erythrophagocytosis of human senescent erythrocytes by autologous monocytes and their inhibition by β-galactosyl derivatives. Proc Natl Acad Sci USA. 1986; 83:1339-43.

220. McEvoy L, Williamson P, Schlegel RA. Membrane phospholipid asymmetry as a determinant of erythrocyte recognition by macrophages. Proc Natl Acad Sci USA. 1986; 83:3311-5.

221. Arese P, Turrini F, Schwarzer E. Band 3/complement-mediated recognition and removal of normally senescent and pathological human erythrocytes. Cell Physiol Biochem. 2005; 16:133-46.

222. Ando K, Kikugawa K, Beppu M. Induction of band 3 aggregation in erythrocytes results in anti-band 3 autoantibody binding to carbohydrate epitopes of band 3. Arch Biochem Biophys. 1997; 339:250-7.

223. Ensnick A, Biondi CS, Marini A, et al. Effect of membrane-bound IgG and desialysation in the interaction of monocytes with senescent erythrocytes. Clin Exp Med. 2006; 6:138-42.

224. Sambrano GR, Parthasarathy S, Steinberg D. Recognition of oxidatively damaged erythrocytes by a macrophage receptor with specificity for oxidized low density lipoprotein. Proc Natl Acad Sci USA. 1994; 91:3265-9.

225. Sambrano GR, Steinberg D. Recognition of oxidatively damaged and apoptotic cells by an oxidized low density lipoprotein receptor on mouse peritoneal macrophages: role of membrane phosphatidylserine. Proc Natl Acad Sci USA. 1995; 92:1396-400.

226. Tanaka K, Usui Y, Kojo S. Role of serum components in the binding and phagocytosis of oxidatively damaged erythrocytes by autologous mouse macrophages. Cell Mol Life Sci. 2001; 58:1727-33.

227. Terpstra V, van Berkel TJC. Scavenger receptors on liver Kupffer cells mediate the in vivo uptake of oxidatively damaged red blood cells in mice. Blood. 2000; 95:2157-63.

228. Aderem AA, Underhill DM. Mechanisms of phagocytosis in macrophages. Annu Rev Immunol. 1999; 17:593-623.

229. Peiser L, Gordon S. The function of scavenger receptors expressed by macrophages and their role in the regulation of inflammation. Microbes Infect. 2001; 3:149-59.

230. Taylor PA, Martinez-Pomares L, Stacey M, et al. Macrophage receptors and immune recognition. Annu Rev Immunol. 2005; 23:901-44.

231. Rettig MP, Low PS, Gimm JA, et al. Evaluation of biochemical changes during in vivo erythrocyte senescence in the dog. Blood. 1999; 93:376-84.

232. Kay MMB. Band 3 and its alterations in health and disease. Cell Mol Biol 2004; 50:117-38.

233. Glader B: Destruction of erythrocytes; in Lee GR, Foerster J, Lukens J et al. (eds): Wintrobe's Clinical Hematology. Williams and Wilkins, Baltimore, 2004, 11th edition, 249-65.

234. Lutz HU. Innate immune and nonimmune mediators of erythrocyte clearance. Cell Mol Biol. 2004; 50:107-16.

235. Oldenborg PA, Zheleznyak A, Fang YF, et al. Role of CD47 as a marker of self on red blood cells. Science. 2000; 288:2051-4.

236. Avent N, Judson PA, Parsons SF, et al. Monoclonal antibodies that recognize different membrane proteins that are deficient in Rhnull human erythrocytes. One group of antibodies reacts with a variety of cells and tissues whereas the other group is erythroid-specific. Biochem J. 1988; 251:499-505.

237. Reinhold MI, Lindberg FP, Plas D, et al. In vivo expression of alternatively spliced forms of integrin-associated protein (CD47). J Cell Sci. 1995; 108:3419- 25.

238. Mateo V, Lagneaux L, Bron D, et al. CD47 ligation induces caspase-independent cell death in chronic lymphocytic leukemia. Nat Med. 1999; 5:1277-84.

239. Cocco RE, Ucker DS. Distinct modes of macrophage recognition for apoptotic and necrotic cells are not specified exclusively by phosphatidylserine exposure. Mol Bio Cell. 2001; 12:919-30.

240. Oldenborg PA, Gresham HD, Lindberg FP. CD47-signal regulatory protein alpha (SIRPalpha) regulates Fcgamma and complement receptor-mediated phagocytosis. J Exp Med. 2001; 193:855-62.

241. Kuypers FA , De Jong K. The role of phosphatidylserine in recognition and removal of erythrocytes. Cell Mol Biol. 2004; 50:147-58.

242. Krieser RJ, White K. Engulfment mechanism of apoptotic cells. Curr Opin Cell Biol. 2002; 14:734-8.

243. Alper SL. Molecular physiology of SLC4 anion exchangers. Exp Physio. 2006; 911:153-61.

244. Werre JM, Willekens FLA, Bosch FH, et al. The red cell revisited: matters of life and death. Cell Mol Biol. 2004; 50:139-45.

245. Kay MMB. Immunoregulation of cellular life span. Ann N Y Acad Sci. 2005; 1057:85-111.

246. Campanella ME, Chu H, Low PS. Assembly and regulation of a glycolytic enzyme complex on the human erythrocyte membrane. Proc Natl Acad Sci USA. 2005; 102:2402-7.

247. Willekens FLA, Bosch FH, Roerdinkholder-Stoelwinder B, et al. Quantification of loss of haemoglobin components from the circulating red blood cell in vivo. Eur J Haematol. 1997; 58:246-50.

248. Bosch FH, Werre JM, Schipper L et al. Determinants of red blood cell deformability in relation to cell age. Eur J Haematol. 1994; 52:35-41.

249. Greenwalt TJ. The how and why of exocytic vesicles. Transfusion. 2006; 46:143-52.

250. Bosman GJ, Werre JM, Willekens FL, et al. Erythrocyte ageing in vivo and in vitro: structural aspects and implications for transfusion. Transfus Med. 2008. 6:335-47.

251. Willekens FLA, Werre JM, Kruijt JK, et al. Liver Kupffer cells rapidly remove red blood cell-derived vesicles from the circulation by scavenger receptors. Blood. 2005; 105:2141-5.

252. Chang TL, Cubillos FF, Kakhniashvili DG, et al. Band 3 is a target of protein of spectrin's E2/E3 activity: implication for sickle cell disease and normal red blood cell aging. Cell Mol Biol. 2004; 50:171-7.

253. Salzer U, Prohaska R. Stomatin, flotillin-1, and flotillin-2 are major integral proteins of erythrocyte lipid rafts. Blood. 2001; 97:1141-3.

254. Salzer U, Hinterdorfer P, Hunger U, et al. Ca++-dependent vesicle release from erythrocytes involves stomatin-specific lipid rafts, synexin (annexin VII), and sorcin. Blood.

2002; 99:2569-77.

255. Peters LL, Shivdasani RA, Liu S-C, et al. Anion exchanger 1 (band 3) is required to prevent erythrocyte membrane surface loss but not to form the membrane skeleton. Cell. 1996; 86:917-27.

256. Willekens FLA, Roerdinkholder-Stoelwinder B, Groenen-Döpp YAM et al. Hemoglobin loss from erythrocytes in vivo results from spleen-facilitated vesiculation. Blood. 2003; 101:747-51.

257. Lang F, Lang KS, Wieder T, et al. Cation channels, cell volume and the death of an erythrocyte. Pflügers Arch. 2003; 447:121-5.

258. Lang KS, Duranton C, Poehlmann H, et al. Cation channels trigger apoptotic death of erythrocytes. Cell Death Differ. 2003; 10:249-56.

259. Huttner W, Zimmerberg J. Implications of lipid microdomains for membrane curvature, budding and fission. Curr Opin Cell Biol. 2001; 13:478-84.

260. Hynes RO. Integrins: versatility, modulation, and signaling in cell adhesion. Cell. 1992; 69:11-25.

261. Rupp PA, Little CD. Integrins in vascular development. Circ Res. 2001; 89:566- 72.

262. Pierschbacher MD, Ruoslahti E. Cell attachment activity of fibronectin can be duplicated by small synthetic fragments of the molecule. Nature. 1984; 309:30-3.

263. Xiong JP, Stehle T, Zhang R, et al. Crystal structure of the extracellular segment of integrin alphaVbeta3 in complex with an Arg-Gly-Asp ligand. Science. 2002; 296:151-5.

264. Gabriel HM, Oliveira EI. Role of abciximab in the treatment of coronary artery disease. Expert Opin Biol Ther. 2006; 6:935-42.

265. Lawler J, Weinstein R, Hynes RO. Cell attachment to thrombospondin: the role of ARG-GLY-ASP, calcium, and integrin receptors. J Cell Biol. 1988; 107:2351- 61.

266. Engleman VW, Nickols GA, Ross FP, et al. A peptidomimetic antagonist of the alpha(v)beta3 integrin inhibits bone resorption in vitro and prevents osteoporosis in vivo. J Clin Invest. 1997; 99:2284-92.

267. Albelda SM, Mette SA, Elder DE, et al. Integrin distribution in malignant melanoma: association of the beta 3 subunit with tumor progression. Cancer Res. 1990; 50:6757-64.

268. Cheresh DA, Harper JR. Arg-Gly-Asp recognition by a cell adhesion receptor requires its 130-kDa alpha subunit. J Biol Chem. 1987; 262:1434-7.

269. Teitelbaum SL. Osteoclasts, integrins, and osteoporosis. J Bone Miner Metab. 2000; 18:344-9.

270. Clover J, Dodds RA, Gowen M. Integrin subunit expression by human osteoblasts and osteoclasts in situ and in culture. J Cell Sci. 1992; 103:267-71.

271. Brooks PC, Silletti S, von Schalscha TL, et al. Disruption of angiogenesis by PEX, a noncatalytic metalloproteinase fragment with integrin binding activity. Cell. 1998; 92:391-400.

272. Eliceiri BP, Cheresh DA. The role of alphav integrins during angiogenesis: insights into potential mechanisms of action and clinical development. J Clin Invest. 1999; 103:1227-30.

273. Felding-Habermann B, O'Toole TE, Smith JW, et al. Integrin activation controls metastasis in human breast cancer. Proc Natl Acad Sci USA. 2001; 98:1853-8.

274. Taverna D, Moher H, Crowley D, et al. Increased primary tumor growth in mice null for beta3- or beta3/beta5-integrins or selectins. Proc Natl Acad Sci USA. 2004; 101:763-8.

275. Taverna D, Crowley D, Connolly M, et al. A direct test of potential roles for beta3 and beta5 integrins in growth and metastasis of murine mammary carcinomas. Cancer Res. 2005; 65:10324-9.

276. Reynolds LE, Conti FJ, Lucas M, et al. Accelerated re-epithelialization in beta3-integrin-deficient- mice is associated with enhanced TGF-beta1 signaling. Nat Med. 2005; 11:167-74.

277. Weng S, Zemany L, Standley KN, et al. Beta3 integrin deficiency promotes atherosclerosis and pulmonary inflammation in high-fat-fed, hyperlipidemic mice. Proc Natl Acad Sci USA. 2003; 100:6730-5.

278. Kieffer N, Phillips DR. Platelet membrane glycoproteins: functions in cellular interactions. Annu Rev Cell Biol. 1990; 6:329-5.

279. Hodivala-Dilke KM, McHugh KP, Tsakiris DA, et al. Beta3- integrin -deficient mice are a model for Glanzmann thrombasthenia showing placental defects and reduced survival. J Clin Invest. 1999; 103:229-38.

280. Ruschitzka FT, Wenger RH, Stallmach T, et al. Nitric oxide prevents cardiovascular disease and determines survival in polyglobulic mice overexpressing erythropoietin. Proc Natl Acad Sci USA. 2000; 97:11609-13.

281. Vogel J, Kiessling I, Heinicke K, et al. Transgenic mice overexpressing erythropoietin adapt to excessive erythrocytosis by regulating blood viscosity. Blood. 2003; 102:2278-84.

282. Bogdanova A, Mihov D, Lutz H, et al. Enhanced erythro-phagocytosis in polycythemic mice overexpressing erythropoietin. Blood. 2007; 110:762-9.

283. Hermand P, Gane P, Callebaut I, et al. Integrin receptor specificity for human red cell ICAM-4 ligand. Critical residues for alphaIIbeta3 binding. Eur J Biochem. 2004; 271:3729-40.

APPENDIX

PREFACE

This part contains

1. A published article named “What is the optimal anesthetic protocol for measurements of cerebral autoregulation in spontaneously breathing mice?” by Zhenghui Wang, Beat Schuler, Olga Vogel, Margarete Arras and Johannes Vogel.

2. Curriculum Vitae of Zhenghui Wang.

Exp Brain Res (2010) 207:249–258
DOI 10.1007/s00221-010-2447-4

RESEARCH ARTICLE

What is the optimal anesthetic protocol for measurements of cerebral autoregulation in spontaneously breathing mice?

Zhenghui Wang · Beat Schuler · Olga Vogel · Margarete Arras · Johannes Vogel

Received: 17 May 2010 / Accepted: 30 September 2010 / Published online: 24 October 2010

Abstract Autoregulation, an important feature of the cerebral circulation, is affected in many diseases. Since genetically modified mice are a fundamental tool in biomedical research, including neuro(bio)logy also in this specie measurements of cerebral autoregulation (CA) are mandatory. However, this requires anesthesia that unfortunately significantly impacts cerebral perfusion and consequently might distort CA measurements directly or by altering arterial pCO_2. The latter can be avoided by artificial ventilation but requires several control measurements of blood gases, each consuming at least 100 µl of blood or 5% of a mouse's blood volume. To avoid such diagnostic hemorrhage, we systematically analyzed the effect of different common anesthetic protocols used for rodents in spontaneously breathing mice on CA measured with Laser speckle perfusion imaging. Halothane, Isoflurane and Pentobarbital abrogated CA and Ketamin/Xylazine as well as Chloralose had a moderate reproducibility. In contrast, the rather rarely used anesthetic Ethomidate applied in low doses combined with local anesthetics had the best reproducibility. Although with this anesthesia the lower CA limit was lower than with Ketamin/Xylazine and Chloralose as reported in the handful of papers so far dealing with CA in mice, we suggest Ethomidate as the anesthetic of choice for CA measurements in spontaneously breathing mice.

Z. Wang · B. Schuler · O. Vogel · J. Vogel (✉)
Institute of Veterinary Physiology,
Vetsuisse Faculty University of Zürich and Zürich Center for Integrative Human Physiology (ZIHP),
Winterthurerstr. 260, 8057 Zürich, Switzerland
e-mail: jvogel@vetphys.uzh.ch

M. Arras
Department of Clinical Research,
University Hospital Zürich, Zürich, Switzerland

Keywords Cerebral blood flow · Laser Doppler flowmetry · Cerebral circulation · Pial arteries · Anesthetics · Mice

Introduction

Normally, in the brain, perfusion and local metabolic demand are closely linked (Kuschinsky 1990, 1991), and as long as the metabolic demand of the brain remains constant, a homeostatic regulatory mechanism called cerebral auto-regulation (CA) allows the cerebral blood flow (CBF) to remain relatively constant during variations in arterial blood pressure (Paulson et al. 1990). When CA is abolished, fluctuations of arterial blood pressure are accompanied by either passive reduction or increase in CBF, leading to syncope and falls, severe cerebral ischemia and edema (Faraci and Heistad 1998). Mostly, disturbed CA is due to chronic hypertension (Immink et al. 2004) resulting in higher CA limits thereby making chronic hypertensive patients highly vulnerable to brain ischemia in response to unforeseen hypotension (Strandgaard 1976). Although the upward shift of the CA limits in chronic hypertension has been described many years ago (Vorstrup et al. 1984; Harper 1987; Werber et al. 1990), its cause(s) are still poorly understood. However, genetically modified mice raise new options to answer also this question. Thus, there is a certain need for a reliable technique to measure CA in mice.

Measurements of the CBF response to blood pressure changes consider either dynamic or static CA (Panerai 2008). Dynamic CA is a transient response to spontaneous fluctuations in systemic arterial blood pressure, changes in posture or other maneuvers resulting in a sudden blood pressure change. In man, dynamic CA can be assessed with

transcranial Doppler ultrasound and (noninvasive) blood pressure recordings together with wavelet analysis (Novak et al. 2004; Hu et al. 2008; Lo et al. 2008). Unfortunately, such a technique is not available for mice. In rodents including mice, dynamic CA can be assessed by carotid clamping (Rosengarten et al. 2006; Schubert et al. 2008). Static CA is defined as the steady-state relationship between CBF and mean arterial blood pressure characterized in humans by a constant CBF between mean arterial blood pressures of approximately 50 and 150 mmHg. Static CA is measured in experimental animals using Laser Doppler flowmetry after exposure of the skull or brain surface together with manipulations of the blood pressure by controlled bleeding (until complete exsanguination) sometimes combined with phenylepinephrine infusion via catheters inserted to the femoral vessels. It is obvious that such measurements require sufficient anesthesia. However, anesthetics themselves influence the reactivity of the brain arterioles either directly e.g. volatile anesthetics dilate arteries due to attenuation of Ca^{2+} entry through voltage-gated Ca^{2+} channels on vascular smooth muscle cells (Bosnjak et al. 1992) or, especially in spontaneously breathing animals, indirectly by respiratory depression that increases arterial pCO_2. Brain vessels are very sensitive to CO_2, and therefore, increased pCO_2 values are accompanied by cerebral vasodilatation (Kuschinsky 1997) and failure of CA. The impact of the arterial pCO_2 becomes even more obvious when considering reports showing that the CA disturbed by Isoflurane anesthesia could be improved by hypocapnia (McCulloch et al. 2005). Although the CO_2 problem can be circumvented by artificial ventilation of the animal, the latter introduces an additional trauma and lengthens surgery. More importantly, the adjustment of the respirator requires several blood gas analyses, each of it consuming at least 100 µl blood. In larger animals, such as rats, this is no problem, but in mice 100 µl equals about 5% of the total blood volume. In mice blood loss, prolonged operations and increased operative trauma per se easily distort the blood acid base status, most evident from a drop in base excess (own unpublished observations). The reduced base excess is either accompanied by a drop in arterial pH and/or compensatory decrease of the arterial pCO_2. Since pial arteries are also sensitive to hydrogen ions (Kuschinsky 1982), both changes again influence either way the constriction state of brain arterioles.

The present study aimed to systematically evaluate different commonly used anesthetic protocols on static CA in spontaneously breathing mice. Specifically, for measurement of CA in rats Barbiturates (Merzeau et al. 2000; Paterno et al. 2000), volatile anesthetics such as Halothane (Verhaegen et al. 1993; Pedersen et al. 2003) or Isoflurane (Ayata et al. 2004; Tonnesen et al. 2005), Ketamine/Xylazine, Chloralose urethane (Niwa et al. 2002) or Chloralose alone (Ayata et al. 2004; Rosengarten et al. 2006) have been used. In general, in the mentioned studies, the rats were artificially ventilated. In a previous study with a setting that is very sensitive to impaired cerebral vasoreactivity on spontaneously breathing rats, we were using Ethomidate (Vogel and Kuschinsky 1996) that is known to have relatively little effect on CBF (Janssen et al. 1975; Famewo and Odugbesan 1978). The present study shows that Ethomidate provides the most consistent measurements, appears to preserve the cerebral vasoreactivity best and is thus recommended as the anesthetic of choice for CA measurements in spontaneously breathing mice.

Methods

All experiments were performed on C57Bl6 mice and conformed to the Guide for the Care and Use of Laboratory Animals published by the US National Institutes of Health (NIH Publication No. 85–23, revised 1996) and institutional guidelines and were approved by the Cantonal Veterinary Department, Zurich, Switzerland. Since there was no gender difference for any anesthetic protocol, mice of both genders were used for the study except for telemetric blood pressure and heart rate measurements where only males were used.

Generally, the same anesthetic was used for surgery and the subsequent experiments. Since in case of Ethomidate this is not possible, surgery was performed during Isoflurane anesthesia (2–2.5%) and the animals were allowed to adapt for at least 30 min after discontinuing Isoflurane and commencing the Ethomidate infusion before the CA measurements were started. All anesthetic protocols are summarized in Table 1. During surgery and the subsequent experiment, the body temperature of the animals was kept constant at 37°C using a temperature controlled heating pad.

After induction of anesthesia, the mice were equipped with catheters in both femoral arteries and veins for the measurement of blood pressure, heart rate (PlugSys, Hugo Sachs Electronics, Germany and PowerLab, ADInstruments, Germany), blood gases and acid–base status (AVL700, Radiometer Medical, Denmark) and hematocrit and the infusion of anesthetics (cf. Table 1) and phenylepinephrine. Before closing the wounds, a drop of 2% Lidocain (Streuli, Switzerland) was applied to the wound. Thereafter the mice were placed in a stereotactic frame, the scull was exposed and flushed with 2% Lidocain. Then a Laser speckle perfusion imager (moorFLPI, Moor Instruments, UK) was adjusted to its maximal magnification and five regions of interest (ROI's, 3 on the left and 2 on the right hemisphere) were defined avoiding visible vessels. In accordance with others (Ayata et al. 2004), preliminary

Table 1 Anesthetic protocols

Active component	Trade name	Provider	Route	Initial dosage	Maintenance dosage
Ethomidate	Ethomidate Lipuro	B. Braun Medical AG, Sempach, Germany[a]	i.v.	80 µg/min for 3 min	14–26 µg/min
Ketamine/Xylazine	Rompun/ Narketan	Ratiopharm, Ulm, Germany/Bayer, Leverkusen, Germany	i.p.	90 mg kg^{-1}/ 9 mg kg^{-1}	40 mg kg^{-1} every 30 min/4 mg kg^{-1} every 30 min
Alpha-chloralose		Siqma-Aldrich GmbH, Buchs, Switzerland[b, c]	i.p./i.v.	25 mg kg^{-1}	75 mg kg^{-1} h^{-1}
Isoflurane	IsoFlo	Abbott AG, Baar, Switzerland	Inhalation	5%	1.50%
Haiotnane	Halothane	Arovet AG, Zollikon-Station, Switzerland	Inhalation	4%	0.90%
Pentobarbital	Vetanarcol	Veterinaria AG, Zurich, Switzerland[c]	i.p./i.v	100 mg kg^{-1}	1 mg kg^{-1} h^{-1}

[a] After finishing the preparation during Isoflurane anesthesia

[b] 16.6 mg Chloralose dissolved together with 25 mg sodiumtetraborate * $10H_2O$/ml H_20

[c] After finishing the preparation changed to i.v. application

experiments have shown that the transparency of the scull of mice is high enough to not reduce significantly the laser signal as long as it is kept wet with artificial cerebrospinal fluid or 0.9% saline warmed to 37°C. The images were acquired at 25 Hz and the traces of the ROI's were sampled with a time constant of 0.5 s. During surgery and the subsequent measurements of static CA, animals were allowed to breathe pure oxygen spontaneously.

At the very beginning of the recordings, a screwdriver handle was dropped onto the arterial line connected to the blood pressure transducer. This produced an artifact simultaneously in both the blood pressure and the laser perfusion trace that was later used to synchronize both traces for offline calculation of the CA limits. Then the mice were slowly exsanguined via the second arterial line while continuously recording the laser speckle perfusion and blood pressure signal. The exsanguination rate was adjusted manually by continuous inspection of the blood pressure trace to get a linear and constant decrease of the blood pressure (about 1 mmHg/min, total exsanguination time: 35–40min). In addition, some animals anesthetized with Ethomidate, Chloralose or Ketamine/Xylazine received an infusion of phenylepinephrin (Sintetica, Switzerland, 1 ng/g/min) that was started 3 min before starting the CA measurement and lasted until its end.

For determination of the CA limits, all laser speckle perfusion and blood pressure values before the marker artifact were discarded and then the data were averaged in ten-second intervals using macros written in Excel (Microsoft). The laser speckle perfusion values obtained this way were then plotted as a function of the corresponding blood pressure values. Then the lower CA limit was determined by linear extrapolation by starting with the lowest blood pressure values and the upper limit in a similar way by starting with the highest blood pressure values as described elsewhere for the "plateau constraint" (Pedersen et al. 2003). This was done separately for each of the five ROI's. The final CA limits for each animal were defined as the mean of those determined for each ROI, and these mean values were used for statistical analysis. The intra-individual variation of the ROI's was very low (coefficient of variation: 1.3–2.8%).

Another experimental group was equipped with telemetric blood pressure sensors (TA11PA-C10 transmitter, Data-Sciences International, USA) as described recently (Schuler et al. 2009, 2010) to assess the effect of anesthesia on arterial blood pressure and heart rate in comparison with conscious animals. In an additional control experiment, the effect of switching from normal air to pure oxygen on Laser speckle imaging during Isoflurane and Ethomidate anesthesia has been assessed.

Data are presented as means ± standard deviation and were analyzed with the GraphPad PRISM 4 Software (version 4.01) using ANOVA and Students *t* test or Kruskal–Wallis test (in case the number of values were not equal for all groups) for unpaired samples with Bonferroni's or Dunn's post hoc test, respectively. *P* values of <0.05 were considered significant.

Results

Table 2 shows the physiologic variables of all naïve animals used for the study. The blood gas values of mice treated with phenylepinephrine were similar, but mean arterial blood pressure as well as heart rate were considerably higher by 53 and 61%, respectively (not shown). The most striking difference between the groups of naïve mice was found concerning the arterial pCO_2 with highest values in Pentobarbital and Ketamine/Xylazine anesthetized mice and lowest during Isoflurane anesthesia. In addition, heart rate

Table 2 Physiologic variables

	Weight (g)	pH	$pC0_2$ (mmHq)	pO_2 (mmHg)	BE (mmol/L)	HCT	Mean arterial blood pressure (mmHg)	Heart rate (min^{-1})	Anesthesia (abbr.)	*n*
Mean	31.00	7.44	36.71	369.00	1.58	43.32	81.52	407.B1	Ethomidate (E)	6
SD	3.79	0.06	7.07	46.62	2.20	3.05	5.90	84.40		
Mean	27.00	7.17*	53.98$^{\&}$	486.28	−4.37	43.17	92.03	248.14*	Ketamine/ Xylazine (K)	6
SD	4.10	0.02	8.62	131.67	3.86	1.22	7.79	42.12		
Mean	35.00*	7.43	40.43	366.36	3.30*	40.60	86.73	467.75	Chforaiose (C)	6
SD	2.83	0.05	5.51	145.64	2.87	1.38	12.55	76.22		
Mean	25.17	7.46	27.38	383.28	−4.77$^{\#}$	47.94	94.82$^{\#}$	430.00	Isofluran 1.2% (I)	6
SD	1.47	0.04	5.65	89.02	2.47	4.34	3.30	54.25		
Mean	27.50	7.29$^{\#}$	46.80/*	389.96	−3.43	44.50	84.40	402.55	Halothane 0.9% (H)	6
SD	4.85	0.03	4.12	124.03	1.07	1.49	4.69	60.70		
Mean	24.40	7.18*	69.14*	439.71	−3.92	43.10	78.93	304.93$^{\#}$	Pentobarbital (P)	5
SD	0.89	0.09	9.85	65.04	4.26	2.04	4.96	20.43		
Mean	25.68					42.87	104.19*	506.34	Telemetry (conscious) (T)	6
SD	1.01					3.82	2.33	49.06		
	*$P < 0.05$ vs. K, I, H, P, T	*$P < 0.05$ vs. I, H, E, C $^{\#}P < 0.05$ vs. I, E, C	*$P < 0.01$ vs. I, H, E, C $^{\&}P < 0.01$ vs. I, E, C $^{\#}P < 0.01$ vs. I	ns	*$P < 0.05$ vs. K, I, H, P $^{\#}P < 0.05$ vs. E	ns	*$P < 0.01$ vs. E, C, H, P $^{\#}P < 0.05$ vs. E, P	*$P < 0.01$ vs. E, C, I, H, T $^{\#}P < 0.01$ vs. C, T		

is lower in those anesthetic regimes that result in respiratory depression such as Ketamine/Xylazine and Pentobarbital. Most likely this is an effect of hypercapnia that has been shown to induce bradycardia in mice (Campen et al. 2004). The high pO_2 values in all experimental groups are due to pure oxygen breathing. The telemetric blood pressure and heart rate data had been obtained in the context of a recent study (Schuler et al. 2010). In comparison with these data, all anesthetics reduced blood pressure and heart rate. Switching from air to pure oxygen did not affect the blood pressure or the Laser speckle signal (data not shown).

Figure 1 shows example autoregulation curves (mean of all ROIs of a single animal) of all anesthetics tested without parallel phenylepinephrine infusion. Halothane as well as Isoflurane resulted in complete abrogation of CA that is for Isoflurane in agreement with previous reports (Ayata et al. 2004). A bit surprisingly, since also used in several studies dealing with CA, Pentobarbital anesthesia also was associated with a complete loss of CA. This is most probably due to the anesthesia-induced hypercapnia of the spontaneously breathing mice (cf. Table 2).

In Ketamine-/Xylazine- and Chloralose-anesthetized mice, the lower CA limit was around 44 and 53 mmHg, respectively, which is in agreement with previous reports on mice investigated using Chloralose (Ayata et al. 2004). In contrast, the lower CA limit in Ethomidate-anesthetized mice was considerably lower at around 25 mmHg and the drop was more abrupt than in Ketamine-/Xylazine- or Chloralose-anesthetized mice (cf. Fig. 1). However, in naïve animals, the differences in lower limit of CA reached statistical significance only for the comparison between Ethomidate and Chloralose. For Ethomidate, Ketamine/Xylazine and Chloralose, the lower limit was also determined during phenylepinephrine infusion resulting in the same limits (Fig. 2); however, between these groups, none of the differences were statistically significant. This is most likely due to much larger data scatter in Ketamine/Xylazine and

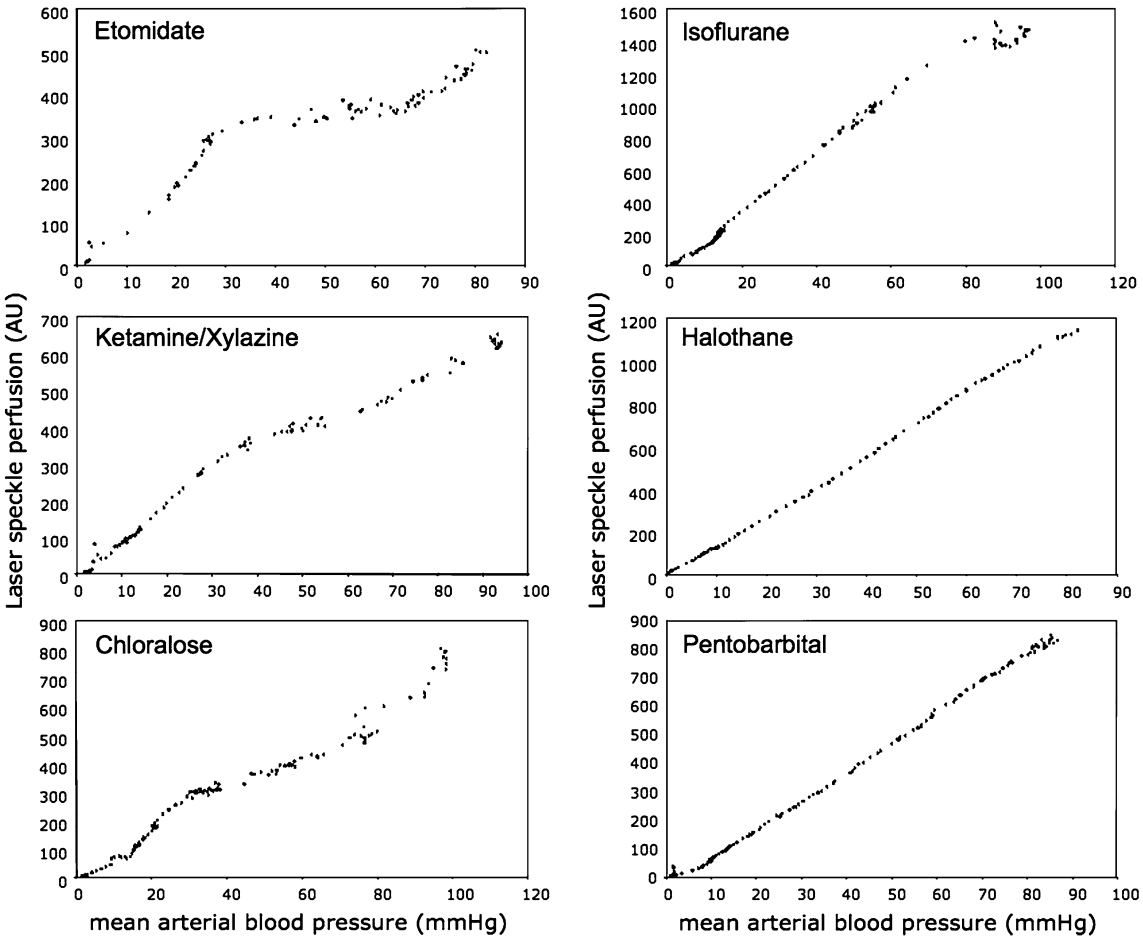

Fig. 1 Representative examples of autoregulation curves (mean of all five ROI's of a single animal) obtained with the different anesthetics as indicated. The anesthetics shown on the *right* completely abrogated cerebral autoregulation (CA). For Ethomidate, the range of CA is largest. Also in Ketamine-/Xylazine-anesthetized mice, the lower as well the upper CA limit can be seen, whereas in Chloralose-anesthetized mice, the upper limit is not visible since with falling blood pressure cerebral perfusion is reduced rather in an exponential fashion until the lower CA limit is reached

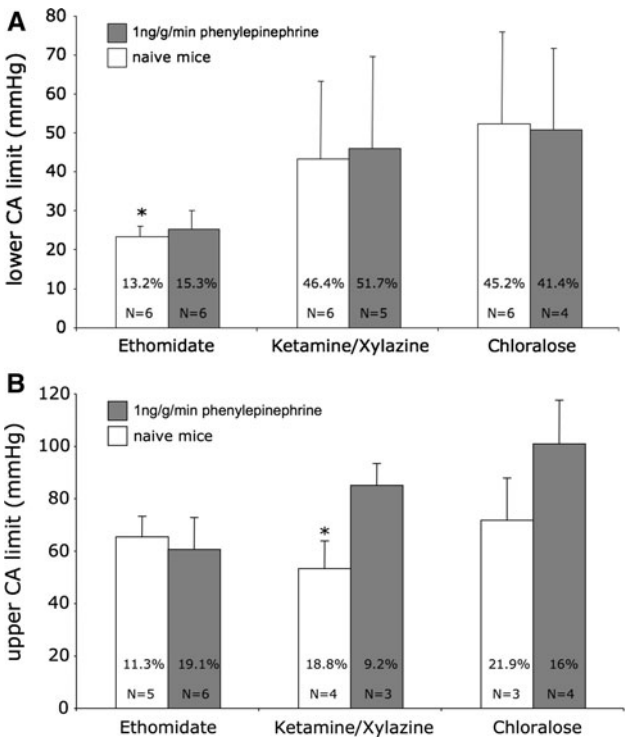

Fig. 2 Mean lower (**a**) and upper (**b**) CA limits determined mice with and without phenylepinephrine treatment. **a** The lower CA limit was the same with or without phenylepinephrine treatment but lowest during Ethomidate anesthesia. However, this was statistically significant only compared to Chloralose (both untreated, $*P < 0.05$), most likely due to the high data scatter in the Ketamine/Xylazine and Chloralose groups as indicated by the coefficient of variation (numbers in the first row). The more than 3-times smaller coefficient of variation indicates a better reproducibility during Ethomidate anesthesia compared to both, Ketamine/Xylazine and Chloralose. **b** Determination of the upper limit was hampered by the fact that some traces showed an exponential shape above the lower CA limit (cf. Fig. 1, Chloralose). In keeping with this limitation, the upper CA limits in Ketamine-/Xylazine- and Chloralose-anesthetized animals tended to be higher in case of phenylepinephrine treatment in contrast to Ethomidate-anesthetized mice. In Ketamine-/Xylazine- and Chloralose-anesthetized mice, the coefficient of variation was lower than that for the lower CA limit and in Ethomidate-anesthetized mice similar to that of the lower limit. $*P < 0.05$ vs. Chloralose + phenylepinephrine, means ± SD, N = number of animals per group

Chloralose anesthetized mice compared to those anesthetized with Ethomidate. Accordingly the coefficient of variation was between 3- and 3.9-times lower during Ethomidate anesthesia than during Ketamine/Xylazine and Chloralose anesthesia. These latter data indicate that Etomidate has the best reproducibility concerning the measurement of the lower CA limit.

Regarding the upper limit in some animals of all anesthetic protocols, the determination was not possible since above the lower limit the CA curves showed an exponential shape. This was even more the case in phenylepinephrine-treated mice. However, the best detection rate of an upper limit was found in Ethomidate-anesthetized mice. In contrast to the lower limit, there were no major differences in the upper limit between naïve mice anesthetized with Ethomidate, Ketamine/Xylazine or Chloralose. In phenylepinephrine-treated mice, the upper limit tended to be higher during Ketamine/Xylazine and Chloralose anesthesia. In contrast to the lower limit, the measurements of the upper limit appeared to be more stable (maximum coefficient of variation of about 22%) irrespective of the fact that sometimes the upper limit could not be determined at all.

By taking the measurements of the lower and upper limits together in naïve Ethomidate anesthetized mice, the CA range was considerably larger (42 mmHg vs. 9.9 and 19.2 mmHg during Ketamine/Xylazine and Chloralose anesthesia). During phenylepinephrine treatment, the differences between lower and upper limit were quite similar (34.6, 35.6 and 36.8 mmHg). The latter data however are based only on a few mice and thus should be taken with caution.

In addition, we aimed to assess the vasodilatation induced by the anesthetics themselves as well as the vasodilator capacity (defined as the difference between the initial and maximum perfusion per mmHg) in response to the falling blood pressure during the different anesthetic protocols. Although Laser speckle perfusion imaging does provide only semi-quantitative data, the measurements are quite stable as determined with a motility standard provided by the manufacturer of the imager along with the device. Thus, we calculated the initial Laser speckle perfusion/mmHg before exsanguination was started. In addition, we calculated the difference between the initial perfusion/mmHg and the maximal perfusion/mmHg before the final drop of the cerebral perfusion. In case there was no increase observed from the initial value, the perfusion/mmHg value at a blood pressure of 50 mmHg was taken. Figure 3 shows that there were large differences in the initial perfusion between the different anesthetics with a maximum factor of nearly 3 between Ethomidate and Halothane. Note that Halothane, Isoflurane, and Pentobarbital, which abrogated CA, exhibit the highest initial laser speckle perfusion as well as perfusion/mmHg values. This indicates anesthesia-induced vasodilatation. In line with this, the maximal increase in perfusion/mmHg as a result of the falling blood pressure was found also in Ethomidate-anesthetized mice (Fig. 4). In contrast, in Halothane-, Isoflurane-, and Pentobarbital-anesthetized mice, sometimes no increase at all could be observed but rather a continuous decrease of perfusion/mmHg from the very beginning until the end of the experiments. These findings indicate that Halothane, Isoflurane as well as Pentobarbital abrogate the vasoreactivity of brain vessels in spontaneously breathing mice and are therefore unsuited for CA measurements in this specie.

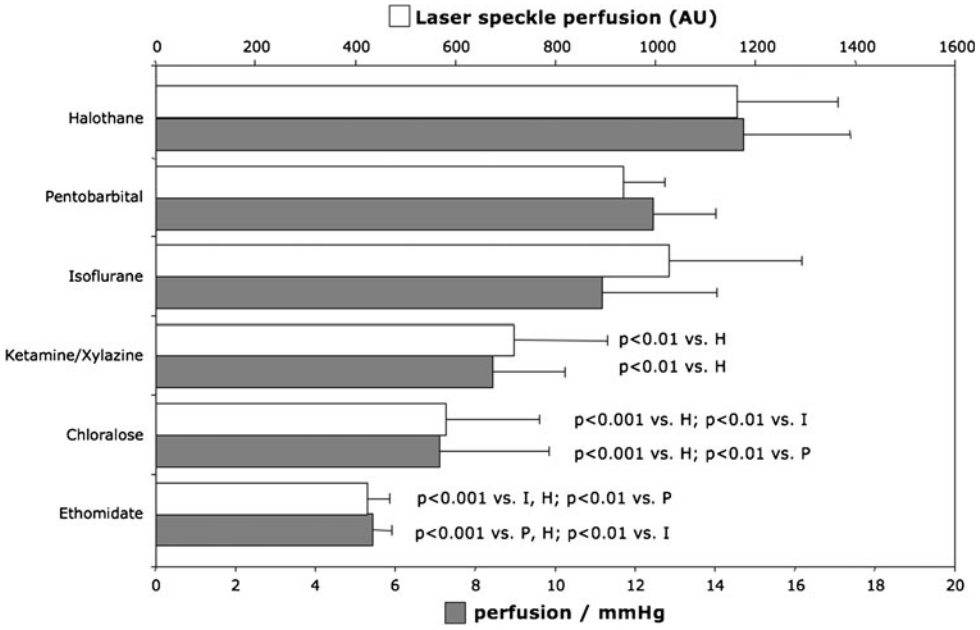

Fig. 3 Initial laser speckle perfusion (*white bars*) and initial perfusion normalized to the mean arterial blood pressure (*gray bars*). These data should be indicative for the vasodilatation state induced by the different anesthetics. Halothane, Isoflurane, and Pentobarbital that abrogated CA have the highest initial laser speckle perfusion as well as perfusion/mmHg values. *I* Isoflurane, *P* Pentobarbital, *H* Halothane

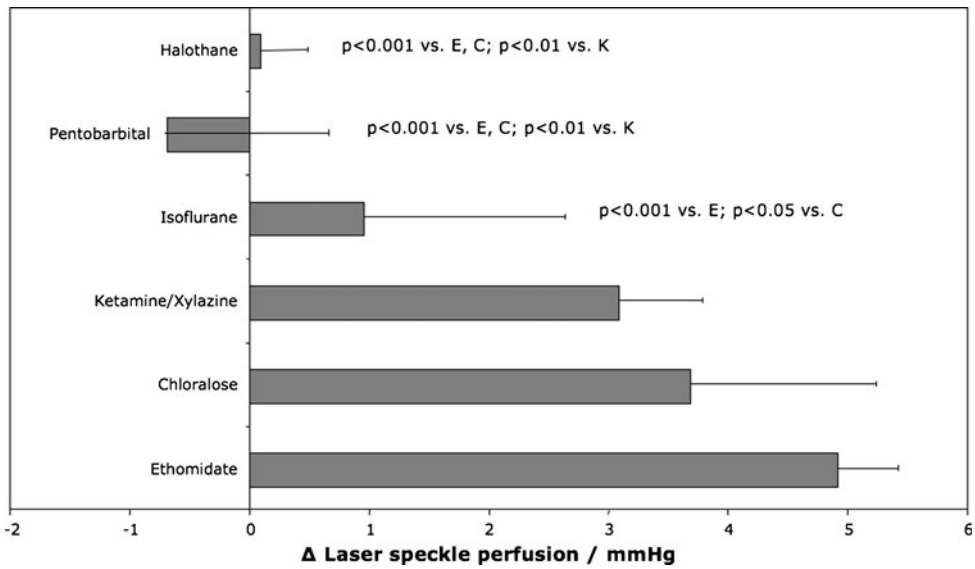

Fig. 4 Difference between the initial perfusion/mmHg and the maximal perfusion/mmHg. In contrast to Ethomidate, Ketamine/Xylazine and Chloralose anesthetized mice in Halothane, Pentobarbital and Isoflurane anesthetized mice more (Halothane) or less often (Isoflurane) no increase at all from the initial perfusion/mmHg value could be observed. In such a case, the perfusion/mmHg value at a blood pressure of 50 mmHg was taken. These data indicate that the highest vasodilatation reserve is present during Ethomidate anesthesia. *E* Ethomidate, *K* Ketamine/Xylazine, *C* Chloralose

Discussion

The present study clearly indicates that in spontaneously breathing mice, the anesthetic protocol for measurement of CA affects both the absolute values as well as the reproducibility of the measurements. In view of the high value of transgenic mice which are often also costly pre-treated before CA is finally measured, good reproducibility is an important point in choosing the anesthetic protocol to detect small but nevertheless biologic relevant differences between experimental groups. Here, we show that Ethomidate has an excellent reproducibility and retains reactivity of the cerebral vasculature best. Therefore, from all anesthetics tested in the present study, Ethomidate appears to be the anesthetic of choice for the measurement of CA in spontaneously breathing mice.

The best way to exclude any influence of anesthetics on mice appears to measure CA in the conscious state (Lacombe et al. 2005; Joutel et al. 2010). In these papers, the perfusion was quantified with Laser Doppler flowmetry via optical fibers glued to the scull of mice also equipped with catheters inside the femoral vessels. The animals had been placed in restrainers for 2 h before starting the final measurements. Laser speckle perfusion imaging that has been used in the present study, however, requires the scull to be fixed since it cannot distinguish tissue from red cell movements. In addition, restraining animals equipped with optical probes at the scull and catheters inside the femoral

vessels, even when treated with local anesthetics, for such a long period with final exsanguinations in the conscious state is difficult to get permitted in countries with strong animal protection laws such as Switzerland. Nevertheless CA measurements in conscious mice might allow assessing where the real limits are lying in this specie. In the aforementioned papers, the CA limits were determined in a different way when compared to the present study. These authors defined the lower limit as 90% and the upper limit as 110% of the initial blood flow. This way they obtained in wt mice a lower limit of about 60 mmHg, a value that is 15–20 mmHg above those reported by others for Ketamine/Xylazine and Chloralose (Niwa et al. 2002; Ayata et al. 2004; Tonnesen et al. 2005; Rosengarten et al. 2006) and that of the present study using the same anesthetics. However, when trying to apply the method for calculating the lower limit used in the present study (Pedersen et al. 2003) to the data of Lacombe et al. (2005) and Joutel et al. (2010) a lower limit of about 40–45 mmHg appears to be present also in their data. Thus, the lower CA limit in conscious mice is most close to our values and those of others obtained during Ketamine/Xylazine and Chloralose anesthesia. In Ethomidate-anesthetized mice, however, the lower limit is clearly lower, although there was only minor significance to the other anesthetics most likely due to much high data scatter in the Ketamine-/Xylazine- and Chloralose-anesthetized groups (cf. coefficients of variation, Fig. 2a). Concerning the upper limit, Lacombe et al. (2005) found during phenylepinephrine infusion and using their 110% method a value of 120 mmHg. Again when applying the method of the present study for determining the upper limit to their data the upper limit appears to be different, namely about 90 mmHg. Thus, the range of CA in mice appears to be about 40 mmHg. In naïve mice, a similar CA range was found only for Ethomidate-anesthetized mice, whereas in Ketamine-/Xylazine- and Chloralose-anesthetized mice, the range was 4- and 2-times smaller, respectively. In contrast, in phenylepinephrine treated mice, the CA range was not different between the different anesthetic protocols and with 35 mmHg also comparable to that found in naïve Ethomidate-anesthetized mice and that estimated from the data of conscious mice (Lacombe et al. 2005). Thus, Ethomidate appears to preserve the CA range best but to shift the autoregulation curve slightly leftward. In contrast, in naïve Ketamine-/Xylazine-and Chloralose-anesthetized mice, the CA range was clearly reduced suggesting an impaired vaso-reactivity that is also evident from the reduced maximal perfusion change per mmHg in response to the blood pressure drop (cf. Fig. 4). This is also in line with the lowest initial perfusion per mmHg in Ethomidate anesthesia (cf. Fig. 3), indicating a higher initial cerebrovascular constriction state and thus a higher vasodilatatory reserve.

Concerning Halothane only studies in rats could be found (Verhaegen et al. 1993; Pedersen et al. 2003), but Halothane slowly disappears from the market. In principle, the pharmacological action of Halothane is similar to that of Isoflurane but the wash-in and -out of Isoflurane is faster (Yasuda et al. 1989) enabling better control of the anesthesia. Thus, in recent years, Isoflurane became the standard volatile anesthetic also in animal research and was used in rats and mice for the measurement of cerebral blood flow under different conditions including functional stimulation (Ayata et al. 2004; Joutel et al. 2010) and cerebral autoregulation (Ayata et al. 2004; Tonnesen et al. 2005). One paper directly compared in mice Isoflurane with Choralose concerning CA as well as functional stimulation (Ayata et al. 2004) and found according to our results an abrogation of CA during Isoflurane anesthesia. In contrast, functional stimulation was not different between Isoflurane and Chloralose that is in line with the data of others also reporting in mice a preserved functional stimulation during Isoflurane anesthesia (Lacombe et al. 2005; Joutel et al. 2010) at an inspired concentration of 1.2–1.5%. We did not yet test Isoflurane and functional stimulation in mice, but previously in a study on rats, we used Ethomidate (Vogel and Kuschinsky 1996) because any functional stimulation-related CBF effect was abolished during Halothane anesthesia. This is in line with studies showing that the reactivity of the smooth muscle is impaired by volatile anesthetics (Bosnjak et al. 1992) as well with the data of the present study showing that Isoflurane like Halothane results in a complete loss of CA (cf. Fig. 1). However, a study dealing with the orthostatic regulation of mice claimed that CA was preserved during 1% Isoflurane anesthesia (Foley et al. 2005). Without measuring CA directly, this was concluded from the fact that phenylepinephrine increased mean arterial blood pressure but not CBF. However, phenylepinephrine results in a considerable tachycardia (in the present study by 61%) that in turn impairs cardiac output. Thus, an increased mean arterial blood pressure during phenylepinephrine treatment paralleled by a reduced cardiac output might leave CBF unchanged independent of an autoregulatory action of the cerebral vasculature.

The most significant problem when using Pentobarbital in spontaneously breathing animals is ventilatory depression that results in hypercapnia induced cerebral vasodilatation and subsequent loss of CA (cf. Table 2 and Fig. 1). To our knowledge, it has not yet been shown whether Barbiturates have also direct (pCO_2-independent) effects on CA, but dosages of pentobarbital previously published for paralyzed and artificially ventilated rats (Paterno et al. 2000) were not sufficient to keep our mice in the tolerance state. Consequently, we had to increase the dosage resulting in the highest arterial pCO_2 values of all groups. The present study was designed to test the effects of the different anesthetic

protocols in spontaneously breathing mice, because the great disadvantage of artificial ventilation is additional trauma and the necessity of several determinations of the arterial blood gases to adjust the respirator. Each blood gas determination requires at least about 100 µl of arterial blood. Thus, 2–3 determinations of blood gases can bring the animals close to a hemorrhagic shock. Although the lost blood can be replaced, e.g., by saline, this reduces the hematocrit and consequently the oxygen transport capacity of the blood that in turn increases CBF (Waschke et al. 1994). Of note, we supplemented the mice during the experiments with pure oxygen. In contrast to the vasodilating effect of hypoxia, CA is not different in man breathing either normal air or pure oxygen (Ogoh et al. 2010). In line with this study, we found no difference in the Laser speckle signal when switching from air to pure oxygen.

Using anesthetics for CA measurements has the principle and unavoidable disadvantage of influencing CBF and thus the CA measurement itself. In addition, anesthesia-induced hypercapnia might disturb CA. The same hold for intermittent sometimes un-recognized hypoxia that can occur during anesthesia especially when induced by injections. Since the brain is very sensitive to shortage of oxygen hyperoxia has been found to be very effective as emergency treatment in traumatic brain injury or stroke (Kumaria and Tolias 2009). Because it drastically reduces the risk of hypoxia during anesthesia but does not alter brain perfusion (cf. previous paragraph), we recommend supplying the mice with pure oxygen during surgery and subsequent CA measurements. Although hypercapnia and hypoxia can be avoided by artificial ventilation, this requires several determinations of the arterial blood gases, in mice easily resulting in a "diagnostic hemorrhage". In addition, one should be aware that transferability of data from animal experiments to the clinics could be hampered by the fact that different researchers perform CA measurements in a different way. One underestimated difference between protocols is anesthesia. Here, we aimed to find an anesthetic protocol that requires as little surgery as possible, to allow measurements in spontaneously breathing animals and has a high reproducibility. Such an anesthetic protocol reduces uncontrolled influences of side parameters on the data and thus increased the transferability of the data into clinics. Reproducibility is also a very important point in light of using valuable genetically modified mice that might be available only in limited numbers e.g. due to reduced breeding success. In this context also small systematic errors can be tolerated as long as the good reproducibility exceeds this disadvantage. Taken together, we feel that Ethomidate is—of the anesthetics tested here—the best due to its ability to keep the arterial pCO_2 in the normal range without the need of artificial ventilation, its excellent reproducibility, and a CA range closest to that of conscious animals (Lacombe et al. 2005; Joutel et al. 2010). The fact that Ethomidate shifts the CA curve slightly leftward could even be interpreted as an advantage, since this allows catching also the upper CA limit without phenylepinephrine treatment.

Acknowledgments J. V. is supported by the Swiss National Science Foundation (310000_120321/1).

Conflict of interest The authors declare no conflicts of interest.

References

Ayata C, Dunn AK, Gursoy OY, Huang Z, Boas DA, Moskowitz MA (2004) Laser speckle flowmetry for the study of cerebrovascular physiology in normal and ischemic mouse cortex. J Cereb Blood Flow Metab 24:744–755

Bosnjak ZJ, Aggarwal A, Turner LA, Kampine JM, Kampine JP (1992) Differential effects of halothane, enflurane, and isoflurane on Ca^2 + transients and papillary muscle tension in guinea pigs. Anesthesiology 76:123–131

Campen MJ, Tagaito Y, Li J, Balbir A, Tankersley CG, Smith P, Schwartz A, O'Donnell CP (2004) Phenotypic variation in cardiovascular responses to acute hypoxic and hypercapnic exposure in mice. Physiol Genomics 20:15–20

Famewo CE, Odugbesan CO (1978) Further experience with etomidate. Can Anaesth Soc J 25:130–132

Faraci FM, Heistad DD (1998) Regulation of the cerebral circulation: role of endothelium and potassium channels. Physiol Rev 78:53–97

Foley LM, Hitchens TK, Kochanek PM, Melick JA, Jackson EK, Ho C (2005) Murine orthostatic response during prolonged vertical studies: effect on cerebral blood flow measured by arterial spin-labeled MRI. Magn Reson Med 54:798–806

Harper SL (1987) Antihypertensive drug therapy prevents cerebral microvascular abnormalities in hypertensive rats. Circ Res 60:229–237

Hu K, Peng CK, Czosnyka M, Zhao P, Novak V (2008) Nonlinear assessment of cerebral autoregulation from spontaneous blood pressure and cerebral blood flow fluctuations. Cardiovasc Eng 8:60–71

Immink RV, van den Born BJ, van Montfrans GA, Koopmans RP, Karemaker JM, van Lieshout JJ (2004) Impaired cerebral autoregulation in patients with malignant hypertension. Circulation 110:2241–2245

Janssen PA, Niemegeers CJ, Marsboom RP (1975) Etomidate, a potent non-barbiturate hypnotic. Intravenous etomidate in mice, rats, guinea-pigs, rabbits and dogs. Arch Int Pharmacodyn Ther 214:92–132

Joutel A, Monet-Lepretre M, Gosele C, Baron-Menguy C, Hammes A, Schmidt S, Lemaire-Carrette B, Domenga V, Schedl A, Lacombe P, Hubner N (2010) Cerebrovascular dysfunction and microcirculation rarefaction precede white matter lesions in a mouse genetic model of cerebral ischemic small vessel disease. J Clin Invest 120:433–445

Kumaria A, Tolias CM (2009) Normobaric hyperoxia therapy for traumatic brain injury and stroke: a review. Br J Neurosurg 23:576–584

Kuschinsky W (1982) Role of hydrogen ions in regulation of cerebral blood flow and other regional flows. Adv Microcirc 11:1–19

Kuschinsky W (1990) Coupling of blood flow and metabolism in the brain. J Basic Clin Physiol Pharmacol 1:191–201

Kuschinsky W (1991) Coupling of function, metabolism, and blood flow in the brain. Neurosurg Rev 14:163–168

Kuschinsky W (1997) Neuronal-vascular coupling. A unifying hypothesis. Adv Exp Med Biol 413:167–176

Lacombe P, Oligo C, Domenga V, Tournier-Lasserve E, Joutel A (2005) Impaired cerebral vasoreactivity in a transgenic mouse model of cerebral autosomal dominant arteriopathy with subcortical infarcts and leukoencephalopathy arteriopathy. Stroke 36:1053–1058

Lo MT, Hu K, Liu Y, Peng CK, Novak V (2008) Multimodal Pressure Flow Analysis: Application of Hilbert Huang Transform in Cerebral Blood Flow Regulation. EURASIP J Appl Signal Processing 2008:785243

McCulloch TJ, Boesel TW, Lam AM (2005) The effect of hypocapnia on the autoregulation of cerebral blood flow during administration of isoflurane. Anesth Analg 100:1463–1467 table of contents

Merzeau S, Preckel MP, Fromy B, Leftheriotis G, Saumet JL (2000) Differences between cerebral and cerebellar autoregulation during progressive hypotension in rats. Neurosci Lett 280:103–106

Niwa K, Kazama K, Younkin L, Younkin SG, Carlson GA, Iadecola C (2002) Cerebrovascular autoregulation is profoundly impaired in mice overexpressing amyloid precursor protein. Am J Physiol Heart Circ Physiol 283:H315–H323

Novak V, Yang AC, Lepicovsky L, Goldberger AL, Lipsitz LA, Peng CK (2004) Multimodal pressure-flow method to assess dynamics of cerebral autoregulation in stroke and hypertension. Biomed Eng Online 3:39

Ogoh S, Nakahara H, Ainslie PN, Miyamoto T (2010) The effect of oxygen on dynamic cerebral autoregulation: critical role of hypocapnia. J Appl Physiol 108:538–543

Panerai RB (2008) Cerebral autoregulation: from models to clinical applications. Cardiovasc Eng 8:42–59

Paterno R, Heistad DD, Faraci FM (2000) Potassium channels modulate cerebral autoregulation during acute hypertension. Am J Physiol Heart Circ Physiol 278:H2003–H2007

Paulson OB, Strandgaard S, Edvinsson L (1990) Cerebral autoregulation. Cerebrovasc Brain Metab Rev 2:161–192

Pedersen TF, Paulson OB, Nielsen AH, Strandgaard S (2003) Effect of nephrectomy and captopril on autoregulation of cerebral blood flow in rats. Am J Physiol Heart Circ Physiol 285:H1097–H1104

Rosengarten B, Hecht M, Kaps M (2006) Carotid compression: investigation of cerebral autoregulative reserve in rats. J Neurosci Methods 152:202–209

Schubert GA, Schilling L, Thome C (2008) Clazosentan, an endothelin receptor antagonist, prevents early hypoperfusion during the acute phase of massive experimental subarachnoid hemorrhage: a laser Doppler flowmetry study in rats. J Neurosurg 109:1134–1140

Schuler B, Rettich A, Vogel J, Gassmann M, Arras M (2009) Optimized surgical techniques and postoperative care improve survival rates and permit accurate telemetric recording in exercising mice. BMC Vet Res 5:28

Schuler B, Arras M, Keller S, Rettich A, Lundby C, Vogel J, Gassmann M (2010) Optimal hematocrit for maximal exercise performance in acute and chronic erythropoietin-treated mice. Proc Natl Acad Sci USA 107:419–423

Strandgaard S (1976) Autoregulation of cerebral blood flow in hypertensive patients. The modifying influence of prolonged antihypertensive treatment on the tolerance to acute, drug-induced hypotension. Circulation 53:720–727

Tonnesen J, Pryds A, Larsen EH, Paulson OB, Hauerberg J, Knudsen GM (2005) Laser Doppler flowmetry is valid for measurement of cerebral blood flow autoregulation lower limit in rats. Exp Physiol 90:349–355

Verhaegen MJ, Todd MM, Hindman BJ, Warner DS (1993) Cerebral autoregulation during moderate hypothermia in rats. Stroke 24:407–414

Vogel J, Kuschinsky W (1996) Decreased heterogeneity of capillary plasma flow in the rat whisker barrel cortex during functional hyperemia. J Cereb Blood Flow Metab 16:1300–1306

Vorstrup S, Barry DI, Jarden JO, Svendsen UG, Braendstrup O, Graham DI, Strandgaard S (1984) Chronic antihypertensive treatment in the rat reverses hypertension-induced changes in cerebral blood flow autoregulation. Stroke 15:312–318

Waschke KF, Krieter H, Hagen G, Albrecht DM, Van-Ackern K, Kuschinsky W (1994) Lack of dependence of cerebral blood flow on blood viscosity after blood exchange with a Newtonian O2 carrier. J Cereb Blood Flow Metab 14:871–876

Werber AH, Fitch-Burke MC, Harrington DG, Shah J (1990) No rarefaction of cerebral arterioles in hypertensive rats. Can J Physiol Pharmacol 68:476–479

Yasuda N, Targ AG, Eger EI 2nd (1989) Solubility of I-653, sevoflurane, isoflurane, and halothane in human tissues. Anesth Analg 69:370–373

Curriculum Vitae

Personal Information	
Name	**WANG**
First Name	**Zhenghui**
Birth Date	6 February 1975
Nationality	Canada
Marriage Status	Married
Professional Experience	
04.2008 - 06.2008	**Trainee** in Center for Integrative Genomics, Université de Lausanne.
01.2006 - 03.2006	**Trainee** in Lady Davis Institute, McGill University, Canada.
08.1996 - 09.1998	**Assistant** in Environmental Science Institute, China.
Education	
06.2008 - 09.2011	**PhD** in Institute für Veterinärphysiologie, Universität Zürich, Switzerland. Thesis Title: Decreased Stability of Erythroblastic Islands in Integrin β3 Deficient Mice.
09.2003 - 06.2007	**Master** in Science (Cell Biology), Université du Québec à Montréal, Canada. Thesis Title: The role of Oxidative Stress in Heat-shock Induced Apoptosis in CHO cells.
09.1992 - 07.1996	**Bachelor** in Science (Biology), University Liaoning, China.
09.1980 - 08.1992	Primary and Secondary School, Liaoning, China.
Publications	
Wang Z, Schuler B, Vogel O, Arras M, Vogel J. What is the optimal anesthetic protocol for measurements of cerebral autoregulation in spontaneousness breathing mice? Exp Brain Res. 2010. **Zhenghui Wang**, Olga Vogel, Gisela Kuhn, Max Gassmann, Johannes Vogel. Decreased stability of erythropoietic islands in integrin β3 deficient mice. (Manuscript accepted by "physiological reports")	

ACKNOWLEDGMENTS

First and foremost, I would like to express the deepest appreciation to my supervisor Prof. Dr. Med. Johannes Vogel for his guidance, motivation and a multitude of priceless discussions and valuable suggestions. I feel lucky to have been encouraged along the way. I am highly grateful for the time and energy he has dedicated to this project and refining of this thesis.

I wish to thank Prof. Dr. med. vet. Max Gassmann for his insightful comments and suggestions. Sincere appreciation also goes to my committee members for their valuable reviewing of this thesis.

This research project would not have been possible without the support of many people. I am grateful to all the members of the institute, especially Manuela Gianella and Olga Vogel, who have not only been there for me as my colleagues, but also as friends, were abundantly helpful and offered invaluable assistance. I would like to extend a special word of gratitude to our secretary Gabriela for her help.

I extend my final and most sincere thanks to my family. Their love and support lights the way for each new adventure I embark on.